UNIVERSIDAD AUTÓNOMA DE MADRID
Departamento de Bioquímica

K_v modulation by polyunsaturated fatty acids. Functional study of a new K_v7.1 mutation associated to short QT syndrome.

CRISTINA MORENO VADILLO

Madrid 2013

Departamento de Bioquímica
Facultad de Medicina
UNIVERSIDAD AUTÓNOMA DE MADRID

K_v modulation by polyunsaturated fatty acids. Functional study of a new K_v7.1 mutation associated to short QT syndrome.

Memoria presentada para optar al grado de Doctor con Mención Internacional por:

CRISTINA MORENO VADILLO
Licenciada en Bioquímica y Biología

Bajo la dirección de:

Dra. Carmen Valenzuela Miranda
Dra. Teresa González Gallego

Realizada en el Instituto de Investigaciones Biomédicas Alberto Sols

Madrid 2013

MINISTERIO DE ECONOMÍA Y COMPETITIVIDAD

CSIC Consejo Superior de Investigaciones Científicas

UAM Universidad Autonoma de Madrid

Dña. CARMEN VALENZUELA MIRANDA, Doctora en Biología e Investigadora Científica del Instituto de Investicaciones Biomédicas CSIC-UAM y

Dña. TERESA GONZÁLEZ GALLEGO, Doctora en Biología e Investigadora Ramón y Cajal del Instituto de Investicaciones Biomédicas CSIC-UAM,

CERTIFICAN:

Que Dña. CRISTINA MORENO VADILLO ha realizado bajo su dirección el trabajo de investigación titulado "*K_V modulation by polyunsaturated fatty acids. Functional study of a new K_V7.1 mutation associated to short QT syndrome*" para alcanzar el Grado de Doctor, el cual reúne los requisitos de originalidad y contenido exigidos, por lo que autorizan su presentación para que pueda ser juzgada por el Tribunal correspondiente.

Y para que así conste, expiden el presente certificado en Madrid a 18 de diciembre de 2012.

Fdo. Carmen Valenzuela Miranda

Fdo. Teresa González Gallego

A mi familia

Hace ya más de 10 años, cuando estudiaba bachillerato decidí que quería empezar la carrera de bioquímica porque me parecía muy atractiva la investigación. Recuerdo que mis padres, pensando en mi futuro, me recomendaban que estudiara otra carrera con más salida pero yo lo tenía claro, quería dedicarme a la ciencia. Pasaron los años de universidad (muy rápido) y en el 2008 la Dra. Carmen Valenzuela me abrió las puertas de su laboratorio para hacer el doctorado. Hoy, casi cinco años más tarde empiezo a escribir las últimas páginas de esta Tesis, los agradecimientos.

Durante este periodo he crecido personal y profesionalmente. Académicamente he aprendido muchísimas cosas, llegué con una formación bioquímica más clásica al campo de la fisiológía y más concretamente al de la electrofisiología. No fue fácil al principio, pero que con el tiempo me ha conseguido atrapar. He vivido muy diferentes experiencias, he vivido en distintas ciudades, he asistido a numerosos congresos gracias a los cuales he cruzado por primera vez el charco y he podido escuchar a algunos de los mejores científicos de éste y otros campos. Guardo un cariño especial al congreso de la RECI y al de la Biofísica del año 2010. En ellos vivimos algún que otro accidente pero sobre todo momentos muy emocionantes y divertidos. Allí descubrí y me enamoré de la ciencia en mayúsculas. Del laboratorio me llevo también muy buenos recuerdos principalmente el buen ambiente que allí se respira y el trabajo en equipo. Creo firmemente que cuanto más a gusto se está en un sitio mejor se trabaja y esto en el 1.13 se cumple a rajatabla. Me llevo las cervecitas del primer año que tan bien nos venían para desconectar en primavera. Largos días de “patch” amenizados con las aplicaciones asociadas a las versiones de clampex (buscaminas y solitario), con videos, bromas y nuestras versiones de canciones de hoy, ayer y siempre. También me llevo productivas discusiones científicas ambientadas en diversos puntos de la geografía mundial y un sinfín de momentos más. Pero no todo ha sido fácil. También ha habido momentos de dudas, cansancio, desesperación…en los cuales sin el apoyo de estas personas no habrá sido posible la realización de ésta Tesis

En primer lugar quisiera agradecer a la Dra. Carmen Valenzuela por su admirable disposición tanto en las labores de investigación como fuera del laboratorio en el ámbito personal. Porque más allá de la relación profesional, Carmen me ha guiado en esta experiencia como una segunda madre. Me siento muy honrada de haber contado con su ayuda, confianza, su cariño, y por haberme transmitido toda su pasión por la electrofisiología y la ciencia. Quisiera hacer extensible ésta agradecimiento a La Dra. Teresa González mi codirectora de Tesis, otro pilar sin el cual ésta Tesis no habría llegado a buen término. Muchas gracias por todo lo que me habéis enseñado y porque sé que siempre contaré con vuestro apoyo.

A todos los miembros que han pasado por el laboratorio. A Miren David que me enseñó todos los trucos del laboratorio y con sus presentaciones de power point y su sentido del humor me hizo mucho más llevadero mi

primer año. Además quiero darle gracias por la calidad científica de sus comentarios y sugerencias que aun hoy me sigue ofreciendo. A Álvaro Macías, con el que he compartido casi todo este viaje. Juntos hemos aprendido y nos hemos complementado siempre con el mejor humor y disposición posible. Nuestro camino se inició en este laboratorio pero no acaba aquí. Como hemos comentado muchas veces, seguirá dentro de años porque quedaremos en futuros congresos en los que otros becarios nos señalarán con el dedo y dirán: Mira, no son ellos los del trabajo… A Gema Y Ulyana, dos estudiantes llenas de energía que que con sus conversaciones y locuras nos sacaron más de una sonrisa, pero sobre todo pero sobre todo por su continuo ofrecieminento y contribución en las diversas tareas del laboratorio. A Carmen y Mariela nuestras cardiólogas murcianas que nos han aportado su visión de la electrofisiología cardiaca desde un punto de vista más clínico. Con su frescura y vitalidad he vivido los dos meses más divertidos e intensos en el laboratorio. A Alicia y Ángela, las últimas incorporaciones nos traído aire fresco y mucha alegría al laboratorio. Os dejasteis engañar y habéis caído en las redes del patch-clamp pero las dos valéis mucho, sois muy trabajadoras y generosas y hacéis que uno tenga ganas todos de venir a trabajar todas los días.

A los compañeros de otros laboratorios, en especial a Rafa, Pilar, Antonio, Alejandra, Mario, Eva Maria, Ana Rosa, Blanca, Pepa, Toño, Miryam, Daniela, Irene…una gran familia científica. El significado de este grupo se refleja en el vacío que queda cuando alguno de vosotros se ha ido. Por hacer de los cafecitos en los bancos y de la hora de comer el mejor momento del día. Juntos hemos conseguido hacer la mesa más larga del IIB. Hemos compartido las penas y alegrías de la ciencia, porque nadie entiende mejor a un becario que otro becario y también muchas falconadas, salidas culturales y nocturnas. En definitiva muchas gracias por hacer fácil este camino.

A Bianca, Quique, Javi, Laura, Carmen, Dani y Raquel miembros de nuestro laboratorio hermanado de la Complutense dirigidos por los Profesores Francisco Pérez-Vizcaíno y Ángel Cogolludo con los que hemos colaborado a lo largo de estos años en diversos proyectos científicos que nos aportado muchas éxitos. Porque siempre se puede contar con ellos, pero sobre todo porque es un placer haber compartido celebraciones profesionales y personales.

Al Dr. Lisardo Boscá y a los miembros de su laboratorio María, Paqui y Patricia. Una parte importante del trabajo que aquí se presenta se ha realizado en colaboración con ellos. Esperemos que dentro de muy poco tiempo salga a la luz. Muchas gracias por vuestro trabajo y colaboración.

Al Dr. Antonio Felipe que me acogió en su laboratorio en mi primera estancia. Él ha sido un excelente mentor para mí en otra rama de la ciencia, la biología molecular. Tanto Antonio como todos los miembros de su

equipo Núria, Anna, Laura Joasssia, Mireia y Ramón se implicaron mucho y me hicieron sentir desde el primer momento como en casa y tengo que reconocer que me sentí muy orgullosa cuando al cabo de un tiempo me comenzasteis a llamar “la Cristina”. Trabajamos muchísimo pero los días pasaban muy rápido entre risas y travesuras con Anna y Núria.. No quisiera olvidarme de mi compañera de piso Antonella con la que recorrí todos los rincones de Barcelona.

En mi segunda estancia me fui un poco más lejos; Dresden, Alemania. Me gustaría agradecer a la Profesora Ursula Ravens por darme la oportunidad de trabajar en uno de los mejores laboratorios de Europa de electrofisiología cardiaca ya los profesores Erich Wettwer y Torsten Christ por guiarme día a día en el proyecto. Los tres pusieron toda su experiencia científica a mi disposición. Esta estancia hubiera sido mucho más difícil sin el apoyo de mis compañeros de residencia Chiara, Alina, Prasad, Ahmed y Lucas a los que me une un lazo muy fuerte. Todos estábamos lejos de nuestras casas en aquel momento y formamos un inolvidable grupo de amigos.

Esta sección de agradecimientos no tendría sentido si no me acordara de mis compañeros de facultad, Teresa, Nadia, Jorge y David porque entre clases, horas en la cafetería, excursiones al campo, apuntes, prácticas de fisiología y de bioquímica comenzó a forjarse nuestro interés por la ciencia. Y de toda la gente que ha ocupado la mayor parte del tiempo libre que el trabajo me dejaba y sin la que no habría podido llevar a término esta Tesis. Vicky, Sara, Jose David y María, con respecto al laboratorio, vosotros habéis sido mi “equipo 0” dispuestos a animar y echar una mano en lo que hiciera falta.

A mi familia y a mi hermano Álvaro que me han apoyado y han seguido muy de cerca esta aventura. Y por último quiero expresar mi más sincero gracias a mis padres Emilio y Blasa. Ellos han sufrido y disfrutado conmigo paso a paso la evolución de esta Tesis. Ellos me inculcaron el valor del esfuerzo y de la superación. Durante estos años han tenido una paciencia infinita al oírme hablar de experiementos y cosas raras, me han animado a seguir en los momentos difíciles, me han dado todo su cariño, han aguantado mis malos humos y han sido mi mayor soporte. Todo sin pedirme nada a cambio. No tengo líneas suficientes para agradecérselo. Ésta Tesis es tan mía como vuestra

Los canales de potasio dependientes de voltaje (K_v) son proteínas de membrana que se encuentran altamente moduladas en diversos procesos fisiológicos, y patológicos tales como la respuesta inmune y la función cardiaca. Los canales iónicos, y en particular los canales de potasio, juegan un papel esencial en la fisiología de los macrófagos. Se ha descrito que un incremento en la dieta de ácidos grasos poliinsaturados (AGPIs) posee propiedades antiinflamatorias. Es más, mediadores lipídicos derivados de AGPIs n-6 y n-3, como lipoxinas y resolvinas (cuya producción aumenta tras la ingesta de aspirina), han surgido como nuevos y potentes agentes que regulan la inflamación aguda promoviendo la resolución. En la presente Tesis Doctoral se estudió la modulación por lipoxinas de los canales K_v y K_{ir} presentes en macrófagos derivados de médula ósea (MDMO) mediante la técnica de *patch-clamp.* El tratamiento agudo con e-LXA_4 de MDMO estimulados con LPS disminuyó la corriente K_v, lo que es compatible con la atenuación de la respuesta inflamatoria. De manera más relevante, el pretratamiento con e-LXA_4 de MDMO estimulados con LPS revertió los efectos producidos en las corrientes K_v y K_{ir}, en los niveles de Ca^{2+} intracelular, disminuyó la actividad de NF-κB e IKKβ y protegió contra la apoptosis inducida por LPS. Estos efectos fueron mediados, al menos en parte, a través de la vía dependiente del receptor de lipoxinas (ALX). Este trabajo describe un nuevo mecanismo por el cual la e-LXA_4 contribuye a la resolución de la inflamación que consiste en la prevención de los efectos del LPS sobre las corrientes K_v y K_{ir} de MDMO. Además, se ha descrito que los AGPIs modifican la actividad eléctrica del corazón a través de la modulación de canales iónicos. En la presente Tesis Doctoral, se analizaron los efectos de la aplicación aguda y crónica de EPA y DHA en la corriente generada por K_v7.1/KCNE1 expresados transitoriamente en células COS7 mediante la técnica de *patch-clamp*, western blot y aislamiento de balsas lipídicas. En función del modo de administración, los AGPIs modificaron dicha corriente de manera diferencial. La perfusión aguda con EPA aumentó la magnitud de K_v7.1/KCNE1, enlenteció la cinética de activación y desplazó la curva de activación (CA) hacia la izquierda. Por el contrario, el EPA crónico no modificó la corriente K_v7.1/KCNE1 pero desplazó la CA en dirección opuesta. Además, EPA crónico disminuyó la expresión de K_v7.1 pero no de KCNE1, e indujo una redistribución de K_v7.1 en la membrana celular. Experimentos con metil-β-ciclodextrina mostraron que la depleción de colesterol aumenta la magnitud de K_v7.1/KCNE1. En estas células, EPA ejerció efectos similares a los producidos tras su administración aguda, efectos que fueron revertidos tras el posterior lavado con solución libre de AGPI, sugiriendo una interacción directa con el canal. Por otro lado, mutaciones en canales iónicos cardiacos alteran la formación y propagación normal de los potenciales de acción, lo que puede generar la aparición de arritmias. El síndrome de QT corto es una nueva entidad clínica que se caracterizada por un acortamiento del intervalo QTc en el ECG y por una falta de adaptación durante el ejercicio. En la presente Tesis Doctoral, se caracterizó mediante la técnica de *patch-clamp* la nueva mutación F279I K_v7.1 encontrada en un varón de 23 años con un QTc de 356 ms con una historia clínica familiar de MSC. En ausencia de KCNE1, la corriente silvestre y F279I K_v7.1 exhibieron propiedades biofísicas similares. Sin embargo, el canal F279I K_v7.1 expresado en homo o heterozigosis con el canal silvestre y en presencia de KCNE1 mostró un pronunciado desplazamiento de la CA y una aceleración de la cinética de activación, permitiendo una ganancia de función en I_{Ks}. Se concluye, por tanto, que la mutación F279I provoca un aumento sustancial en la corriente de repolarización durante el PA debido a una modulación defectuosa de KCNE1 del "*gating"* de K_v7.1.

Abstract

Voltage dependent potassium channels (K_v) are membrane proteins highly modulated by several physiological, pharmacological and pathological events. Also, K_v channels are involved in a plethora of pathophysiological process, including immune response and cardiac arrhythmias. Ion channels and in particular, potassium channels play a pivotal role in the modulation of macrophage physiology. It has been described that an increased consumption of PUFAs in the diet possesses anti-inflammatory actions. In fact n-6 and n-3 derived lipid mediators, such as the lipoxins and resolvins (whose production is increase in the presence of aspirin) have emerged as novel potent agents that counter-regulate excessive acute inflammation and stimulate molecular and cellular events that define resolution. In the present Doctoral Thesis, the modulation of K_v and K_{ir} channels by lipoxins was analyzed. Currents were recorded in bone marrow derived macrophages (BMDM) using the *patch-clamp* technique. Acute treatment of LPS-stimulated BMDM with e-LXA_4 resulted in a decrease of K_v currents, compatible with attenuation of the inflammatory response. More importantly, long-term treatment of LPS-stimulated BMDM with e-LXA_4 significantly reverted LPS effects on K_v and K_{ir} currents, intracellular calcium levels, diminished NF-κB and IKKβ activity, and protected against LPS activation-dependent apoptosis. These effects were mediated, at least in part, via the lipoxin receptor (ALX). We provide evidence for a new mechanism by which e-LXA_4 contributes to inflammation resolution consisting in the revertion of LPS effects on K_v and K_{ir} currents in macrophages. In addition, it has been report that PUFAs can modify the electrical activity of the heart due to their ability to modulate cardiac ion channels. In the present Doctoral Thesis, we analyzed the effects of acute and chronic application of EPA and DHA on the current and the expression of K_v7.1/KCNE1 channels transiently expressed in COS7 cells by using *patch-clamp*, Western blot, and lipid rafts extraction techniques. Depending on the way of administration, PUFAs differentially modified this current. Acute perfusion with EPA increased K_v7.1/KCNE1 current magnitude, slowed the activation kinetic and induced a leftward shift of the activation curve. On the contrary, chronic EPA did not modified K_v7.1/KCNE1 current and shifted the activation curve towards the opposite direction. In addition, chronic EPA decreased the expression of K_v7.1 but not of KCNE1, and induced a wider distribution of K_v7.1 over the cell membrane. Experiments with methyl-β-cyclodextrin demonstrated that removal of cholesterol increased the K_v7.1 current magnitude. In cholesterol depleted cells, EPA produces similar effects than those produced acutely that could be reverted after wash-out with drug-free external solution, suggesting a direct effect on the channel. Mutations involving cardiac ion channels result in abnormal action potential (AP) formation or propagation, leading to cardiac arrhythmias. They constitute approximately 10–20% of all sudden cardiac death (SCD). The short QT syndrome is a new congenital entity characterized by a shortened QTc interval in the ECG and a lack of adaptation during increasing heart rates. In the present Doctoral Thesis, we used the *patch-clamp* technique to characterize the novel F279I K_v7.1 mutation found on a 23 years old man with a QTc of 356 ms and a familial history of SCD. In the absence of KCNE1, WT and F279I K_v7.1 currents had similar biophysical properties. However, functional analysis of F279I K_v7.1 (alone or co-expressed with the WT channel, in the presence of KCNE1) revealed a pronounced shift of the half-activation potential and an acceleration of the activation kinetics leading to a gain of function in I_{Ks}. We conclude that the F279I mutation would predict to augment substantially repolarizing current during the AP due to an impaired coupling of the K_v7.1 gating modulation induced by KCNE1.

Content

Figure list

Supplemental Figures

Table list

Supplemental tables

Abbreviations Index

4-AP	4-aminopyridine
Å	Angstrom
O	Open state of the channel
Ab	Antibody
AKAP	A-kinase anchoring protein
ALA	Alpha-linolenic acid
Ala	Alanine
ALX	Activated lipoxin receptor
AP	Action potential
ATP	Adenosin triphosphate
BocPLP	N-terminus Boc-Phe-Leu-Phe-Leu-Phe formyl peptide
BMDM	Bone marrow derived macrophages
BSA	Bovine serum albumin
C	Closed state of the channel
Ca^{2+}	Calcium ion
CaM	Calmodulin
cAMP	Cyclic adenosine monophosphate
cGMP	Cyclic guanine monophosphate
cDNA	Complementary desoxyribonucleic acid
Cm	Membrane capacitance
CMV	Citomegalovirus
COS7	CV-1 (simian) cell line in origin carrying the SV40 genetic material
COX-2	Cyclooxygenase-2
CRAC	Calcium release activated channels
C-terminus	Carboxyl terminal domain of proteins
CVD	Cardiovascular disease
Cys	Cysteine
DAG	Diacylglycerol
DHA	Docosahexaenoic acid
DMEM	Dulbecco´s Modified Eagle Medium
E_K	Equilibrium potential for K^+
ECG	Electrocardiogram
e-LXA_4	15-Epi-lipoxin A_4
EPA	Eicosapentaenoic acid
ER	Endoplasmic Reticulum
FBS	Fetal bovine serum
FCS	Fetal Calf serum
GΩ	Gigaohmn
GLUT4	Glucose transporter 4
HEK293	Human embrionic kindey cell line
HTRF	Homogeneous time-resolved fluorescence
IFNγ	Interferon gamma
IL	Interleukin
IV	Current voltage relationship
I_{CaL}	Inward L-type calcium current
I_{CRAC}	Calcium release activated calcium current
I_{K1}	Inward rectifying potassium current
$I_{K,ACh}$	Inward rectifying acetylcholine-sensitive K^+ current
$I_{K,ATP}$	Inward rectifying ATP-sensitive K^+ current
I_{Kr}	Rapidly activating delayed rectifying potassium current
I_{Ks}	Slowly activating delayed rectifying potassium current
I_{Kur}	Ultrarapidly activating delayed rectifying potassium current
I_{Na}	Inward sodium current.

I_{to}	Transient outward potassium current
IP	Immunoprecipitation
K^+	Potassium ion
KDa	Kilodalton
kHz	Kilohertz
K_v	Voltage dependent potassium channel
$K_v\beta$	Ancillary β-subunit of voltage-gated potassium channels
LOX	Lipoxygenase
LPS	Lipopolysaccharide
Ltk$^-$	Leukocyte tyrosine kinase less mouse derived cell line
Mg^{2+}	Magnessium ion
MβCD	Methyl beta cyclodextrin
M-CSF	Macrophage colony-stimulating factor
mRNA	Messenger ribonucleic acid
n-3 PUFAs	Omega 3 polyunsaturated fatty acids
Na^+	Sodium ion
NO	Nitric oxide
N-terminus	Amino-terminal domain of proteins
P	P-loop
PBS	Phosphate buffer saline
PCR	Polimerase chain reaction
PI	Propidium iodide
PIP_2	Phosphatidylinositol bisphosphate
PKA	Protein kinase A
PKC	Protein kinase C
PKG	Protein kinase G
Pro	Proline
PVP	Proline-Valine-Proline motif
QT	QT interval of the electrocardiogram
QTc	Bazett corrected QT interval for the cardiac frequency
RT-PCR	Retrotranscriptase polimerase chain reaction
SCD	Sudden cardiac death
SEM.	Standard error of the mean
τ	Time constant
TEA	Tetraethylammonium
TM	Transmembrane
TG	Thapsigargin
TRPM8	Transient receptor potential cation channel subfamily M member 8

1 INTRODUCTION

1.1 ION CHANNELS

Ion channels are part of the mechanism of cellular signaling of almost all live cells. Our ability to do gymnastic, to perceive a colorful world and to process language relies on rapid communication among cells. Such signaling, the fastest in our bodies, involves electrical fluxes produced when ion channels open and close. Fast electrical signaling is made possible by the homeostatic mechanisms that establish the standard environment and content of animal cells: high Na^+ concentration [Na^+] in the blood and extracellular fluid, and high [K^+] (but low [Na^+] and [Ca^{2+}]) in the cytoplasm. Gradients are established and maintained by active transporters and pumps, which prepare the way for rapid changes in membrane voltage to be produced by passive transport through ion channels. These pore-forming proteins allow ions to flow only "downhill", as dictated by their electrochemical gradients, but they do it rapidly (the rate of passage of ions through one open channel is often more than 10^6 ions per second) and selectively. Opening a Na^+ or Ca^{2+} selective channel permits Na^+ or Ca^{2+} to flow down its gradient into a cell, making the intracellular voltage more positive. Opening a K^+ selective channel permits K^+ to flow from the cell and restores the voltage to a negative value. The dimensions of a typical cell and its membrane allow the voltage to be changed rapidly back and forth many times, with relatively small changes in concentration. This is essentially how all cellular electrical signaling is produced (2).

1.2 CLASSIFICATION OF POTASSIUM CHANNELS

Voltage-gated ion channel protein superfamily, formed by more than 140 members, is one of the largest groups of signal transduction proteins (3,4). Among them, potassium channels are the largest and most diverse family of ion channels. The first K^+ channel to be identified came from the cloning of the *Shaker* gene of *Drosophila* which causes flies to shake when exposed to ether (5). However, ion channels are found in bacterial, archeal, and eukaryotic cells both plant and animal and their amino acid sequences are very easy to recognize because K^+ channels contain a highly conserved segment called the potassium signature sequence (GYG) (6). This sequence forms a structural element known as the selectivity filter, which prevents the passage of sodium ions but allows potassium ions through the ion channel pore at rates approaching the diffusion limit. Diversity among different members of the K^+ channel family is related mainly to the various ways in which K^+ channels are gated. Some K^+ channels are ligand gated, which means that pore opening is energetically coupled to the binding of an ion (7), a small organic molecule, or even in some cases a protein (8). Other K^+ channels are voltage-gated, in which case pore opening is energetically coupled to the movement of a charged voltage-sensor within the membrane electric field (9,10). Based on their molecular architecture, different channel classes are distinguished (Figure 1) (11-14). The simplest structural type of K^+ channels is visible in the 2TM/1P class, named after their typical composition of two transmembrane helices (TM) and one P-loop (P), and is represented by the inward rectifier K^+ channels (K_{ir}). The second group is referred to as voltage-gated K^+ channels (K_v). They are composed of six TM helices (S1-S6) and one P-loop, resulting in the 6TM/1P class. The two-P K^+ channels

family is constituted by the non voltage-gated outward rectifier channels that have an eight TM architecture that contains two P-regions per subunit (8TM/2P) and the class of the so-called "background" or "leakage" channels made up of two P-regions, hence structurally referred to as 4TM/2P type (15,16).

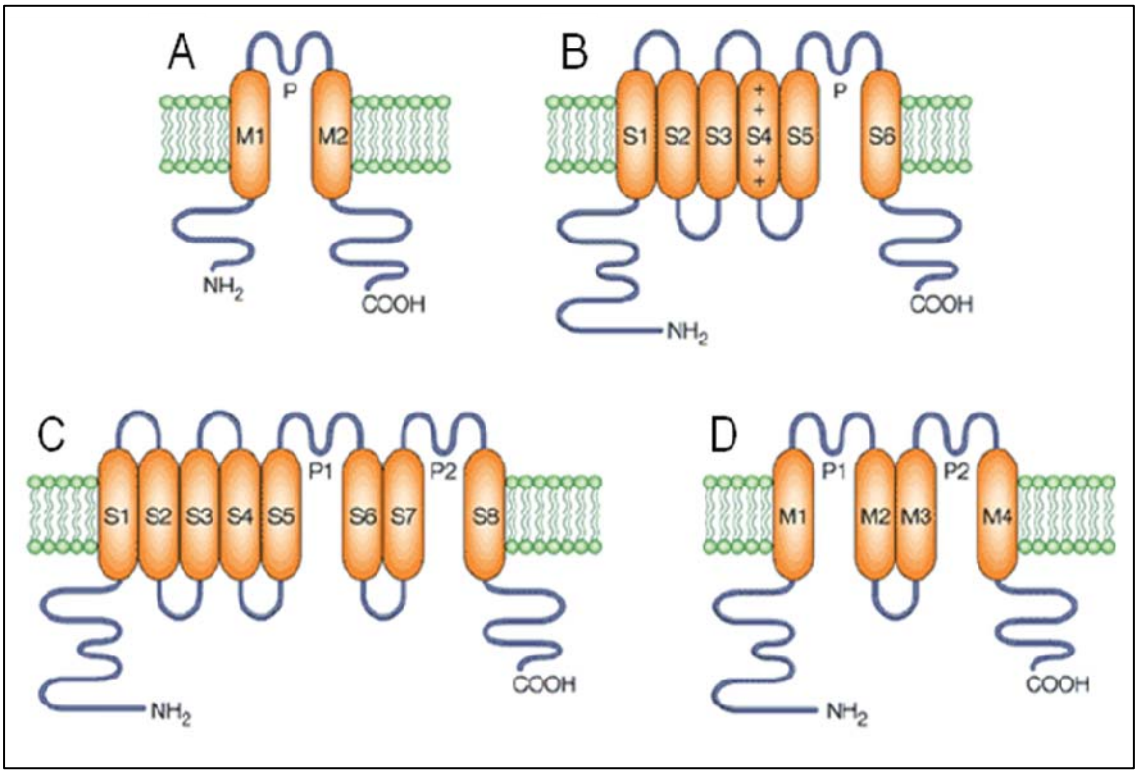

Figure 1. The four main classes of potassium channels. **(A)** 2TM/P channels, which consist of two transmembrane (TM) helices with a P loop between them, exemplified by inwardly rectifying K^+ channels and by bacterial K^+ channels such as KcsA. **(B)** 6TM/P channels, which are the predominant class among ligand-gated and voltage-gated K^+ channels. **(C)** 8TM/2P channels, which are hybrids of 6TM/P and 2TM/P, and were first found in yeast. **(D)** 4TM/2P channels, which consist of two repeats of 2TM/P channels. 8TM/2P and 4TM/2P probably assemble as dimers to form a channel. 4TM/2P channels are far more common than was originally thought. These so called 'leakage' channels are targets of numerous anaesthetics. S4 is marked with plus signs to indicate its role in voltage sensing in the voltage-gated K^+ channels. Taken from Choe et al 2002 (3).

1.3 VOLTAGE-GATED POTASSIUM CHANNELS

Voltage-gated K^+ channels (K_v) "sense'' voltage differences across the cell membrane and open or close in response to changes in the membrane potential. To date, twelve different subfamilies of K_v channels subunits have been described (K_v1-12) (17,18). K_v channels are formed by co-assembly of four α subunits, each containing six α-helical TM segments (S1-S6), with both N- and C-termini on the intracellular side of the membrane. Each subunit comprises two membrane-integrated functionally distinct modules; one forms the voltage-sensor (S1-S4) and the other the K^+ selective pore with the gate (S5-P-S6) (Figure 2A).

The N-terminus of K_v1-4 channels contains a "tetramerization domain" (T1 domain) (Figure 2B). It determines the specificity of channel subunit assembly and also serves as a platform for binding of auxiliary K_v cytoplasmic β-subunits. The cytoplasmic C-terminus of *Shaker* K^+ channels has no obvious domain structure. By

contrast, other K_v channels are characterized by the presence of a subunit assembly domain and/or a sensor domain in the C terminus. These include K_v7 and K_v10-12 channels, as well as potassium channels gated by

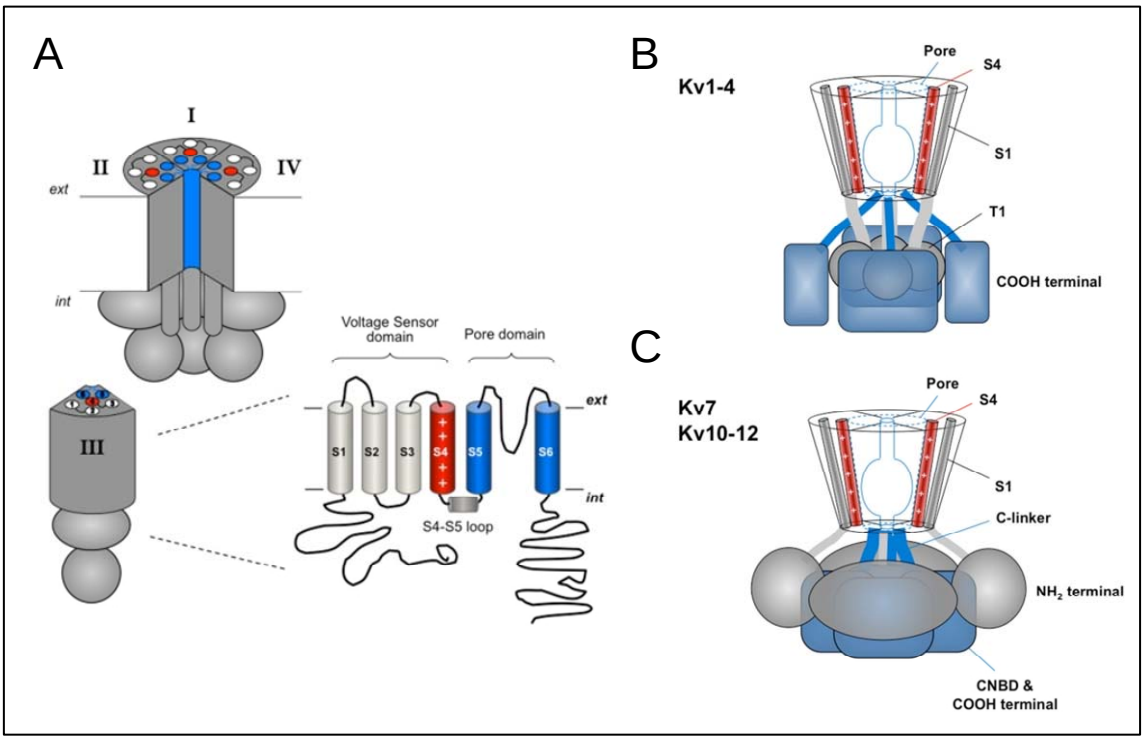

Figure 2. Summary of structural components of K_v channels. **(A)** Schematic representation of the tetrameric organization of a K_v channel. A structural folding model of one of the four α subunits is shown on the right. **(B)** General organization of the K_v1–K_v4 channels group with the T1 "tetramerization domains" hanging centrally below the transmembranal core and attached to it through four linkers continued from the first transmembrane helices. In this case, the C-terminus structures probably track to the periphery surrounding T1 and extending to its bottom. **(C)** General architecture of the K_v7 and K_v10–K_v12 channels characterized by a C-terminus (i.e., the C-linker/cyclic nucleotide-binding domain (CNBD) region of the K_v10–K_v12 channels or the A–D helical regions of the K_v7 channels) forming a compact tetrameric structure in a central position immediately below the cytoplasmic pore opening. In this case the N-terminus probably surrounds the C-terminus and extends to its bottom establishing extensive contacts with its top and side surfaces. Note that in both models the initial N-termini structures are likely to interact with the gate surroundings in the transmembrane core. S4 segment is also depicted as a reference. Adapted from Barros and de la Peña 2012(19)

voltage and intracellular Ca^{2+} (e.g. $K_{Ca}1$ channels) and channels gated exclusively by intracellular ligands like Ca^{2+} (e.g. $K_{Ca}2$ channels) (Figure 2C). The auxiliary subunits known to be associated with this family (KCNE, β1- β4) are transmembrane proteins; they appear to be intimately associated with the pore domain and may displace the voltage-sensor domain or interact with it directly (19,20).

1.3.1 Ion pore and selectivity filter of K_v channels

The essential role of all K^+ channels is to conduct K^+ ions across the cell membrane. The atomic radius of K^+ is 1.33 Å and that of Na^+ is 0.95 Å. With only this difference in ionic radius to work with, K^+ channels manage to select for the K^+ ion over the Na^+ ion by a factor of more than 1000. Moreover, this strong selectivity for K^+ is achieved without compromising the rates of conduction, which approach the diffusion limit. The K^+ channel pore is comprised of four usually identical subunits that encircle with four-fold symmetry a central ion

conduction pathway (21,22). The first K^+ to be crystallized was the bacterial KcsA channel.Two of the four subunits of the KcsA are shown in Figure 3. Each subunit contains two fully transmembrane α-helices termed inner (nearest the ion pathway) and outer (nearest the membrane) helices (equivalent to S5 and S6 of K_v channels), and a tilted pore helix that runs half way through the membrane, pointing its C-terminus negative charge toward the ion pathway. Near the midpoint of the membrane, the ion pathway is nearly 10 Å in diameter, forming a central water-filled cavity. A hydrated K^+ ion remains suspended at the center of the cavity in the crystal structure (23).

Potassium selectivity is determined by the selectivity filter, located in the extracellular third of the ion pathway in between the central cavity and the extracellular solution. The K^+ channel signature sequence amino acids (GYG), conserved in K^+ channels throughout the phylogeny, form the selectivity filter. Here, conducting K^+ ions encounter four evenly spaced layers of carbonyl oxygen atoms and a single layer of threonine hydroxyl oxygen atoms, which create four K^+ ion binding sites numbered 1 to 4 from the extracellular to the intracellular side. At these sites, K^+ ions bind in an essentially dehydrated state, surrounded by eight oxygen atoms from the protein, four 'above' and four 'below' each ion. The arrangement of protein oxygen atoms surrounding each binding site in the selectivity filter is very similar to the arrangement of water molecules around the hydrated K^+ ion observed in the central cavity. Thus, the crystal structure provides an explicit demonstration of the selectivity

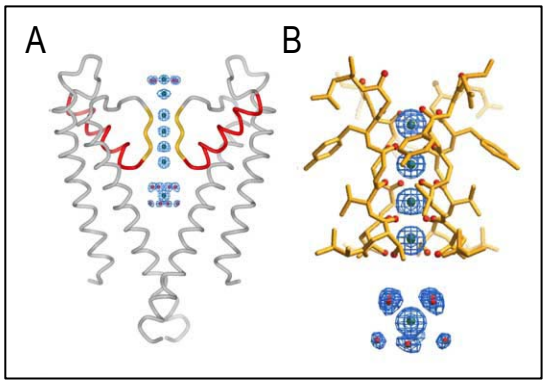

Figure 3. The ion conduction pore of K^+ channels. **(A)**: Two of the four subunits from the KcsA pore are shown with the extracellular side on top. Each subunit contains an outer helix close to the membrane, an inner helix close to the pore, a pore helix (red) and a selectivity filter (gold). Blue mesh shows electron density for K^+ ions and water along the pore**. (B)** Close-up view of the selectivity filter with dehydrated K^+ ions at positions 1 through 4 (external to internal) inside the filter and a hydrated K^+ ion in the central cavity below the filter. Taken from Mackinnon 2003 (22)

filter's role, to create a queue of K^+ binding sites that mimic the waters of hydration surrounding a K^+ ion. Potassium ions are therefore able to diffuse from water into the selectivity filter where the energetic cost of dehydration is compensated. Sodium ions, on the other hand, do not seem to enter the selectivity filter in crystal structures even when Na^+ is present in vast excess (22,24). In fact, reduction of K^+ to 3 mM in the presence of 150 mM Na^+ causes the selectivity filter to undergo a conformational change to a 'collapsed' state. The structure of K_v channels differs from that of the non-voltage-gated bacterial potassium channel KcsA due to a sharp-bend in the S6 helices (equivalent to the inner helices of the KcsA channel). This bend occur at a Pro-X-Pro sequence that is absolutely conserved in the K_v channels (25).

1.3.2 Voltage-sensor of K_v channels

For K_v channels the membrane voltage determines whether they are open and therefore, they provide a

way for the membrane voltage to feed back onto itself, a key property for generating electrical impulses (26). Different reports have revealed that the S1-S4 region acts as the voltage-sensor of K_v channels (27) (Figure 4). The S4 segment (which exhibits seven positively charged residues) is the major component of the -sensor for gating, although negative charges in S1, S2 and S3 also contribute to this process. S3 is actually formed by two

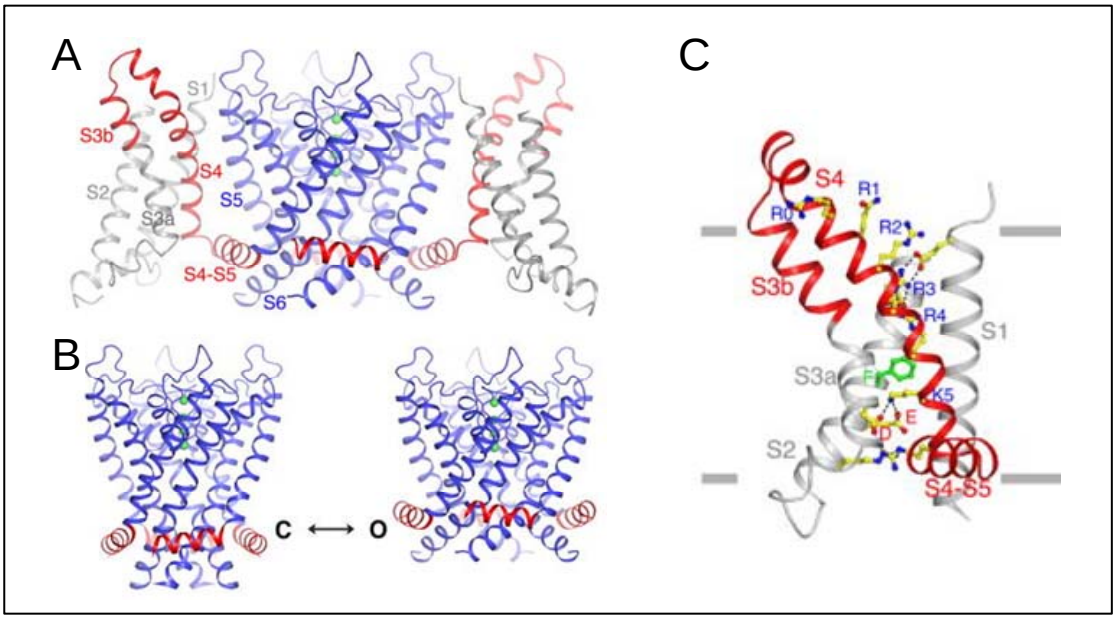

Figure 4. Schematic view of the voltage-sensor of K^+ channels. **(A)** Ribbon representation of the transmembrane region of K_v2.1 paddle–K_v1.2 chimera channel tetramer ($K_v$chim, viewed from the side, and oriented with the extracellular solution above. The pore is colored blue; the voltage sensor paddle (S3b and S4) and the linker helix (S4-S5) between voltage sensor and the pore red; and S1, S2, and S3a gray. The voltage sensor closest to the viewer was removed for clarity. K^+ ions in the selectivity filter are shown as green spheres. **(B)** Ribbon representation of the pore and S4-S5 linkers in the hypothetical closed conformation (C) from a model constructed from the $K_v$chim and KcsA structures and in the open conformation (O) from the crystal structure of $K_v$chim. In the hypothetical closed state, based on the closed conformation of KcsA, the S4-S5 linker helices are pushed down to maintain their same contacts with the pore. **(C)** View of the voltage sensor and S4-S5 linker helix of the open conformation from $K_v$chim. Side chains of the positively charged residues on S4 (labeled as R0, R1, R2, R3, R4, and K5) and the negatively charged residues forming ionizing hydrogen bonds (dashed black lines) with the positive charges, as well as those of the three residues (labeled F, E, and D) forming an occluded binding site in the voltage sensor, are shown as sticks and colored according to atom types (yellow, carbon; blue, nitrogen; red, oxygen; and green, phenylalanine). Taken from Tao et al 2010 (30).

helices referred to as S3a and S3b (Figure 4C). In all of the crystal structures determined, S3b forms with S4 a helix-turn-helix structure called the voltage-sensor paddle (28,29). Depolarization of the cell membrane causes a physical outward movement of S4, which induces further conformational changes that open the channel pore and permit selective K^+ permeation. This movement has been monitored electrically as the gating current (29,30), or by means of fluorescence (30,31).

1.3.3 Coupling of voltage sensing to gating of K_v channels

The gate region in K^+ channels controls whether K^+ ions can traverse the ion conduction pore. Comparison of the structural data from K^+ channels trapped in the open conformation, MthK, K_vAP and K_v1.2

(28,32-35), and channels trapped in the closed conformation, KcsA and K_{ir}Bac1.1 (21,36), indicates that gate opening is associated with a conformational change of the S6 helix. Bending of the S6 helix at a glycine hinge may well explain gating in bacterial K^+ channels. However, the S6 helix of many eukaryotic K_v channels has a PVP motif. Results of accessibility studies (25,37-40) suggest that opening of the S6 bundle takes place at the PVP motif of K_v1 channels. The crystal structure of the rat K_v1.2 (28,35) supports this view and shows that widening of the S6 occurs because of a bend at the PVP motif. Apparently, opening of the gate is associated with the bending of inner TM2/S6 helix which can occur at either a glycine or a PVP motif. It is not well understood how motion of the voltage-sensor couples to the channel opening. Several studies on *Shaker* and related channels suggest the S4-S5 linker and the end of S6 are involved in coupling (41-48). The crystal structure of K_v1.2 demonstrates this interaction clearly. The distal end of the S4-S5 linker comes close to the internal end of S5 below the PVP motif, with extensive contacts between side chains of the two regions. This structural picture of the activated conformation suggests that to close the gate, the S4-S5 linker would have to move inward, shutting down the S6 gate (28,35). As discussed above, the S4-S5 linker and C-terminus end of S6 are critical for coupling between voltage-sensor movement and channel opening. In addition, studies on a triple mutant of *Shaker* (named ILT) where three positions in S4 were mutated to the corresponding residues in *Shaw* (49,50), revealed that in ILT, the voltage ranges over which the voltage-sensor movement and the channel opening occur were quite well separated. It is suggested that S4 itself plays a role in coupling voltage sensing with gating (51). The effect of the ILT mutations was proposed to be due to interactions between a hydrophobic face of S4 and the neighbouring subunit's S5, which is consistent with the crystal structure of K_v1.2 (28,35).

1.3.4 Characteristics of K_v channels

A brief description of the electrophysiological properties of K_v channels studied in the present Doctoral Thesis is given in this section.

1.3.4.1 K_v1.3 channels

K_v1.3 channel was first cloned in rat and mouse brain, where it was named RCK3 (52), KV3 (53) or RGK5 (54) and MK3 (55) respectively. In addition, this channel was also cloned from mouse (56), rat (57) and finally from human T lymphocytes and was identified as HLK3, HGK5 (57,58). The channel gating characteristics and the distinctive pharmacological profile provided unique biophysical fingerprint that enabled to identify all these clones as K_v1.3 with the standardized nomenclature. K_v1.3 channels expressed in olfactory bulb neurons are involved in the mechanism of signal transduction (59,60). These proteins also participate in the translocation of the glucose transporters, GLUT4, to the plasma membrane in adipocytes, suggesting that ion channels are important in insulin sensitivity (59,61,62). In the immune response, K_v1.3 channels play a crucial role in the regulation of the resting potential and calcium signaling and thus, in the activation of T lymphocytes and macrophages (63-67). In the presence of lipopolysaccharide (LPS), protein levels of these channels increase

(63,68,69). K_v1.3 selective blockers have been used in the treatment of autoimmune diseases. The activation threshold for K_v1.3 channels is ~ -50 mV, and the midpoint for the activation curve is ~ -33 mV. K_v1.3 current activates with an exponential time course (τ_{act} <10 ms). After depolarization to + 60 mV, the current reaches the maximum peak amplitude and then, C-type inactivation proceeds with a time constant of ~200–400 ms (Figure 5 top panel) (70,71). C-type inactivation occurs by a conformational change at the external side of the channel pore (60,72-74), and results in use-dependent or cumulative inactivation during repeated episodes of depolarization (Figure 5 low panel) (73,75). Interaction studies between K_v1.3 and auxiliary β subunits are scarce. It was shown that T lymphocytes, in which K_v1.3 channels are the major contributors to K_v current, K_vβ1.1 and K_vβ2.1 are also expressed (76). The expression of these modulator subunits is also increased after stimulating lymphocyte with proliferative cytokine interleukin 2 (IL2). Also, all splice variants of the K_vβ1.1 gene (K_vβ1.1, K_vβ1.2, and K_vβ1.3) were detected in these cells, as well as the only K_vβ2 gene product described to date (K_vβ2.1) (77). This study suggested that differential K_vβ expression modifies the electrical properties of K_v current in macrophages, and that this modulation is dependent on proliferation and the mode of activation of immune cells. K_v1.3 channel has different target sequences susceptible to be phosphorilated by protein kinase C (PKC). However, several reports demonstrated that phosphorylation at these positions did not modify the physiological current properties (78,79). It has been described that K_v1.3 channels are regulated by PKA in human T lymphocytes, being this effect mediated by LcK and Dlg1 (78,80). Blockers of K_v1.3 channels belong to two large classes: peptide toxins and small molecule blockers. K_v1.3 blocking toxins from scorpions, sea anemones or other animals such as charybdotoxin and margatoxin carry a large positive net charge and consequently are impermeant through cell membranes. Peptide toxins utilize a “cork in the bottle” blocking strategy, covering and plugging the external end of the channel pore, thereby preventing the efflux of K^+ ions (81-83). In contrast, small molecule blockers including correolide are hydrophobic and thus, easily permeate through cell membranes. They bind from the intracellular side to the internal end of the selectivity filter. Due to their smaller size, these molecules have fewer contact points with the channel than peptide toxins, which generally results in lower affinity and poorer selectivity (84-86). A notable exception to the typical small molecule behaviour is the membrane impermeant K^+ channel blocker tetraethylammonium (TEA), which is capable of blocking the channel from both sides.

1.3.4.2 K_v1.5 channels

K_v1.5 channel was first cloned from human ventricle (87) and then from atrium (88). It is highly homologous with the *Shaker* K^+ channel in *Drosophila* (5). In the heart, K_v1.5 channels generate the I_{Kur} current. Despite mRNA and protein expression of K_v1.5 in both atria and ventricles (89), I_{Kur} is confined to atrial myocytes and virtually absent in ventricular myocytes of most species. K_v1.5 channels are also expressed in many other organs, including pulmonary arteries (90), skeletal muscle (91), rat brain (53), and immune cells (92). K_v1.5 are also involved in the maintenance of vascular smooth muscle tone, glucose-stimulated insulin release by β-

pancreatic cell, cell volume regulation and cell growth (15). Heterologous expression of $K_v1.5$ results in a robust outward current with a midpoint for activation potential of ~0 mV (Figure 5). At room temperature, current activates rapidly at potentials between 0 and +60 mV (τ_{act} <10 ms) and inactivates only partially, i.e. by 10-20% after 250 ms at +60 mV. Inactivation follows a bi-exponential time course with time constants of ~240 and 2700 ms (93,94). $K_v1.5$ channels display outward rectification and very slow inactivation during strong depolarizations (Figure 5). Inactivation is temperature dependent and accelerates at more physiological temperature (95-97). The electrophysiological properties of $K_v1.5$ are modified by the assembly of $K_v\beta$ subunits ($K_v\beta1.2$, $K_v\beta1.3$, and $K_v\beta2.1$) (98,99). The $K_v\beta1.3$ subunit provides a number of functions, including a fast and partial inactivation

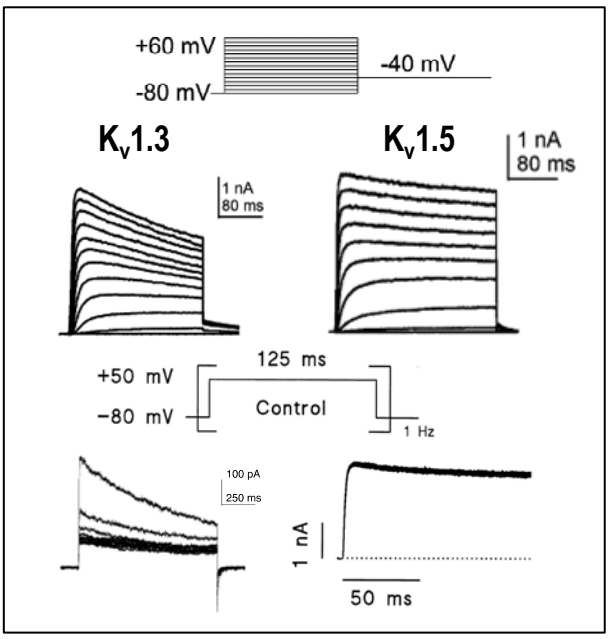

Figure 5: Electrophysiological characteristics of $K_v1.3$ and $K_v1.5$ channels. Top panel shows $K_v1.3$ and $K_v1.5$ current traces recorded using the protocol shown on the top in *Ltk*$^-$ and HEK293 heterologous expression systems. Adapted from Tang et al 2007 (70) and Macias et al 2010 (92) respectively). At the end of the depolarizing pulse, the degree of inactivation is greater for $K_v1.3$ channels Bottom panel shows the use dependence of $K_v1.5$ and $K_v1.3$ channels after applying a train of depolarizing pulses at 1 Hz. Adapted from Fadool et al 2004 (59) and Valenzuela et al 1996 (93) Respectively. The different electrophysiological properties of these channels allow to differentiate the composition of K_v channels in the cell membrane when various types of K^+ channels are expressed.

component, that is mediated by an equilibrium binding of the N-terminus of $K_v\beta1.3$ between PIPs and the inner pore region of the channel which overlaps with the Kvβ1.3 binding site (100), a greater degree of slow inactivation, a shift of the activation curve toward more negative potentials, a 7-fold decrease in the sensitivity of the channel to the block induced by antiarrhythmic drugs and local anaesthetics, and a decrease in the degree of stereoselective blockade (100-104). In addition, interaction of $K_v\beta$ subunits with $K_v1.5$ controls channel trafficking to the plasma membrane. Although the major groups of ancillary subunits that associate with $K_v1.5$ channels are $K_v\beta$ subunits, KChIP2 also modifies channel properties (105). $K_v1.5$ channels are highly susceptible to adrenergic regulation, which is differentially modulated by α and β stimulation (106) via PKC and protein kinase A (PKA), respectively (107-109). PKC and PKA activities are also required for the $K_v1.5$ modulation by the auxiliary subunits $K_v\beta1.2$ and $K_v\beta1.3$. (107,108,110). Moreover, it has been described that in rat ventricle, $K_v1.5$ associates with $K_v\beta1.3$, various PKC isoforms and other proteins forming a “channelosome” which is a novel mechanism for signal transduction (111). Channels are also regulated by nitric oxide (NO) via a cyclic guanosine monophosphate/Protein kinase G (cGMP/PKG) dependent pathway. NO donors decrease $K_v1.5$ in an expression system (112). Based on molecular modelling, these authors showed that S-nitrosylation of two cystein residues in S2 (Cys331 and Cys 346) are involved in this effect. The current is sensitive to most class I

antiarrhythmic drugs and local anesthetics (94,113-116), to low concentrations of 4-aminopyridine (4-AP), but is rather insensitive to (TEA) (97)or dendrodotoxin (117). Most of these compounds are open channel blockers that bind to a common internal receptor site at $K_v1.5$ channels.

1.3.4.3 $K_v7.1$ channels

The *KCNQ1* gene was first identified by Wang and colleagues (118) in a linkage study of patients with long QT interval syndrome type 1. Its gene product, $K_v7.1$ (also termed K_vLQT1 or KCNQ1), is a voltage-gated K^+ channel α-subunit, and its expression was detected in several mammalian tissues, including heart, epithelia, lung, stomach, adrenal and thyroid glands, kidney, pancreas, small intestine and inner ear (119,120). The other four K_v7 channels ($K_v7.2$-7.5) from the K_v7 family are highly expressed in the central and peripheral nervous system. K_v7 channels exhibit, as a distinctive feature, a C-terminal domain much longer than that of other K_v channels,. It contains several structural motifs including coiled-coils, calmodulin-binding structures, and basic aminoacid clusters, which are critical for K_v7 assembly and trafficking, and also gating (Figure 6B). $K_v7.1$ channels expressed in heterologous systems generate a classical delayed rectifier potassium-selective channel with fast activation kinetics (τ_{act} <100 ms at +60 mV) and relatively slow deactivation. The midpoint for the activation curve of $K_v7.1$ channels is ~ -23 mV. Upon long depolarizing steps, a fraction of $K_v7.1$ channels undergo partial inactivation (121-123). The inactivated current component can be visualized upon repolarization as a hook on the current trace, since the $K_v7.1$ channel has to go to the open state from the inactivated one before it closes (deactivates) (Figure 6A top). This inactivation property of $K_v7.1$ channels is determined by the S5 transmembrane domain and the P-loop, and changes of just a single residue in this area can abolish the inactivation (124,125). $K_v7.1$ channels have a small single-channel conductance ranging from 2 to 8 pS, depending on the composition of the intra- and extracellular recording solution (121,126-128). $K_v7.1$ channels are selectively blocked by chromanol 293B (129), azilamide (130) and I_{Ks}124 (131), but almost insensitive to TEA (132) and 4A-P (133). The extensive versatility of $K_v7.1$ channel function is widely due to the channel ability to interact with ancillary subunits from the KCNE family. $K_v7.1$ channels associate with all five members of the KCNE β-subunit family to fulfil a variety of physiological functions.

The cardiac repolarizing potassium current, consists of two major components, the rapid delayed rectifier potassium current (I_{Kr}) and the slow delayed rectifier potassium current (I_{Ks}) (134). $K_v7.1$ co-assembles with the KCNE1 beta subunit to form the channel complex that mediates I_{Ks} (135,136). Although KCNE1 is the major accessory subunit assembling with $K_v7.1$ in the heart, other subunits of the KCNE family might be present (137), serving as additional regulators of I_{Ks} (138). The significance of $K_v7.1$ and its accessory beta subunits for maintaining normal rhythmicity is further emphasized by the numerous $K_v7.1$ and KCNE mutations associated with cardiac arrhythmias. Some of these mutations can lead to a loss of channel function causing long QT syndrome, a disorder predisposing affected individuals to Torsade de Pointes arrhythmia and sudden cardiac death (SCD). The presence of KCNE1 drastically modifies $K_v7.1$ activity by increasing unitary conductance as well as macroscopic currents, slowing activation, right-shifting voltage dependence of activation, suppressing

currents at low activating voltages, suppressing partial inactivation, and modulating its pharmacology (121,124,125,127,135,136,139-145). K_v7.1/KCNE1 complexes open at potentials positive to -20 mV and give rise to currents with very slow activation kinetics (Figure 6A bottom). The increased current level compared with that of homomeric K_v7.1 channels is caused both by an increase in the single-channel conductance

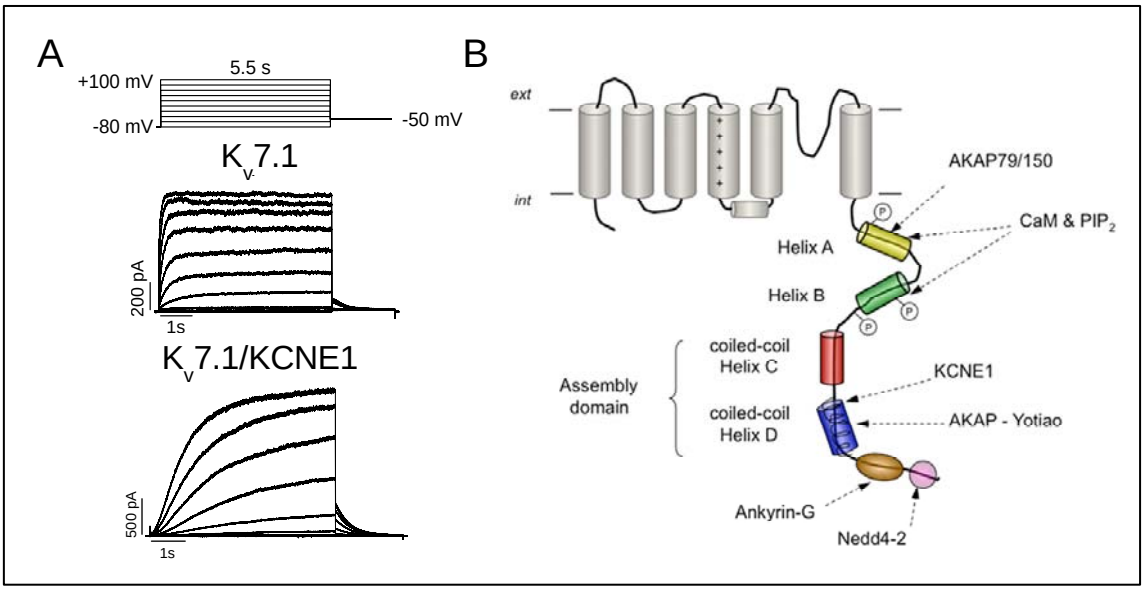

Figure 6. Electrophysiological characteristic of K_v7.1 and K_v7.1/KCNE1 channels and schematic representation of the C-terminus tail structures of K_v7 channels. Left panel **(A)** shows K_v7.1 and K_v7.1/KNCE1 current traces recorded using the protocol shown on the top expressed in COS7 cells **(B).** The four helical regions (helices A–D) are shown as cylinders. Formation of coiled-coil assemblies at the level of helices C and D is indicated. The proposed location of the conserved interaction sites with calmodulin (CaM) and phosphatidylinositol 4,5-bisphosphate (PIP_2), with A-kinase anchoring protein 79/150 (AKAP79/150) in K_v7.2, with the auxiliary β subunit KCNE1 in K_v7.1, with AKAP-Yotiao in K_v7.1, with ankyrin-G in K_v7.2–K_v7.3 and with ubiquitin-protein ligase Nedd4-2 in K_v7.1 and K_v7.2–K_v7.3, are also shown. Phosphorylation sites by Src kinase in helix A and by protein kinase C in helix B are indicated by an encircled P. Adapted from Barros and de la Peña 2012 (19).

(121,127,128) and by a loss of the inactivation state. Seebohm and colleagues (124) found that co-expression of KCNE1 stabilizes the open conformation of the K_v7.1 pore by altering an interaction between the pore helix, the selectivity filter, and the S5-P-S6 domain.

It is known for many years that the cardiac I_{Ks} is upregulated following sympathetic stimulation (146). This upregulation of the K_v7.1/KCNE1 current is mediated by β-adrenergic receptor activation, leading to an increased level of cyclic adenosine monophosphate (cAMP) and thereby PKA stimulation, which interacts with the I_{Ks} complex through an A-kinase anchoring protein 9 (AKAP9) (Figure 6B) (147). Kass and co-workers showed that PKA and protein phosphatase 1 interact with K_v7.1 through the AKAP9, called yotiao, which binds to the C-terminus tail of K_v7.1 via a leucine zipper motif (148). Upon PKA activation, residue S27 in the N-terminus of K_v7 is phosphorylated. However, yotiao seems not only to be important for mediating the phosphorylation of S27, but it is also necessary to transform the phosphorylated K_v7.1 subunit into a channel with altered activity (149). The cAMP-mediated regulation of K_v7.1 channels in mammalian expression systems is dependent on co-expression of KCNE1 and, indeed, mutations described in both K_v7.1 and KCNE1 identified in long QT syndrome patients have been found to disrupt this regulation (148,149). PIP_2 is another key

intracellular regulator of the K_v7.1/KCNE1 channel activity (150). PIP_2 affects the K_v7.1/KCNE1 channel by stabilizing the open state, resulting in increased amplitude, which can be sustained if Mg-ATP is present. Furthermore, PIP_2 slows the deactivation kinetics and shifts the activation curve. The importance of this interaction, occurring primarily with residues in the very proximal C-terminus, is emphasized by the fact that reduced PIP_2 affinity of K_v7.1 mutants found in long QT syndrome patients may underlie this pathology (151).

1.4 INWARD RECTIFYING POTASSIUM CHANNELS

Since the initial cDNA cloning of the first inward rectifiers K_{ir}1.1 (ROMK1) and K_{ir}2.1 (IRK1) in 1993 (152,153), a succession of new members of this family have been discovered. To date, around twenty members, including the G protein-coupled K_{ir}3 and the ATP-sensitive K_{ir}6 of this superfamily have been cloned. K_{ir} channels can be grouped into seven families by sequence similarity, and designated K_{ir}1-7 (154,155). These channels play an important physiological role in the function of many organs, including brain, heart, kidney, endocrine cells, ears, retina, and immune cells, such as T lymphocytes and macrophages (156).

The N- and C- terminus of K_{ir} subunits are exposed to the cytoplasm and associate with each other to form a cytoplasmic domain that is linked to, but distinct from the transmembrane domain. The transmembrane domain is mainly responsible for ion selectivity and gating. The cytoplasmic domain is thought to act as a gating modulator (156). Like K_v channels, K_{ir} channels exhibit the K^+ channel signature (TXGY(F)G) that constitutes the selectivity filter in the transmembrane domain. The four groups of associated N- and C-terminus make up a cylinder that surrounds the so called cytoplasmic pore. This architecture is a characteristic of the K_{ir} channels and extend the ion conduction pathway by ~30 Å. Therefore, in K_{ir} channels, K^+ has to pass over 60 Å through the pore composed by the cytoplasmic and transmembrane domain (Figure 7A).

A brief description of the electrophysiological properties of the K_{ir} channel studied in the present Doctoral Thesis is given in the following section.

1.4.1 K_{ir}2.1 channels

K_{ir}2 is the principal class of 2TM/1P domain potassium channels. The first member of this family to be cloned was from a mouse macrophage cell line and named IRK1/K_{ir}2.1/KCNJ2 (153). Immunolocalization studies have revealed it to be present on many cell types within the forebrain, including neurones, microglia, endothelial, heart, ependymal and vascular smooth muscle cells (153,157,158). Cloned K_{ir} 2 channel cDNAs encode proteins of 370-500 residues. K_{ir}2.1 channel alpha subunits possess only 2TM domains linked with a P-domain. Thus, K_{ir}2.1 channels share similarity with the fifth and sixth domains, and P-loop of the other families. Initially, K_{ir}2.1 subunits were thought to be made up of only homomeric complexes (159). However, recent studies have revealed that K_{ir}2.1 subunits can function as heterotetramers both *in vitro* and *in vivo*. Indeed, *in vitro* electrophysiological experiments have shown that K_{ir}2.1, K_{ir}2.2, and K_{ir}2.3 can assemble with any one of the

other subunits, and the respective heteromer exhibits different properties from that of their homomers (160). The channels of this family are constitutively active and exhibit strong inward rectification (which is described as the ability to allow large inward currents and smaller outward currents) (Figure 7B) (161). Inward rectification is

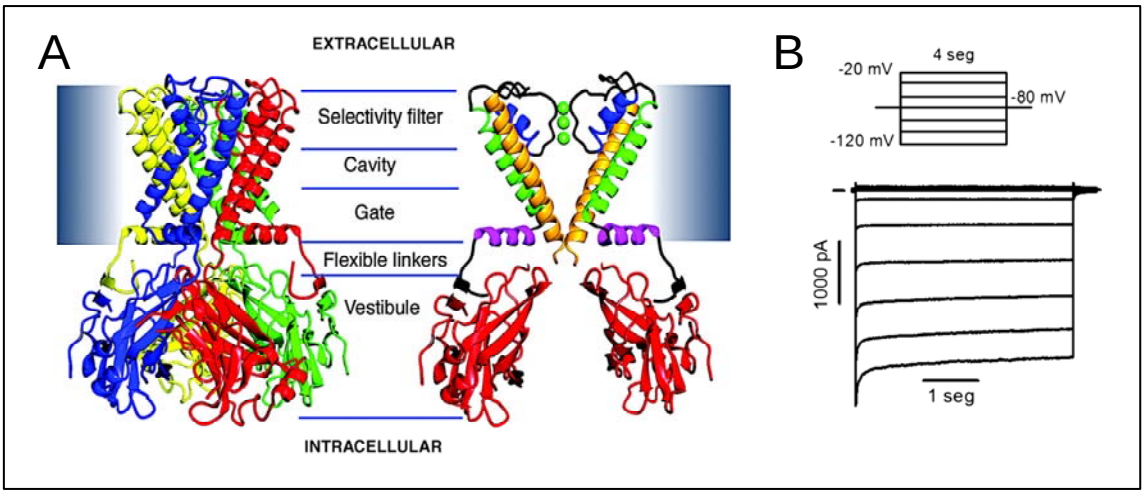

Figure 7. Crystal structure of the bacterial K_{ir}Bac1.1 channel and electrophysiological characteristics of K_{ir}2.1. **(A)** The blue bar represents the position of the lipid membrane. On the right, the main secondary structural elements that make up the channel are highlighted: slide helix (purple), outer helix (green) pore helix (blue), inner helix (yellow), C-terminus domain (red) Taken from Kuo et al 2003 (35). **(B)** Typical K_{ir}2.1 currents recorded using the protocol shown on the top after heterologous expression in HEK293 cells. Adapted from Lopez-Izquierdo 2010 (161).

caused by intracellular Mg^{2+} (162,163) and polyamines (164). Polyamines block the channel pore when the membrane potential is more depolarized than the E_K (164). K_{ir} channels are responsible for regulating diverse processes including: cellular excitability in heart and brain tissue, vascular tone, heart rate, renal salt flow, and insulin release (165). They contribute to the establishment of highly negative resting membrane potential and long-lasting action potential plateau in various cells types including cardiac myocytes. K_{ir}2.x channels are activated by PIPs that are essential for the normal function of the channel (1,166,167). K_{ir}2.1 current is increased by cAMP when the channel is co-expressed with AKAP79 and treated with phosphatase inhibitors (168). In addition, it has been suggested that phosphorylation or pH might modulate channel function by affecting channel PIP_2 interaction (1,169,170). K_{ir} 2.1 is blocked by barium (171), cesium (172) and it is almost insensitive to TEA and 4-AP (173,174).

1.5 PHYSIOLOGICAL ROLES OF K_v CHANNELS

1.5.1 The cardiac action potential

The normal behaviour of the heart is determined by the ordered propagation of excitatory stimuli resulting in rapid depolarization and slow repolarization, generating action potentials (AP) in individual myocytes. At the most generic level, abnormalities of impulse generation, propagation, duration and configuration of individual cardiac APs form the basis of disordered cardiac rhythm. These concepts evolved during the twentieth century from clinical descriptions of arrhythmia, to descriptions of AP in specific regions of cardiac tissue, and

then to identification of specific whole-cell and single-channel ionic currents whose integrated activity generates these APs. In the past decades, cloning efforts have defined genes whose expression generates specific molecular components, including ion channel proteins underlying individual ion currents in cardiac myocytes. K^+ currents control the repolarization process of the cardiac AP, determine membrane potential, heart rates and refractoriness of the myocardium and are important targets for the actions of neurotransmitters, hormones, drugs and toxins known to modulate cardiac function (12,175-177).

The AP of a cardiac myocyte exhibits five distinct phases (Figure 8): phase 0 corresponds to the rapid depolarization (or AP upstroke) that ensures the cell reaches the voltage threshold. Phase 1 corresponds to the brief, rapid repolarization that is initiated at the end of the AP upstroke and that is interrupted when the cell

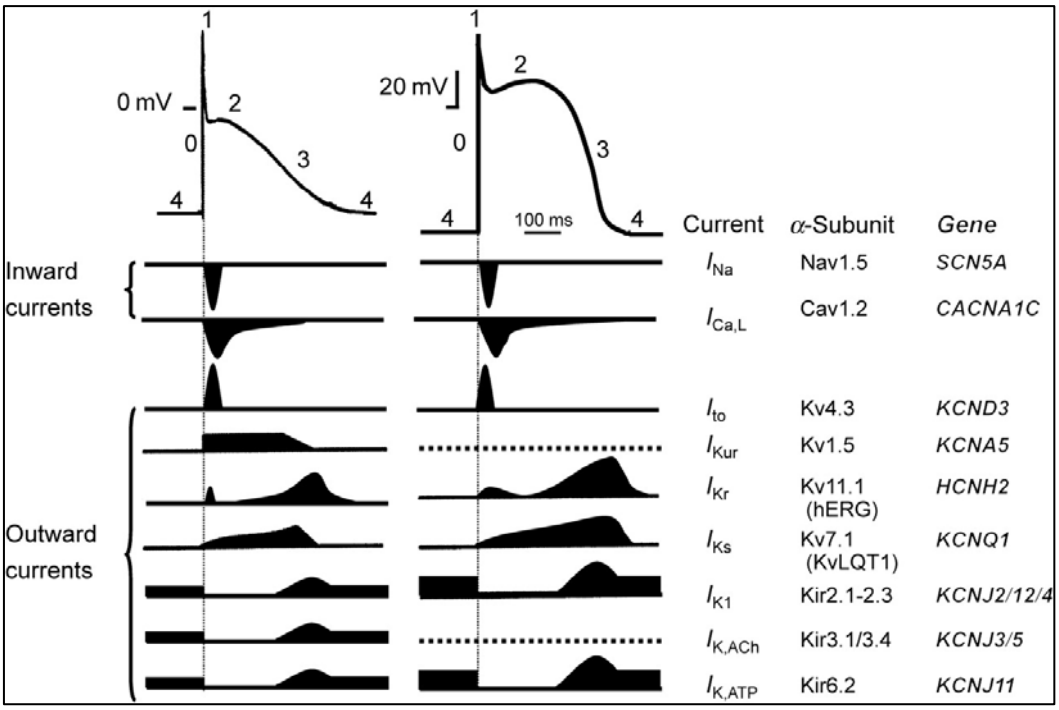

Figure 8. Inward depolarizing and outward repolarizing currents that underlie the atrial and ventricular action potential. Inward currents: I_{Na} sodium current; $I_{Ca,L}$ L-type calcium current; I_{to} transient outward current; I_{Kur} ultra rapidly activating delayed rectifier current; I_{Kr} and I_{Ks} rapidly and slowly activating delayed rectifier current; I_{K1} inward rectifier current; $I_{K,ACh}$ acetylcholine-activated potassium current. Note that I_{Kur} is present in atria only. Phase 0, rapid depolarization; phase 1, rapid early repolarization phase; phase 2, slow repolarization phase ('plateau' phase); phase 3, rapid late repolarization phase; phase 4, resting membrane potential. Adapted from Ravens and Cerbai 2008 (177).

reaches the "plateau level" or phase 2. During the plateau, repolarization progresses slowly; but eventually a phase of rapid repolarization, or phase 3, ensures it. Finally, phase 4 is the period between the last repolarization and the onset of the subsequent AP. It corresponds to the resting membrane potential

*Phase 0: Action potential upstroke***.** At rest, the dominant membrane conductance is provided by the potassium channels. However, once the cell reaches a threshold level of approximately −65 mV, membrane sodium channels open. Hence, at threshold, the membrane rapidly switches from being mostly permeable to K^+ to being largely permeable to Na^+. The sodium current (I_{Na}) represents a very large and rapid transition. When the conductance to sodium suddenly increases, the large transmembrane gradient of Na^+ leads to a rush of ions into the cell in the form of an inwardly directed negative sodium current (I_{Na}). Thus, the membrane rapidly

becomes less negative; i.e., it depolarizes, and results in the upstroke, or phase 0 of the action potential. In fact, given that during phase 0 the cell is mostly permeable to Na^+, the membrane potential becomes transiently positive as it moves toward E_{Na} (approximately +40 mV). However, the increase in sodium conductance is very brief. After a few milliseconds, the sodium channels enter a nonconductive state. The membrane potential does not quite reach the sodium equilibrium potential, but stops at approximately +20 mV and then begins to repolarize.

*Phase 1: Rapid repolarization***.** As shown in Figure 8, for the most part, the end of the action potential upstroke is brought about by the inactivation of the sodium channels. During the initial phase of repolarization of the AP, potassium channels provide the dominant membrane conductance. Depending on the cardiac region, and also the specie, there can be important differences in the ionic currents that are activated at this stage, depending on the region of the heart from which the cells originate (and also depending on the animal species studied), in most cases the so-called "transient outward current" (I_{to}) provides most of the repolarizing charge. This rapidly activating potassium conductance turns on during the action potential upstroke. When the sodium channels enter their nonconductive state, repolarization begins in earnest, with the membrane potential heading toward the reversal potential for potassium. I_{to} inactivates also very rapidly, and its contribution to the repolarizing process during phases 2 and 3 of the action potential is smaller than that observed during phase 1.

Phase 2: Action Potential Plateau. Other voltage dependent membrane channels are also activated by cell depolarization, although at a slower rate. Consequently, these channels provide a sizable current only several milliseconds after the end of the action potential upstroke. The two dominant currents during the plateau phase of the action potential, or phase 2, are the inward calcium current (I_{Ca}) (including, the L-type calcium current and electrogenic sodium–calcium exchanger), and the delayed rectifier potassium outward current (I_K),. The potassium current I_K includes at least two separate components: a rapid component (I_{Kr}) and a slow component (I_{Ks}). In addition, in atrial myocytes the ultrarapidly delayed rectifying potassium current (I_{Kur}) also contributes to the repolarization of the AP. Given the concentration gradient for Ca^{2+}, opening of calcium channels leads to movement of calcium from the extracellular to the intracellular space (i.e., an inwardly directed, depolarizing current). Potassium ions, on the other hand, move in the opposite direction. The end result is that, while the calcium channels remain open, repolarization by potassium currents is prevented by the presence of calcium current that is moving positive charges into the cell. Thus, during the plateau, the membrane potential depends on the balance between inward I_{Ca} and outward I_K currents. Although in some cells (e.g., Purkinje fibers) outward currents dominate and the plateau tends to have a consistently negative slope, in other cells there may be an actual slight depolarization before repolarization continues (in a "dome like" shape).

Phase 3: Final Repolarization. Inactivation of the calcium channels leads to the end of the plateau (Figure 8). Only potassium channels remain active; consequently, the membrane potential returns relatively rapidly toward E_K. The delayed rectifier currents (I_{Kr} and I_{Ks}) tend to close as the cell repolarizes, and thus the inward rectifier current (I_{K1}) predominates.

Phase 4: Diastolic Potential. In muscle cells, the resting potential remains constant throughout the diastolic interval. In these cell types, the inward-rectifier current I_{K1} remains the dominant conductance at rest

and it is largely responsible for setting the resting membrane potential. An additional small background conductance, with a more positive equilibrium potential, keeps the resting potential slightly more depolarized than the value estimated by the potassium equilibrium potential. Atrial and ventricular myocytes remain at this level of potential until a new excitatory stimulus brings the membrane potential to threshold, thus eliciting a new active response.

1.5.1.1 Channelopathies: The short QT syndrome

In approximately 10–20% of all sudden deaths, no structural cardiac abnormalities can be identified. Important potential causes of sudden cardiac deaths in the absence of heart disease are primary electrical diseases. Mutations involving cardiac ion channels result in abnormal AP formation or propagation, leading to cardiac arrhythmias. In recent years, major advances have been made in the understanding of the molecular substrates of inherited arrhythmogenic diseases. With the contribution of molecular genetics and electrophysiological studies, the genetic basis of numerous cardiac diseases such as the long QT syndrome, the Brugada syndrome, catecholaminergic polymorphic ventricular tachycardia, and familial atrial fibrillation have been established (178-180)

The short QT syndrome is a cardiac channelopathy associated with a predisposition to atrial fibrillation and SCD. The arrhythmogenic potential of a short QT interval was first suggested by Gussak and colleagues (181) in 2000 when they reported an isolated case of sudden cardiac death in a young female, and the presence of early onset atrial fibrillation in a separate family. Cardiac workup in both instances revealed structurally normal hearts. However, electrocardiography (ECG) was notable for markedly abbreviated QT intervals ranging from 260 to 280 ms (Bazett corrected QT interval, (QTc), values ranging from 248 to 300 ms) in affected subjects. Similar findings were reported few years later in a detailed description of 2 unrelated families with short QT intervals who suffered from a high incidence of sudden cardiac death in the absence of structural heart disease (182). These initial reports led to the recognition of short QT syndrome as a distinct clinical entity and have been followed by numerous additional case reports within the past decade that have furthered our insight into this condition. To date, 3 separate genes encoding ion channels present in the cardiomyocyte cell membrane have been implicated in the pathogenesis of short QT syndrome, and further genetic culprits are suspected (183-185). short QT1 syndrome is caused by gain of function of the $K_v11.1$ channels (I_{Kr}). short QT2 is caused by gain of function mutations in the *KCNQ1* gene encoding the α subunit of the $K_v7.1$ channel (I_{Ks}) A gain of function in the *KCNJ2* gene encoding for the inwardly rectifying channel protein $K_{ir}2.1$ is associated with an accelerated repolarizarion process. This short QT is classified it as short QT type 3. The mutations linked to the three forms of short QT shorten the AP duration. However, a variation in the T-wave phenotype distinguishes the different mutations because of the dissimilar time dependence and voltage rates at which I_{Kr}, I_{Ks} and I_{K1} operate. In short QT1 and short QT2 syndrome, significant action potential duration abbreviation starts at the level of the plateau, but the overall morphology of the action potential remains unchanged (185).

Until date, three mutations associated with short QT2 have been found; two in the S1 S140G (186), V141M (187) and another one in the P-loop of $K_v7.1$ V307L (184). Functional studies revealed that S140G and

V141M mutations resulted in a constitutively activated channel. V307L $K_v7.1$ exhibited a pronounced shift of the half-activation potential and an acceleration of the activation kinetics leading to a gain of function in I_{Ks}.

The diagnostic hallmark of the condition is a short ECG QT interval; however, consensus on an appropriate cutoff value and diagnostic criteria sufficient to establish a diagnosis of short QT syndrome are still emerging. In fact Gollob and colleagues systematically reviewed the literature for reported cases of short QT syndrome to develop diagnostic criteria designed to facilitate accurate clinical recognition of the disorder (188).

1.5.1.2 Role of n-3 PUFAs on the cardiovascular function: modulation of cardiac ion channels

Omega-3 (n-3) polyunsaturated fatty acids (PUFAs) are essential nutrients that must be acquired from the diet and that are required for normal development and cellular function. n-3 PUFAs are derived from two sources. Plant derived n-3 PUFAs such as α-linolenic acid (ALA) [(18:3 n-3)] is found in vegetable oils (such as flaxseed, canola, and soy bean oils) and walnuts. Marine n-3 PUFAs include eicosapentaenoic acid (EPA) [20:5(n-3)] and docosahexaenoic acid (DHA) [22:6(n-3)], and they are found in oily fish and seafood. After the industrial revolution, the dramatic increase in the n-6/n-3 ratio in the diet of the populations of Western countries has, at least in part, contributed to the rise in cardiovascular disease (CVD) (189,190). Sinclair et al. described the rarity of CVD in Greenland Inuits, who consumed a diet rich in n-3 PUFAs (whale, seal, and fish; (191,192)). Since that time, a large amount of evidence from cellular and animal studies (193-195), and from clinical trial outcomes (196-199) has suggested that an increased intake of fish oil fatty acids has favourable effects on cardiovascular health. Analyses of these trials have concluded that these beneficial effects mainly occur through the prevention of SCD, which is often preceded by ventricular arrhythmias, indicating that n-3 PUFAs are antiarrhythmic (197,200). However, not all studies have demonstrated the cardioprotective effects on CVD of PUFAs consumption. Pro-arrhythmic actions have been described for n-3 PUFAs in animal models during acute regional myocardial ischemia (201). Moreover, the recent Alpha OMEGA and OMEGA randomized trials, involving patients who had suffered a myocardial infarction, did not show any improvement in the clinical results following n-3 PUFAs supplementation (202,203), and even a deleterious effect due to an increased risk of cardiac death was reported in men with stable angina (without myocardial infarction) who were advised to eat fish (204), or in patients with implantable cardioverter defibrillators. (205). These differences could be explained by the fact that a diet rich in fish oil could be pro- or anti-arrhythmic depending on the underlying arrhythmogenic mechanism. In any case, the mechanism underlying the pro- or anti-arrhythmic effect after n-3 supplementation is thought to be related to the modulation of the cardiac ion channels involved in the genesis and/or maintenance of cardiac APs. n-3 PUFAs inhibit I_{Na}, I_{Kur}, I_{to}, I_{Kr}, I_{Ca}, and I_{NCX}, and enhanced I_{Ks} and I_{K1} (206-214).

Regarding the effects of n-3 PUFAs on I_{Ks}, Doolan and colleagues (209) demonstrated that acute EPA and DHA do not modify the electrophysiological characteristics of $K_v7.1$ channels. On the contrary, these authors observed that DHA, but not EPA, increases the magnitude of the I_{Ks} generated after activation $K_v7.1$/KCNE1 channels expressed in *Xenopus* oocytes, and that this effect is mediated by the interaction between DHA and

the KCNE1 subunit (209). Another study performed in cardiac myocytes obtained from pigs fed with a diet rich in n-3 PUFAs, demonstrated that chronic PUFAs also increases I_{Ks} (213). However, the precise molecular mechanism by which n-3 PUFAs exert their actions on this and other cardiac ion currents remained to be elucidated.

1.5.2 Role of K_V currents in the immune response

Inflammation is a defensive response to trauma or microbial invasions. This response is designed to remove the inciting stimulus and resolve tissue damage. On the contrary, excessive inflammatory responses can cause local tissue damage and remodeling, which may lead to significant and chronic injury. Therefore, acute inflammation in healthy individuals is self-limiting and has an active termination program. Recent studies have suggested that low-grade systemic inflammation is one of the characteristics features of obesity, diabetes mellitus, cancer, Alzheimer's disease and several cardiovascular pathologies, such as atherosclerosis, atrial fibrillation, myocardial infarction or heart failure, implying that prevention or suppression of inflammation decrease the burden of these diseases (215-226).

Acute inflammatory reaction in response to infection or tissue damage is characterized by the classic cardinal signs of inflammation (heat, redness, swelling and pain), and in experimental settings *in vivo* the temporal relationships are well established, e.g. edema and the accumulation of leukocytes, specifically polymorphonuclear leukocytes, followed by monocytes and macrophages. These events in self-limited or resolving inflammatory reactions are coupled with release of local factors that prevent further or excessive trafficking of leukocytes allowing for resolution (227-229). Early in the inflammatory response, pro-inflammatory mediators such as prostaglandins and leukotrienes play an important role (230). The progression from acute to chronic inflammation is commonly viewed as an excess of pro-inflammatory mediators. Although mononuclear cells can sometimes contribute to pro-inflammatory responses, they are also critical in wound healing, tissue repair and remodeling (231). Thus, it is highly plausible that defects associated with mounting endogenous proresolving circuits and local autacoids could underlie some of the pathologic events in chronic inflammation. The complete resolution of an acute inflammatory response and the return of the local tissues to homeostasis are necessary for ongoing health.

Macrophages play an important role in the inflammatory response, acting as professional antigen-presenting cells and modifying the cytokine milieu and the intensity of T-cell signaling. Therefore, macrophages may tune the immune response toward inflammation or tolerance (232,233). The proliferation, activation, and resolution or tolerance of immune cells is mainly modulated by membrane transduction of extracellular signals. Some of these interactions involve changes in transmembrane ion fluxes that, in turn, modulate the network of intracellular signaling (i.e. Ca^{2+} fluxes (234)). The electrophysiological properties of macrophages change depending on their state of functional activation (67). Indeed, changes in membrane potential that occur as a consequence of the modulation of ion channels are among the earliest events in macrophage activation (235,236). Macrophages can undergo different activation processes depending on the stimuli received

(232,237,238). The classic and innate activations, which can be induced by *in vitro* culture of macrophages with interferon gamma (IFN-γ) plus LPS, are associated with high microbicidal activity, proinflammatory cytokine, reactive oxygen and nitrogen species production and cellular immunity. The alternative activation, which can be mimicked *in vitro* after culture with IL-4, IL-13, glucocorticoids, immune complexes, or IL-10, is associated with phagocytosis, tissue repair, tumour progression and humoral immunity (239,240).

Consistent data indicate that ion channels play a pivotal role in the regulation of macrophage immunomodulatory responses. Ion channels are tightly regulated during proliferation and activation in macrophages, and their functional activity is important for cellular responses (63,67,69). The first ion channel described in T lymphocytes and macrophages was the voltage-gated $K_v1.3$ potassium channel, which has a key role in the activation pathway and seems to be the most important target to control T cell and macrophage activation (65,66). Together with $K_v1.3$, $K_v1.5$ and $K_{ir}2.1$ channels are also expressed in the plasma membrane of immune cells and are involved in the maintenance of the membrane potential (Figure 9) (241). The opening of $K_v1.3$ and $K_v1.5$ channels at voltages exceeding their activation threshold creates a K^+ efflux that would increase the driving force for calcium influx. Due to the very high electrical resistance of the lymphocyte membrane, the opening of a few of these channels is sufficient to regulate the membrane potential (Figure 9). Besides potassium channels, Ca^{2+} release activated Ca^{2+} channels (CRAC) are also expressed in the immune cells. Two proteins, named Orai1 and STIM1 are necessary to generate CRAC current. Orai1 is the pore forming subunit of the channel, while STIM1 is the sensor of Ca^{2+} depletion in the endoplasmic reticulum (ER) lumen (242-245). STIM1 is found in the ER membrane with an EF-hand in the ER lumen, while Orai1 is located in the plasma membrane mostly as a dimmer (246). Upon store emptying STIM1 senses the drop in Ca^{2+} concentration and relocalizes to puncta closely associated with the plasma membrane. This translocation brings Orai1 dimmers together to form tetrameric active CRAC channels that allow the influx of Ca^{2+}. The concerted action of the two K^+ channels and the CRAC channel achieves a precisely controlled and long lasting Ca^{2+} signal that is required for the execution of the activation pathway. CRAC channels provide the entry route for Ca^{2+} while tightly regulated K^+ efflux maintains a permissive membrane potential for the prolonged Ca^{2+} influx (Figure 9).

The other plasma membrane potassium channel of immune cells is the Ca^{2+} activated $K_{Ca}3.1$ (formerly called $I_{KCa}1$, for intermediate conductance Ca^{2+} activated K^+ channel), which is activated when the free intracellular Ca^{2+} concentration rises above about 200 nM (247). Thus, at resting Ca^{2+} levels in the cytoplasm are low and the channel remains silent; however, upon activation the influx of Ca^{2+} to the cytoplasm due to I_{CRAC} activates them allowing K^+ efflux through $K_{Ca}3.1$ channels resulting in a negative feedback loop. Ca^{2+} sensing is accomplished by CaM molecules bound to the C-terminus of $K_{Ca}3.1$ subunits (Figure 9) (248).

Proliferation and innate activation trigger the induction of the K_v outward current and, in a parallel way, a decrease of the $K_{ir}2.1$ current; whereas alternative activation down regulates K_v current (63,67,69). Experimental evidence indicates that in macrophages, the major K_v is mainly a heterotetrameric $K_v1.3/K_v1.5$ channel (63,69). Innate activation changes the stoichiometry of these channels increasing the $K_v1.3$:$K_v1.5$ ratio, whereas alternative activation decreases it (63,69). CRAC channels are also increased upon classical stimulation. However, less is known regarding the role of these channels in the resolution phase (63,69).

Lipoxins are endogenous eicosanoids released during the resolution phase of inflammation (249-251)

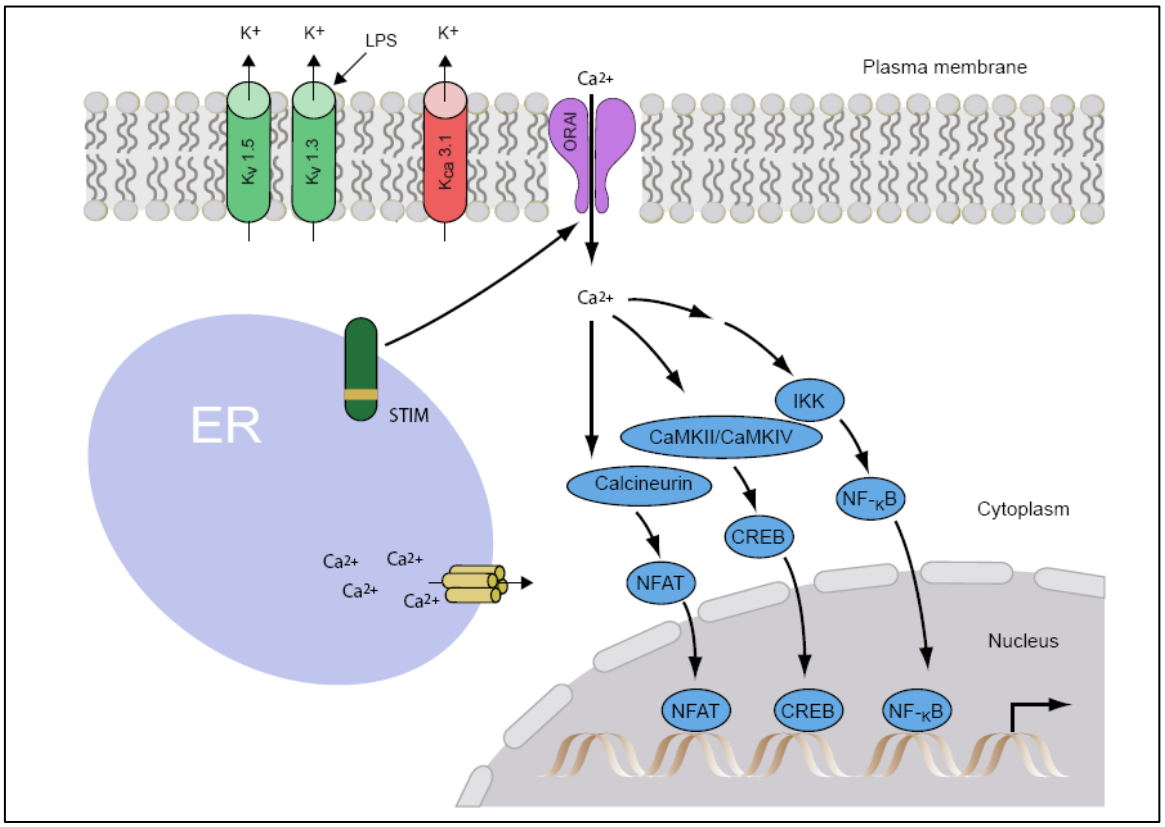

Figure 9. Ion channels in the immune response. $K_v1.5$, $K_v1.3$, $K_{Ca}3.1$ Orai 1 and STIM1 is depicted schematically in the scheme. In macrophages, three types of K^+ channel generate a negative membrane potential (approximately -60 to -70 mV) that is required for Ca^{2+} influx through calcium release-activated calcium (CRAC) channels. Depolarization of the cells reduces the driving force for Ca^{2+} entry, a process that is counteracted by the opening of $K_v1.3$, $K_v1.5$ and $K_{Ca}3.1$ channels. $K_{ir}2.1$ channels, by contrast, open in response to Ca^{2+} influx and increased intracellular Ca^{2+} concentration.

and they might modulate K_v channel activity. These lipids are mainly generated by transcellular metabolism from arachidonic acid (n-6 PUFA) via lipoxygenase (LOX) enzymes (252,253). In addition to LOX-initiated lipoxin biosynthesis, another route involving cyclooxygenase 2 (COX-2) has been described. After aspirin ingestion, acetylated COX-2 loses the activity required to form prostaglandin, but retains oxygenase activity to produce 15*R*-HETE from arachidonate. This intermediate is transformed via 5-LOX in epimeric lipoxins, termed 15-epi-lipoxins (252). The potent antiinflammatory and proresolving actions of lipoxins and epi-lipoxins have been demonstrated in multiple animal models of human diseases (253,254). Both, native lipoxin A_4 (LXA_4) and 15-epi-LXA_4 (e-LXA_4) bind to and activate the lipoxin receptor (ALX) and decrease polymorphonuclear cells infiltration in rodent models of acute peritonitis (255). The endogenous protective role of ALX mediating the biological actions of lipoxins has been demonstrated in mice overexpressing the human ALX in myeloid cells (256)

2 OBJECTIVES

Voltage dependent potassium channels are membrane proteins highly modulated by several physiological, pharmacological and pathological events (257). Also, K_v channels are involved in a plethora of pathophysiological process, including immune response and cardiac arrhythmias.

In the immune system, it has been described that K_v channels initiate the immune response, in such a way that different types of stimulation can increase or decrease the expression of several types of K_v channels in macrophages. Indeed, consistent data indicate that K_v channels play a pivotal role in the regulation of macrophage immunomodulatory responses: K_v channels are tightly regulated during proliferation and activation in macrophages, and their functional activity is important for cellular responses (63,67,69). Proliferation and innate activation trigger the induction of the K_v outward current and, in a parallel way, a decrease of the $K_{ir}2.1$ current; whereas alternative activation downregulates K_v current (63,67,69). Experimental evidence indicates that in macrophages, the major K_v current is mainly generated by heterotetrameric $K_v1.3/K_v1.5$ channels (63,69). Innate activation changes the stoichiometry of these channels increasing the $K_v1.3$:$K_v1.5$ ratio, whereas alternative activation decreases it (63,69). However, less is known regarding the role of these channels in the resolution phase.

In the heart, there have been reported hundreds of mutations in several genes encoding K_v and other ion channels present in the cell membrane of cardiomyocytes as well as other proteins, such as ankyrin or caveolin, which can produce the development of cardiac arrhythmias through different mechanisms. Elucidation of the basis of genetic diseases provides unique insights into the mechanisms responsible for the more prevalent arrhythmias and sudden cardiac arrest while also permitting the identification of therapeutic opportunities for their treatment and prevention. There have been described different mutations in genes that encode potassium channels ($K_v7.1$, $K_v11.1$) associated with long or short QT syndrome. Mutations in $K_v7.1$ and $K_v11.1$ inducing short QT syndrome are associated with an increase in outflow of potassium in phase 3 of the cardiac action potential. Although the general mechanisms by which the short QT syndrome are known, there are only a few cases reported in the literature and the pathogenic role of the short QT syndrome is controversial. The electrophysiological study of mutations in genes that encode ion channels allow advanced knowledge of the pathophysiology of channelopathies and will be able to explain the differences found in those affected, in response to pharmacological agents shedding light on possible therapeutic agents. 80% of the channel mutations trigger an abnormal behavior of the channel that is enough to develop cardiac arrhythmias. In addition, an increase number of mutations in certain regions of the channels may affect the channel function by modifying their interaction with regulatory subunits or impairing traffic and targeting of the complex to specific membrane locations. Moreover, some of these mutations can affect the affinity of the channel to different selective blockers and modulators (antiarrhythmic drugs, kinases, etc.).

Finally, K_v channels can be modulated by lipids such as polyunsaturated fatty acids (either PUFAs or their metabolites, such as lipoxins). Thus, it has been described that n-3 PUFAs can exert antiarrhythmic actions, maybe due to their interaction with cardiac ion channels (206-208,210-212). Lipoxins are endogenous eicosanoids released during the resolution phase of inflammation (249-253). They can exert their anti-inflammatory effects through their initial actions on K_v and K_{ir} channels., and they might modulate K_v channel

activity. The potent antiinflammatory and proresolving actions of these lipids have been demonstrated in multiple animal models of human diseases (253,254). Both native LXA_4 and 15-epi-LXA_4 (e-LXA_4) (252) bind and activate the lipoxin receptor (ALX) and decrease polymorphonuclear cells infiltration in rodent models of acute peritonitis (255). The endogenous protective role of ALX mediating the biological actions of lipoxins has been demonstrated in mice overexpressing the human ALX in myeloid cells (256).

The **Hypothesis** of the present Doctoral Thesis is that K_v channels influence the immune response and the cardiac electrophysiology, and that their changes induced by PUFAs or by point-mutations can trigger antiarrhythmic/proarrhythmic or anti-inflammatory effects.

The **Main Objective** of the present Doctoral Thesis is to analyze the effects of polyunsaturated fatty acids on K_v channels in bone marrow derived macrophages and on Kv7.1/KCNE1 channels, as well as to analyze the electrophysiological characteristics of a new mutation in the KCNQ1 gene that trigger short QT syndrome.

In order to achieve this Objective, our **specific objectives** are to analyze:

- The electrophysiological effects of 15-epi-LXA_4 on K_v and K_{ir} channels in bone marrow derived macrophages.
- The electrophysiological effects of eicosapentaenoic and docohexaenoic acid on K_v7.1/KCNE1 channels.
- The electrophysiological characteristics of a new point mutation of the KCNQ1 gene that triggers type 2 short QT syndrome.

3 MATERIALS AND METHODS

3.1. PRIMARY CELL CULTURE

For the treatment of animals and preparation of bone marrow-derived macrophages (BMDM), BALB/c mice were housed and bred in our pathogen-free facility, and all experimental procedures were performed following the Spanish and European guidelines regarding the use of animals for experimentation. Animals (aged 8 to 12-weeks) were sacrificed by CO_2 chamber euthanasia. Pelvises, femurs and tibiae were dissected removing adherent tissue. The ends of the bones were cut off and the marrow tissue was flushed by irrigation with Dulbecco's Modified Eagle's Medium (DMEM). The marrow plugs were passed through a 25G needle for dispersion. Bone marrow mononuclear phagocytic precursor cells were propagated in suspension by culturing in DMEM containing 10% fetal bovine serum (FBS), 0.5 µM β-mercaptoethanol, 100 U/ml penicillin, 100 µg/ml streptomycin (all from Gibco, Paisley, UK), 1 nM IL-3 (PeproTech, Rocky Hill, NJ, US) and 0.20 nM recombinant murine macrophage colony-stimulating factor (M-CSF) (PeproTech,Rocky Hill, NJ, US) in tissue culture plates. The precursor cells became adherent within 3 days of culturing. For priming of BMDM, the cells were maintained in RPMI1640 medium supplemented with 10% Fetal Calf Serum (FCS) for 14 h prior to use. Experiments were carried out in phenol-red free RPMI 1640 medium and 1% of heat inactivated FCS plus antibiotics.

3.1.1. COS7 culture

The African green monkey kidney-derived cell line COS7 was obtained from the American Type Culture Collection (Rockville, MD, US) and cultured at 37ºC in DMEM supplemented with 10% FCS and antibiotics (100 IU/ml penicillin and 100 µg/ml streptomycin; all from Gibco, Paisley, UK) in a CO_2 humidified atmosphere. The culture medium was changed every 2-3 days and briefly trypsinized every 4-5 days. COS7 cells express a background K^+ current (an endogenous acid-sensitive K^+ channel) (258) but its magnitude is too small to interfere with the recordings obtained after transfecting the cells with the potassium channels of our interest (K_v7). Even more, its biophysical properties widely vary from the transfected ones. These cells do not express endogenously the $K_v7.1$ accessory subunit KCNE1, being a good expression system to study $K_v7.x$ currents.

3.1.1.1 COS7 transfection

For electrophysiological studies of the effects of PUFAs on $K_v7.1$/KCNE1, COS7 cells were transiently transfected with 0.4 µg pcDNA3.1 KCNE1-$K_v7.1$ concatemer (human KCNE1 linked to the N-terminus of human $K_v7.1$ cDNA, kindly supplied by Dr. Isabelle Baró). In some experiments, 0.5 µg pEYFP-N1-$K_v7.1$ plus 0.5 µg pECFP-C1-KCNE1 (kindly supplied by Dr. Antonio Felipe), were used. In both cases, transfection was performed together with 1.6 and 1 µg respectively of the reported plasmid EBO-pcD-Leu2-CD8 (for future selection of the transfected cells) per 35 mm culture dish. The total amount of cDNA transfected in both cases was 2 µg.

For protein expression studies on the effects of PUFAs on $K_v7.1$ and KCNE1 products, cells were transfected with 4 µg pEYFP-N1-$K_v7.1$ alone or with 4 µg pECFP-C1-KCNE1 per 100 mm culture dish.

For electrophysiological studies of the effects of the new mutation F279I in $K_v7.1$ protein found in the clinical practice, the mutation was introduced in the pEYFP-N1-$K_v7.1$ plasmid by PCR reaction using mutant primers and the Quick change site-directed mutagenesis kit (Stratagene, La Jolla, CA, USA) following manufacturer instructions. COS7 cells were transfected with 1 µg of WT or F279I $K_v7.1$ constructs and 1 µg EBO-pcD-Leu2-CD8 and, for co-expression experiments, 0.5 µg of WT or F279I $K_v7.1$ constructs plus 0.5 µg KCNE1 always in combination with 1 µg EBO-pcD-Leu2-CD8 per 35 mm culture dish.

In all cases, transient transfections were carried out in COS7 cells at 60-80% confluence following the FuGENE®6 transfection method (Promega, Southampton, UK). The ratio µg DNA:µl Fugene was 1:3.

3.1.2 HEK293 culture

The Human Embryonic Kidney derived cell line HEK293 was obtained from the American Type Culture Collection (Rockville, MD, US) and cultured at 37ºC in DMEM supplemented with 10% FCS and antibiotics (1% v/v: penicillin G 10.000 U/mL and streptomycin 10 mg/mL; all from Gibco, Paisley, UK) in a CO_2 humidified atmosphere. The culture medium of the cell was changed every 2-3 days and briefly trypsinized every 4-5 days.

3.1.2.1 HEK293 transfection

For coimmunoprecipitation and biotinylation assays of WT and F279I $K_v7.1$ channels, HEK293 cells were transiently transfected with 4 µg of WT or mutant $K_v7.1$ channel plus 4 µg of KCNE1 cDNA per 100 mm culture dish using *Metafectene Pro* (30 µL) at 80% confluence following manufacturer instructions. 24 hours after transfection, the cells were ready for use.

3.2 FLOW CYTOMETRY

Apoptosis was detected either with propidium iodide (PI) nuclei staining or with using flow cytometry by annexin V binding. Cells were harvested and washed in cold phosphate buffered saline (PBS). After centrifugation at 4ºC for 5 min and 1000 × g, cells were resuspended in annexin V binding buffer (10 mM HEPES; pH 7.4, 140 mM NaCl, 2.5 mM $CaCl_2$). Cells were labelled with annexin V–FITC solution (BD/Pharmingen, San Jose, CA) and/or PI (100 µg/ml) for 15 min at room temperature in the dark. PI is impermeable to living and apoptotic cells but stains necrotic and apoptotic dying cells with impaired membrane integrity in contrast to annexin V, which stains early apoptotic cells (22). Analysis was carried out using a FC500 Becton Dickinson FACscan flow cytometer (Mountain View, CA, USA) using a CXP software (Beckman Coulter, Brea, CA, USA)

3.3 MEASUREMENT OF IKKβ ACTIVITY

To determine the direct effect of e-LXA_4 *in vitro,* IKKβ activity was measured by homogeneous time-

resolved fluorescence (HTRF) assay, using cloned and expressed IKKβ and biotinylated-IκBα (amino acids 28 to 40) as substrate. Fluorescence (excitation at 330 nm and emission at 615 and 665 nm) was recorded after addition of europium cryptate phospho-Ab recognizing the S32/S36 phosphorylation peptide and streptavidin-XL665. Inhibition of IKKβ by staurosporine was used as control (Figure 10).

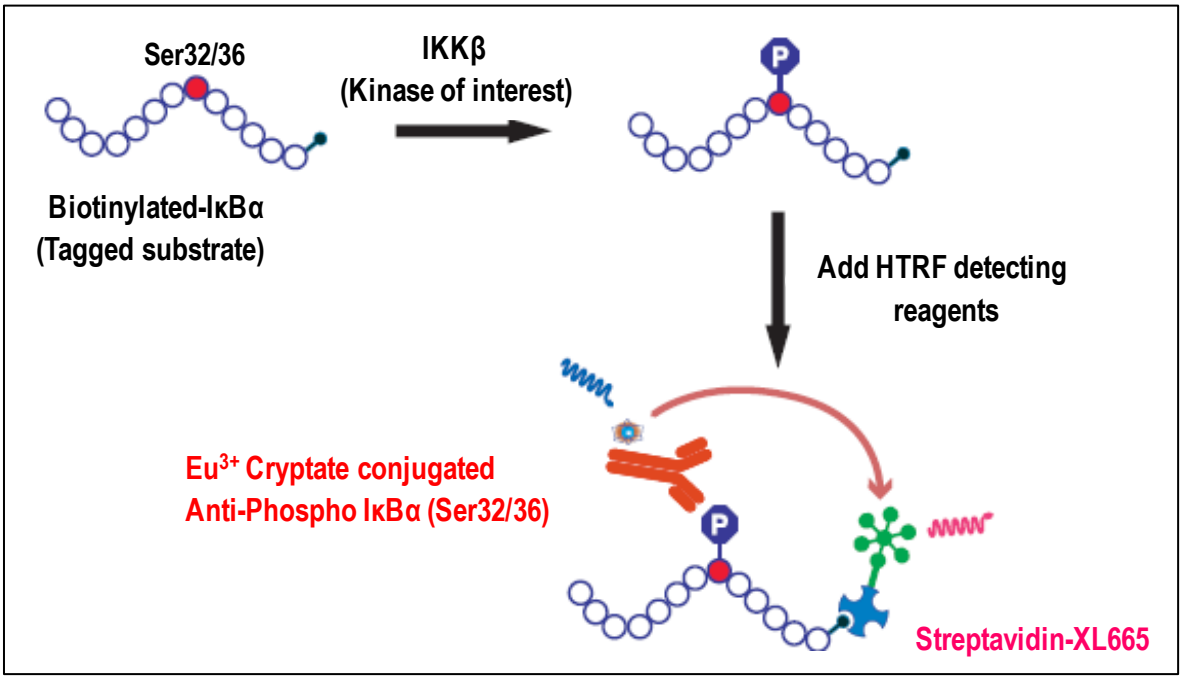

Figure 10. HTRF interaction assay principle. IκBα–biotinylated substrate for IKKβ, binds to a streptavidin-XL665 molecule, which is conjugated with a fluorescent acceptor XL665. The phosphorylated substrate can be detected using the Anti-Phospho IκBα (Ser32/36) monoclonal antibody coupled to Eu^{3+} Cryptate fluorescent donor that becomes in close proximity to the acceptor and fluoresce transfer is detected.

3.4 IMMUNOCYTOCHEMISTRY OF K_v AND K_{ir} PROTEINS

Cells were seeded into sterile 8-wells chamber slides (Falcon, Lincoln Park, NJ) and activated for the indicated time. After fixation with 2% paraformaldehyde for 10 min, cells were then permeabilized in iced methanol and incubated with 3% bovine serum albumin (BSA) for 30 min. After incubating with antibodies against K_v or K_{ir} at 4ºC for 1 h, cells were washed with PBS followed by incubating with Alexa 488 anti-rabbit secondary antibody at 4ºC for 1 h at room temperature (1:500; Molecular Probes, Invitrogen Corporation, Carlsbad, CA, US) and Hoechst 33342. Coverslips were mounted in Vectashield (Vector Laboratories, Burlingame, CA) and examined using an Espectral Leica TCS SP5 confocal microscope. Values of intensity fluorescence and quantification were obtained performed with Image J software (NIH, Bethesda, MD).

3.5 RNA ISOLATION AND RT-PCR ANALYSIS

1 µg of total RNA, extracted with Trizol Reagent (Invitrogen Corporation, Carslbad, CA, US), was reverse

transcribed using Transcriptor First Strand cDNA Synthesis Kit for RT-PCR following the indications of the manufacturer (Roche Diagnosis, Manheim, Germany). For priming, a mixture of random hexamers was used to obtain a uniform representation of all RNA sequences present in the cellular extracts. Real-time PCR was conducted using the SYBR Green method (*SYBR® Green PCR Master Mix,* Applied Biosystems) on a MyiQ Real-Time PCR System (Bio-Rad, Herculaes, CA, US). PCR thermocycling parameters were 95°C for 10 min, 40 cycles of 95°C for 15 s, and 60°C for 1 min. All samples were analyzed in parallel for 36B4 expression, a ribosomal subunit whose expression is not altered under all the conditions tested. Each sample was run in duplicate and was normalized to 36B4. The replicates were then averaged, and fold induction (FI) was determined in a ΔΔCt based fold-change calculations.

3.6 PROTEIN EXTRACTION

3.6.1 Protein extraction from BMDM

The BMDM cultures (6-well dishes) were washed twice with ice-cold PBS and the cells were homogenized in 0.2 ml of buffer A (10 mM Tris-HCl, pH 7.5, 1 mM $MgCl_2$, 1 mM EGTA, 10% glycerol, 0.5% CHAPS, 1 mM β-mercaptoethanol and 0.1 mM PMSF and a protease inhibitor cocktail (Sigma, St Louis, MO, US). The extracts were vortexed for 30 min at 4ºC and centrifuged for 15 min at 13,000 × g. The supernatants were stored at -20ºC.

3.6.2 Protein extraction from COS7 cells

48 hours after transfection, COS7 cells were washed twice in chilled PBS and centrifuged at 3,000 × g for 10 min. The pellet was then lysed with ice-cold lysis solution (50 mM Tris-HCl, pH 7.4, 150 mM NaCl, 1mM EDTA, 1% Triton X-100), supplemented with Complete Protease Inhibitor Cocktail Tablets (Roche Diagnostics, Mannheim, Germany) by repeated passing (10 times) through a 25G (0.45 × 16 mm) needle. Homogenates were further centrifuged at 10,000 × g for 5 min. Samples were separated into aliquots and stored at -20°C.

All steps were carried out at 4ºC and proteins levels were determined using the Bio-Rad detergent-compatible protein reagent (Bio-Rad, Herculaes, CA, US).

3.6.3 Protein extraction from HEK293 cells

24 h after transfection, the homogenates were were lysed in immunoprecipitation buffer 1% (50 mM HEPES, 150 mM NaCl, 1% Triton X-100, 10% glycerol (pH 7.2) supplemented with complete protease inhibitor mixture), and homogenized by orbital shaking at 4 °C for 20 min. Homogenates were then centrifuged at 3000 x g for 10 min, and the supernatant was aliquoted and stored at −20°C. Protein content was determined using the Bio-Rad Protein Assay (Bio-Rad).

3.7 LIPID RAFTS ISOLATION.

Lipid rafts are specific membrane domains rich in cholesterol and sphingolipids. They are resistant to detergent solubilisation at 4°C and are destabilized by cholesterol- and sphingolipid-depleting agents. The methods used to isolate the lipid rafts are based on the insolubility of these structures in the non-ionic detergent Triton X-100. Following ultracentrifugation on sucrose density gradients, lipid rafts will float away from the soluble proteins, forming a cloudy band at the top of the centrifugation tube.

Lipid rafts or low-density Triton-insoluble complexes were isolated as previously described. Briefly, COS7 cells transfected with K_v7.1 and KCNE1 were washed twice in cold PBS, scrapped and centrifuged for 8 min. The pellet was resuspended in 0.5 ml of MES-buffered saline containing 1% (v/v) Triton X-100, MES 25 mM, NaCl 150 mM, pH 6.5, and supplemented with protease inhibitors and homogenized by repeated passing (10 times) through a 25G (0.4 × 1.6 mm) needle. The addition of 1.5 ml of 53.28% sucrose prepared in MES buffer yielded to homogenate to a final concentration of 40% sucrose and it was placed at the bottom of an ultracentrifuge tube. Then, a 5-30% linear sucrose gradient was formed above the homogenate and centrifuged at 39,000 rpm at 4ªC for 20-22 h in a SW41 rotor (Beckman Instruments, Inc, Fullerton, CA, US). A light scattering band confined to the 15-20% sucrose region was observed that contained endogenous caveolin used as a positive control, but excluded most of other cellular proteins. Gradient fractions (1 ml) were collected from the top, separated by SDS-PAGE and analyzed by western blotting.

3.8 COIMMNUNOPRECIPITATION ASSAY

For co-immunoprecipitation, 50 µl of protein G-Sepharose beads were incubated with 4 ng of KCNE1 antibody in immunoprecipitation buffer at a final volume of 200 µl (50 mM HEPES, 150 mM NaCl, 1% Triton X-100, 10% glycerol (pH 7.2)) and homogenized by orbital shaking at 4°C for 1 h. Antibody-bound sepharose beads were then washed three times with wash buffer to remove unbound antibody.

1 mg of crude membrane protein were incubated with 25 µl of immunoprecipitation buffer-prewashed Sepharose protein A/G beads (Santa Cruz Biotechnology) for 1 h at 4 °C, and contaminant-bound Sepharose beads were separated by centrifugation for 30 s at 1000 x g at 4°C. The supernatant was incubated then with the antibody-bound sepharose beads by orbital shaking at 4°C for 1.5 h. During this incubation, the antibody would bind its specific protein (KCNE1). Sepharose beads bound to antibody-protein complexes were precipitated by centrifugation (30 s at 1000 x g at 4°C), and antibody-bound beads were then washed three times with immunoprecipitation buffer and centrifuged for 30 s at 1000 *g* at room temperature. Protein samples and immunoprecipitates were resuspended in 100 µl of Laemmli SDS loading buffer, boiled for 5 min at 100ºC, and then centrifuged for 3 min at 5.000 x g at room temperature. 50 µl of protein extract was separated by SDS-PAGE and analyzed by western blotting.

3.9 BIOTINYLATION OF MEMBRANE PROTEINS

Cell surface biotinylation was carried out with the Pierce Cell Surface Protein Isolation Kit (Pierce) following manufacturer's instructions. HEK293 cells were transfected with WT K_v7.1-YFP or F279I K_v7.1-YFP and their temporal presence at the surface was analyzed by western blotting. 24 hours after transfection, the cells were washed twice with chilled PBS and then, surface proteins were labeled with sulfosuccinimidyl-2-(biotinamide) ethyl-1,3-dithiopropionate (Sulfo-NHS-SS-biotin; Pierce) and incubated at 4°C with constant rotation for 30 minutes. The reaction was stopped by adding quenching solution. The cells were scrapped and homogenated in lysis buffer (provided by the Kit). The cell lysate was sonicated at low frequencies using 5 pulses for 1s followed by incubation on ice for 30 min being vortexed for 5 s every 5 min. Finally the sample was centrifuged at 1000 *x* g for 2 minutes at 4°C. The supernatant was reacted with immobilized NeutrAvidin gel slurry in columns (Pierce) to isolate surface proteins for 1hour at room temperature. Columns were washed and protein was eluted in sample buffer containing DTT. Surface proteins were resolved on a SDS-PAGE gel and the samples were analyzed by western blotting.

3.10 WESTERN BLOT ANALYSIS

Cell lysates containing equal amounts of protein (20-40 µg per lane) were resuspended in Laemmli Buffer (10% w/v SDS, 10% v/v glycerol, 5% w/v 2-β-mercaptoethanol, 0.002% w/v bromophenol blue, 62.5 mM Tris-HCl, pH 7.4) and boiled at 95ºC for 5 min when determining all the antigens with. Protein extracts were loaded and size-separated in 7-15% (acrylamide/bis-acrylamide) SDS-PAGE gels and transferred to PVDF membranes (GE Healthcare, UK) or to nitrocellulose membranes (Immobilon-P; Millipore). Membranes were blocked in 5% dry milk in PBS-Tween20 0.01% for 1 hour at room temperature and processed as recommended by the supplier of the antibodies against the antigens (see Table 1). Horseradish peroxidase-conjugated secondary antibodies were used (dilution1:10,000, Calbiochem, San Diego, CA, US). Inmunoblot signals were visualized by chemiluminescence using ECL-plus reagent (Amersham, GE Healthcare, UK). Quantification of band intensity was performed with the Image J software.

Table 1. Primary antibodies used in the present Doctoral Thesis

Antibody	Type and Host	Dilution	Reference and Origin
Anti-K_v1.5	Polyclonal Rabbit	1:200-1:400	APC-004, Alomone
Anti-K_v1.3	Polyclonal Rabbit	1:200	APC-002, Alomone
Anti-K_{ir}2.1	Polyclonal Rabbit	1:200	APC-026, Alomone

Anti-K_v7.1	Polyclonal Mouse	1:200	APC-028, Alomone
Anti-HO-1	Polyclonal Rabbit	1:1000	AB-1284, Millipore
Anti-Arg-1	Polyclonal Rabbit	1:1000	Sc-20150, Santa Cruz Biotech
Anti-NOS-2	Monoclonal Mouse	1:1000	Sc-7271, Santa Cruz Biotech
Anti-COX-2	Polyclonal Goat	1:1000	Sc-1747, Santa Cruz Biotech
Anti-Arg-2	Polyclonal Rabbit	1:500	Sc-20151, Santa Cruz Biotech
Anti-Nrf-2	Polyclonal Rabbit	1:200	Sc-13032, Santa Cruz Biotech
Anti-p65	Polyclonal Rabbit	1:1000	3034, Cell Signaling
Anti- IκBα	Polyclonal Rabbit	1:1000	Sc-371, Santa Cruz Biotech
Anti- P-IκBα	Monoclonal Rabbit	1:1000	2859, Cell Signaling
Anti-phospho-IKK	Polyclonal Rabbit	1:1000	2681, Cell Signaling
Anti-IKK	Polyclonal Rabbit	1:200	2678, Cell Signaling
Anti-β-Tubulin	Polyclonal Goat	1:5000	Sc-9935, Santa Cruz Biotech
Anti-β-actin	Polyclonal Goat	1:10000	Sc-1615, Santa Cruz Biotech
Anti-GFP	Monoclonal Mouse	1:1000	11814460001 Roche Applied science
Anti-Clathrin	Polyclonal Rabbit	1:1000	AB-9884, Millipore Chemicon
Anti-Pan-Caveolin	Polyclonal Mouse	1:1000	610057, BD Transduction Labs
Anti-KCNE1	Polyclonal Rabbit	1:200	APC-008 Alomone

3.11 ELECTROPHYSIOLOGICAL RECORDINGS

The patch clamp technique was first used by Neher and Sakmann (1976) to resolve currents through single acetylcholine-activated channels in cell-attached patches of membrane of frog skeletal muscle. This method is a refinement of the voltage-clamp technique that uses, as an electrode, a glass micropipette pulled to a fine tip of approximately 1-4 μm. The recording electrode or "patch pipette" is filled with a saline solution and sealed (with a high resistance, GΩ) onto a patch on the surface of the cell membrane, allowing the researcher to keep the voltage constant while measuring the current flowing across the membrane of a cell or even form a

single channel localized in the membrane patch.

Several configurations of the patch-clamp technique have been developed. The most commonly used when studying ion currents across the cell is the whole-cell patch-clamp technique. In this approach, after the seal is formed between the electrode and the cell membrane, a gentle suction is applied, rupturing the cell membrane in the patch and gaining access to the cytoplasm. Consequently, the internal pipette solution enters in direct contact with the intracellular space. The membrane of the whole cell is voltage clamped, and the recorded currents are a composite of the currents flowing through all the active channels (Figure 11).

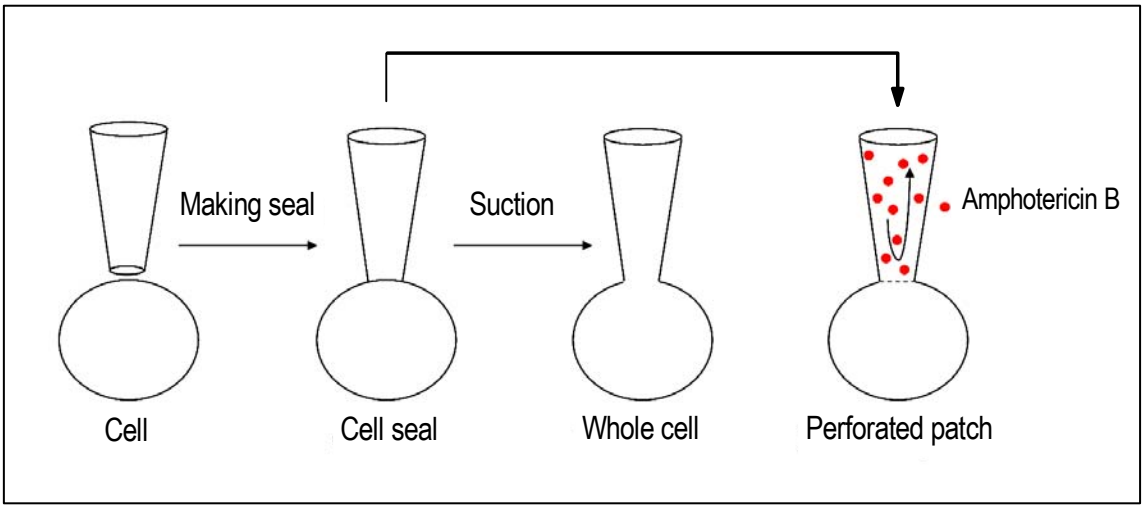

Figure 11. Patch-clamp configurations. In whole cell patch clamp there is continuity between the intracellular space and the pipette-filling solution. Dialysis of the cytoplasm is avoided when the perforated patch is used.

A variation of the same procedure is the perforated-patch technique. Here, the idea is to introduce in the pipette the specific pharmacologic agent amphotericin B (0.5 mg/ml) that creates large pores in the membrane inside the patch. The seal, therefore, is not broken. Instead, the electrode gains electric access to the intracellular compartment through the pores perforated by the drug and the intracellular space is not dialyzed (Figure 11).

Before experimental use, cells were incubated with polystyrene microbeads precoated with anti-CD8 antibody (Dynabeads M450, Dynal, Oslo, Norway). A suspension of transfected cells were placed on a chamber mounted on the stage of an inverted microscope. Current recordings were made with an Axopatch 200B amplifier (Axon Instruments, Foster City, CA, USA) in the whole cell configuration of the patch clamp technique, when measuring $K_v1.3$, $K_v1.5$ and K_{ir} currents, or with the perforated patch configuration when measuring $K_v7.1$ currents. As described above, experiments were performed at room temperature (20-23ºC). Current recordings were low pass-filtered and sampled at 2 kHz with an analog-to-digital converter DigiData 1400A (Axon Instruments, Foster City, CA, USA) (data acquisition system). Command voltages and data storage were controlled with pClamp9 software (Axon Instruments, Foster City, CA, USA). Patch electrodes were pulled from borosilicate glass capillaries (GD-1, Narishige, Tokio, Japan) with a P-87 puller (Sutter Instruments, Co., Novato, CA, EE.UU) and were heat polished (MF-83, Narishige, Tokyo, Japan). After heat-polishing, the resistance of the patch electrodes tip (filled with the internal solution) averaged 1-3 MΩ. The cells were perfused continuously with a bath solution containing the following (in mM): NaCl 130, KCl 4, $CaCl_2$ 1.8, $MgCl_2$ 1, HEPES 10, and glucose

10, and was adjusted to pH 7.4 with NaOH. The electrode solution contained the following (in mM): K-aspartate 80, KCl 50, phosphocreatine 3, KH_2PO_4 10, MgATP 3, HEPES-K 10, EGTA-K 5 and was adjusted to pH 7.25 using KOH. Gigaohm seal formation was achieved by suction (2-5 GΩ). In the experiments performed using the whole-cell configuration, the capacitive transients elicited by symmetrical 5 mV steps from -80 mV were recorded at 50 kHz and filtered at 10 kHz for subsequent calculations of capacitative surface area, access resistance and input impedance. Thereafter, capacitance and series resistance compensation were optimized and, usually, 80% compensation of the effective access resistance was obtained. Uncompensated series resistances were 4-8 MΩ, as currents evoked were less than 1 nA; voltage errors from uncompensated series resistance were less than 2 mV.

The holding potential was set to -80 mV, and the interpulse interval was set to a minimum of 10 seconds. The voltage protocols were adjusted to determine the biophysical properties of wild type and mutant channels adequately. Time constant of activation, inactivation and deactivation were determined by fitting the current recordings with a single or double exponential functions:

$$y = A_s\exp(-t/\tau_s) + A_f\exp(-t/\tau_f) + C$$

where τ_f and τ_s are the system time constants, A_1 and A_2 are the amplitudes of each component of the exponential, and C is the baseline value. The voltage dependence of channel activation was fitted to a Boltzmann equation:

$$y = 1/[1 + \exp(-(E-E_h)/s)]$$

in which *s* represents the slope factor, *E* represents the applied voltage, and E_h the voltage at which 50% of the channels are activated .

Microcal Origin 8.5 (Microcal Software, Northampton, MA) and CLAMPFIT software were used to analyze data, perform least-squares fitting and for data presentation.

3.12 DRUGS AND REAGENTS

Table 2. Drugs and reagents used in the present Doctoral Thesis. See the results section for a more detailed description of each experimental condition.

Drug/Reagent	Function	$[]_{final}$	Origin
LPS	Induction of classical activation of macrophages	100 ng/µl	Invitrogen
Staurosporine	Induction of apoptosis by activating caspases	1-500 ng/ml	Calbiochem
IL4	Induction of alternative activation of macrophages	20 ng/ml	PrePro Tech
IL13	Induction of alternative activation of macrophages	20 ng/ml	PrePro Tech
e-LXA_4	Anti-inflammatory eicosanoid	100-500 nM	Cayman

BocPLP	Lipoxin receptor antagonist	1 μM	Bachem
Amphotericin B	Antifungal used to create small pores in a membrane patch when adding to the internal solution	0.5 mg/ml	Sigma
EPA	K_v7.1 and KCNE1 modulators	20-100 μM	Sigma
DHA	K_v7.1 and KCNE1 modulators	20-100 μM	Sigma
MG132	Potent, reversible, and cell permeable proteasome inhibitor	2 μM	Calbiochem
MβCD	Disruptions of lipid rafts by removing cholesterol from membranes	10 mM	Sigma

3.13 STATISTICAL ANALYSIS

Results are expressed as mean±SEM. Direct comparisons between mean values in control conditions versus mean values in the presence of drug for a single variable were performed by a paired Student's *t* test. ANOVA was used to compare more than two groups. Student's *t* test was also used to compare two regression lines. Differences were considered significant if the *P*-value was less than 0.05.The curve-fitting procedure used a non-linear least-squares (Gauss-Newton) algorithm; results were displayed in linear format. Goodness of fit was judged by the χ^2 criterion and by inspection for systematic non-random trends in the difference plot.

4 RESULTS

4.1 MODULATION OF K_v AND K_{ir} CURRENTS BY 15-EPI-LIPOXIN-A_4 IN ACTIVATED MACROPHAGES. IMPLICATIONS IN INNATE IMMUNITY

4.1.1 Macrophage profiling upon activation

BMDM were challenged with LPS or IL4/IL13 and the expression of genes characteristics of the LPS (NOS-2, COX-2 and IP-10) and IL4/IL13 activation (HO-1 and Arg-1) confirmed the differential phenotype of these populations upon treatment (Figure 12A). Interestingly, less than 20% of the cells exhibited an apoptotic phenotype after LPS challenge (24 h), whereas IL4/IL13 stimulation did not affect cell viability (Figure 12B), allowing the use of the cells for electrophysiological purposes after this primary treatment.

Lipoxins have been described as inhibitors of the pro-inflammatory response to LPS, although the molecular mechanisms involved are only partially characterized (254). In this regard, treatment of BMDM with e-LXA_4 significantly impaired IKK activation and IκBα phosphorylation and subsequent degradation in response to LPS stimulation (Figure 12C), an effect that was further evidenced by the decreased translocation of p65 to the nucleus (i.e., lesser NF-κB activity) and the enhanced accumulation of Nrf-2, a transcription factor activated in response to e-LXA_4 (Figure 12D). In agreement with this pattern of signaling, a decrease in the expression of NOS-2 and COX-2 and, interestingly, a moderate expression of HO-1 (Nrf2-dependent gene) at 10 h after e-LXA_4/LPS challenge were observed (Figure 12E). Arg-1 and Arg-2 were not expressed under these conditions. In addition to this analysis, e-LXA_4 exhibited a moderate but significant direct inhibition of IKKβ when analyzed *in vitro*, using staurosporine as a control inhibitor (13). In agreement with previous data (254) and in part due to the attenuation of the LPS-dependent activation, treatment of BMDM with e-LXA_4 protected against apoptosis (Figure 12F-G).

4.1.2 Acute effects of e-LXA_4 on K_v currents from BMDM

Voltage-dependent potassium currents were evoked in BMDM by applying depolarizing pulses from a holding potential of -80 mV to different voltages from -80 to +60 mV in 10 mV steps. Figure 13 shows original records of K_v currents obtained in control (resting state), activated with LPS or with IL4/IL13 BMDM (Figure 13A-C), before and after perfusion (15 min) with e-LXA_4. Panels D-F show the current-voltage relationships (IV) obtained in the absence and in the presence of e-LXA_4. Resting and IL4/IL13 stimulated BMDM elicited small K_v currents of similar magnitude that were not modified by the external perfusion with e-LXA_4 ($P>0.05$, $n=10$) (Figure 13A, C). However, LPS-stimulated BMDM elicited inactivating K_v currents of greater amplitude and perfusion with e-LXA_4 significantly decreased them at potentials >0 mV (20±3% at +60 mV; $P<0.05$, $n=12$) (Figure 13B, E). Since it has been described that the increase of K_v current induced by LPS is due to an upregulation of $K_v1.3$ channels (67), this early inhibition of K_v current produced by e-LXA_4 could be due, at least in part, to its effects on $K_v1.3$ channels.

Use-dependent inactivation of certain K^+ channels is characterized by an inactivation that accumulates after repetitive depolarizations due to an incomplete recovery during the inter-pulse interval is incomplete (69,75).

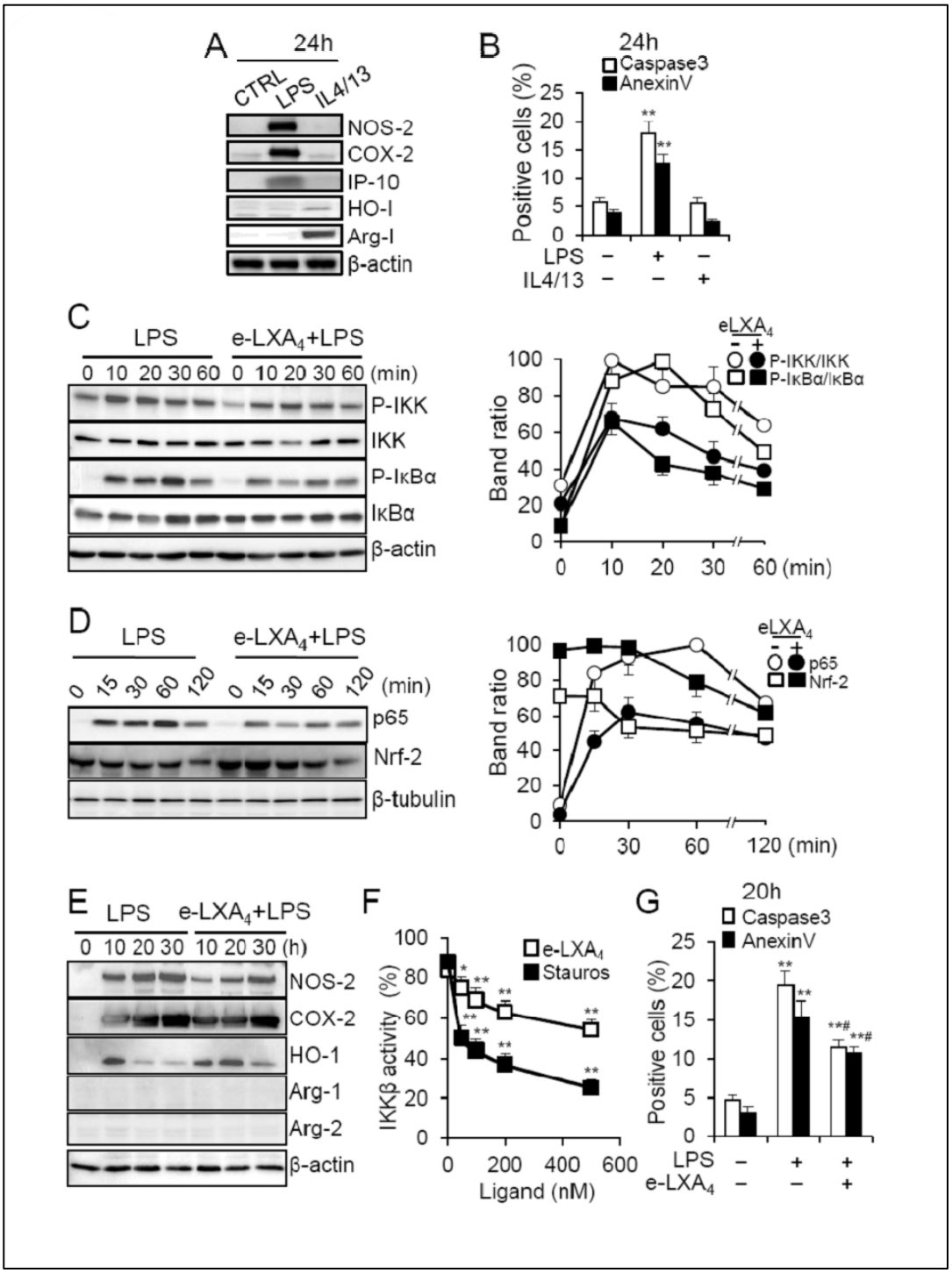

Figure 12. *Macrophage profiling after stimulation through the innate and alternative pathways and effect of e-LXA4 on activation.* BMDM were maintained in culture and activated for the indicated period with LPS (100 ng/ml) or IL-4/IL-13 (20 ng/ml each). The expression of proteins characteristics of each pathway **(A)** were determined by Western blot. The extent of apoptosis/necrosis under these conditions was determined by the staining with annexin V and propidium iodide, respectively **(B)**. Cells were treated with e-LXA4 (200 nM) for 30 min prior the challenge with LPS (100 ng/ml). The activation of IKK **(C)** and the presence of p65 and Nrf-2 in the nuclei of BMDM **(D)** were determined at 0-120 min. Band intensities were normalized for content in β-actin **(C)** or β-tubulin **(D)** and the ratios P-IKK/IKK and P-IκBα/ IκBα **(C)** and the p65 and Nrf-2 levels **(D)** were represented as percentage over the maximal value. The effect of e-LXA4 on the protein levels of NOS-2, COX-2, HO-1, Arg-1 and Arg-2 were determined at 10-30h **(E)**. e-LXA4 inhibited IKKβ activity in TRF in vitro assays, using staurosporine as control inhibitor **(F)**. The effect of e-LXA4 on apoptosis/necrosis in LPS activated BMDM was determined **(G)**. Results show a representative experiment out of four (A, C-E) or the mean±SEM of three experiments. *P<0.05, **P<0.01 *vs.* the control condition (in the absence of stimuli). #P<0.05 vs. values obtained in LPS- activated BMDM cells.

Figure 14A-C shows the use-dependency of K_v currents in resting, LPS- and IL4/IL13-stimulated BMDM before and after perfusion with e-LXA_4.

The degree of use-dependent inactivation observed in resting BMDM was small 15±5% (n=10), but increased to 69±3% (P<0.01, n=10 *vs.* control) in LPS-stimulated BMDM. In contrast, stimulation with IL4/IL13 led to a marked decrease of the use-dependent inactivation (1.6±3, P<0.01, n=8 *vs.* control). In none of these

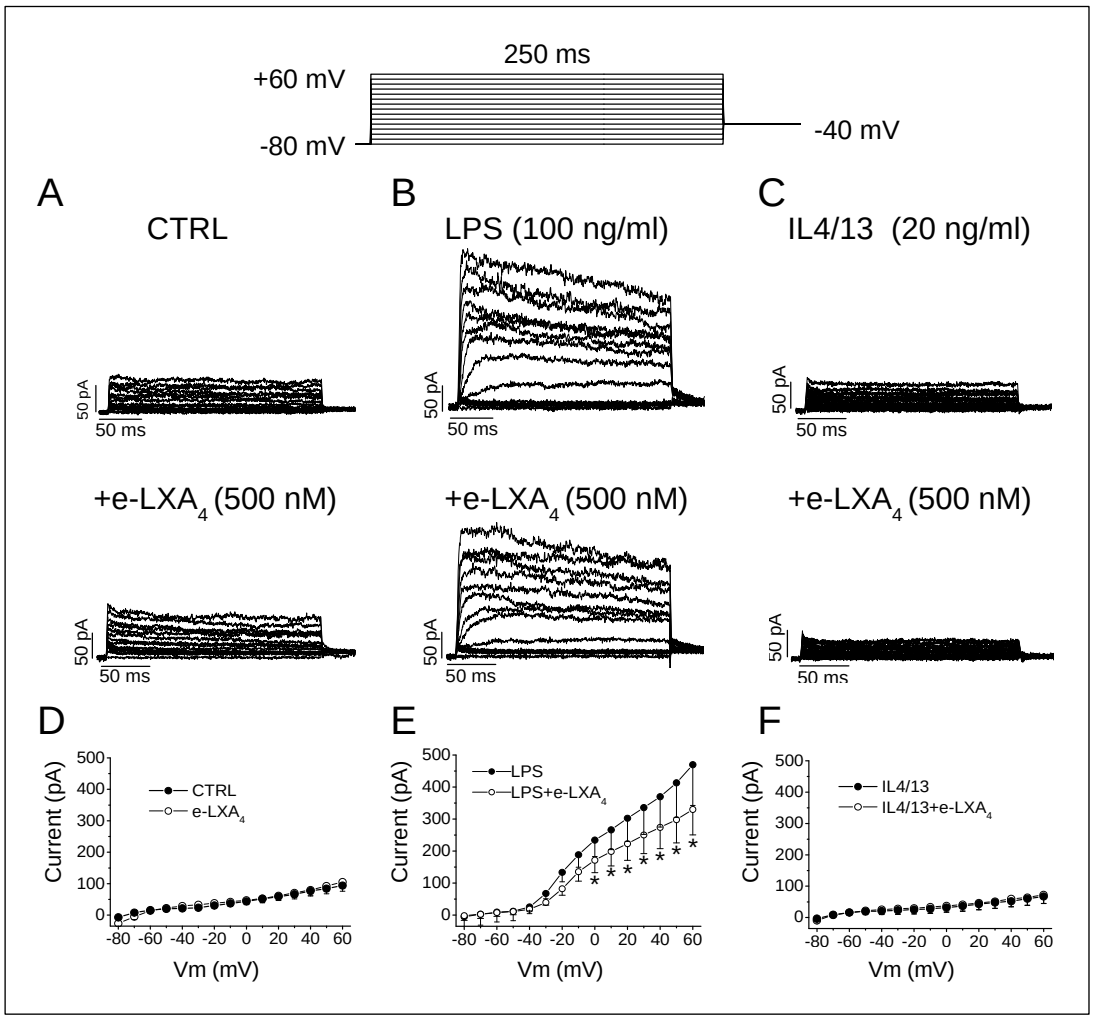

Figure 13. Acute effects of e-LXA_4 on K_v currents. Representative traces of K_v currents recorded in control **(A)**, LPS-stimulated (100 ng/ml) **(B)** and IL4/IL13-stimulated (20 ng/ml) **(C)** BMDM for 18 h. Current recordings were obtained in the absence and after perfusion with e-LXA_4 (500 nM). Currents were elicited by applying depolarizing pulses from a holding potential of -80 mV to different depolarizing voltages from -80 to +60 mV in 10 mV steps (250 ms duration). IV relationships in the absence and in the presence of e-LXA_4 (500 nM) in non-stimulated BMDM cells **(D)**, LPS **(E)** and IL4/IL13 **(F)** activated BMDM cells are shown. IV plots shows the mean±SEM. *P<0.05 *vs.* control; n>10 cells per group.

cases, the perfusion with e-LXA_4 (500 nM) was able to modify the degree of use-dependent decrease of the current.

As shown in Figure 14, K_v currents inactivate with a different time course in resting, LPS- and IL4/IL13-stimulated BMDM. Inactivation parameters are useful to evaluate possible differences in the tetrameric K^+ channel phenotype, as K_v1.3 channels present fast C-type inactivation, which is absent in K_v1.5 (17,69,259). Figure 14D-F shows the time course of K^+ current inactivation after applying a depolarizing pulse from -80 to +60

mV for 1 s. While K_v currents inactivated with a time constant of >1 s (n=5) in control BMDM, this time constant decreased to 456±43 ms in LPS-stimulated cells (P<0.05, n=10, *vs*. control). However, this process became much slower in IL4/IL13-stimulated BMDM (>1 s, P<0.05, n=7, *vs.* control). These results further support the notion that K_v currents generated upon depolarization in BMDM are mediated by K_v channels with different subunit stoichiometry after activation with LPS or with IL4/IL13. Therefore, these cytokines produce similar electrophysiological effects than those elicited by dexamethasone, both conditions counteracting the proinflammatory polarization (67,69)

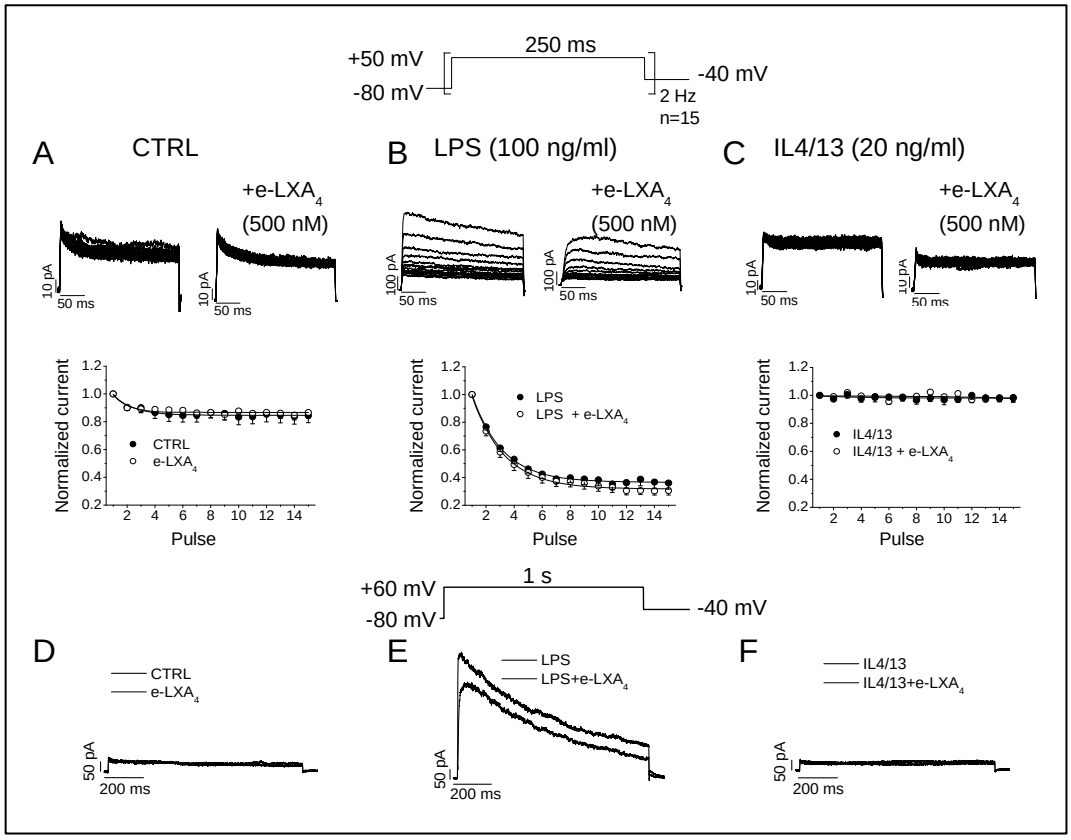

Figure 14. Acute effects of e-LXA4 on use-dependency and kinetics of K_v inactivation. Representative traces of K_v currents recorded in control **(A)**, LPS (100 ng/ml) **(B)** and IL4/IL13 (20 ng/ml) **(C)** activated BMDM after applying the pulse protocol shown in the upper panel of the Figure. Plots show the normalized current measured at the maximum peak current during the application of a train of depolarizing pulses. Current records of K_v currents recorded in control **(D)**, LPS **(E)** and IL4/IL13 **(F)** activated BMDM obtained after applying a depolarizing pulse of 1s at + 60 mV. Graphs show the mean±SEM of normalized current against the pulse number.

4.1.3 Acute effects of e-LXA4 on K_{ir} channels from BMDM

Inward rectifying potassium currents (K_{ir}) were evoked in BMDM by applying pulses from a holding potential of -80 mV to different voltages from -140 to +40 mV in 10 mV steps (Figure 15A-C). Figure 15 shows original records of K_{ir} currents and the mean IV relationships obtained in resting, LPS- and IL4/IL13-stimulated BMDM in the absence or presence of e-LXA4 (500 nM). In cells activated with IL4/IL13, the magnitude of the K_{ir} currents was similar to that recorded in control BMDM. However, cells activated with LPS elicited K_{ir} currents of smaller amplitude (-34±10 pA *vs.* -127±33 pA, P<0.05, n=9-11). Figure 15D-F shows the mean IV relationships

for K_{ir} currents obtained in non stimulated, LPS- and IL4/IL13- stimulated BMDM in the absence and the presence of e-LXA_4. The degree of K_{ir} inactivation was greater in LPS- or IL4/IL13-stimulated BMDM cells than in non-stimulated cells (Figure S1). Under all experimental conditions, e-LXA_4 decreased the current at potentials negative to -120 mV (12±4%, n=10; 18±9%, n=12 and 23±4%, n=7 at -140 mV in not stimulated, LPS and IL4/IL13 stimulated BMDM, respectively). The decrease induced by e-LXA_4 was accompanied, in not stimulated

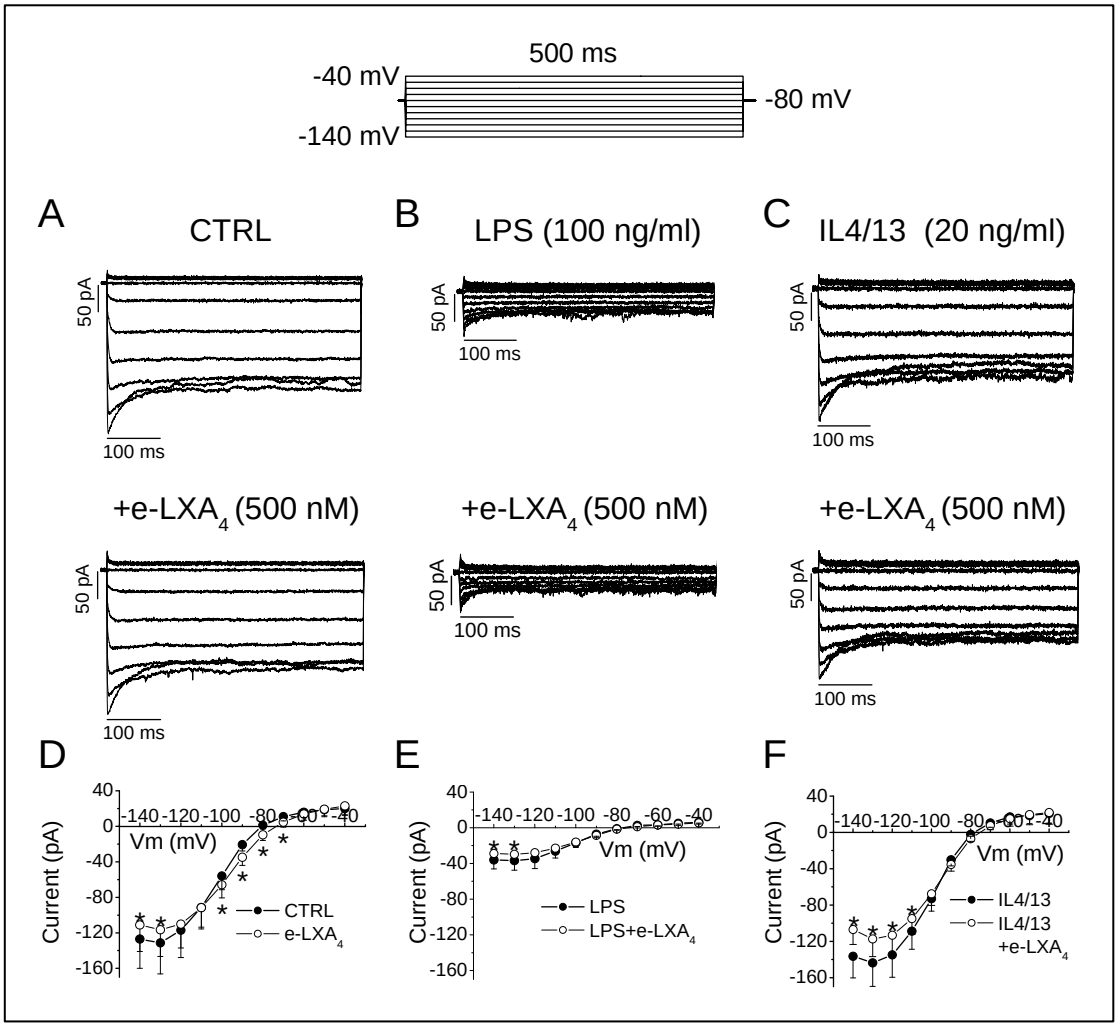

Figure 15. Acute effects of e-LXA_4 on K_{ir} currents. Representative traces of K_{ir} currents recorded in control, LPS and IL4/IL13 activated BMDM. BMDM were not stimulated **(A)** treated with LPS (100 ng/ml) **(B)** or IL4/IL13 (20 ng/ml) for 18h **(C)**. Current recordings were obtained in the absence and after perfusion with e-LXA_4 (500 nM**) (A-C)**. Currents were elicited by applying hyper- and depolarizing pulses from a holding potential of -80 mV to different voltages from -140 to -40 mV in 10 mV steps (500 ms duration). IV relationships in the absence and in the presence of e-LXA_4 (500 nM) in non-stimulated BMDM **(D)**, or LPS **(E)** and IL4/IL13 **(F)** activated BMDM are shown. IV plots show the mean±SEM. *P<0.05 *vs.* control; n>10 cells per group.

and LPS stimulated BMDM, by a higher degree of inactivation of the current. These early effects produced by e-LXA_4 on K_{ir} currents may suggest ALX receptor-independent effects.

4.1.4 Chronic effects of e-LXA_4 on K_v and K_{ir} channels of BMDM

Since e-LXA_4 produces changes in gene expression in addition to early signaling, the long-term effects of

e-LXA_4 were analyzed on K_v and K_{ir} currents. The effects of 18 h treatment with e-LXA_4 in resting or LPS-stimulated BMDM are shown in Figures 16-19. The effects of e-LXA_4 in IL4/IL13-stimulated BMDM were not studied due to the slight changes produced by IL4/IL13 on K_v and K_{ir} currents. Treatment of non-stimulated BMDM with e-LXA_4 (18 h) did not change the K_v outward current at any membrane potential tested (Figure 16A). However, the combined stimulation of BMDM with e-LXA_4+LPS significantly decreased K_v current at membrane potentials positive to -10 mV, reverting the magnitude of the current towards that observed in resting cells (546±152 pA *vs.* 178±48 pA, measured at the end of +60 mV pulses, P<0.05, n=7-9; Figure 16B).

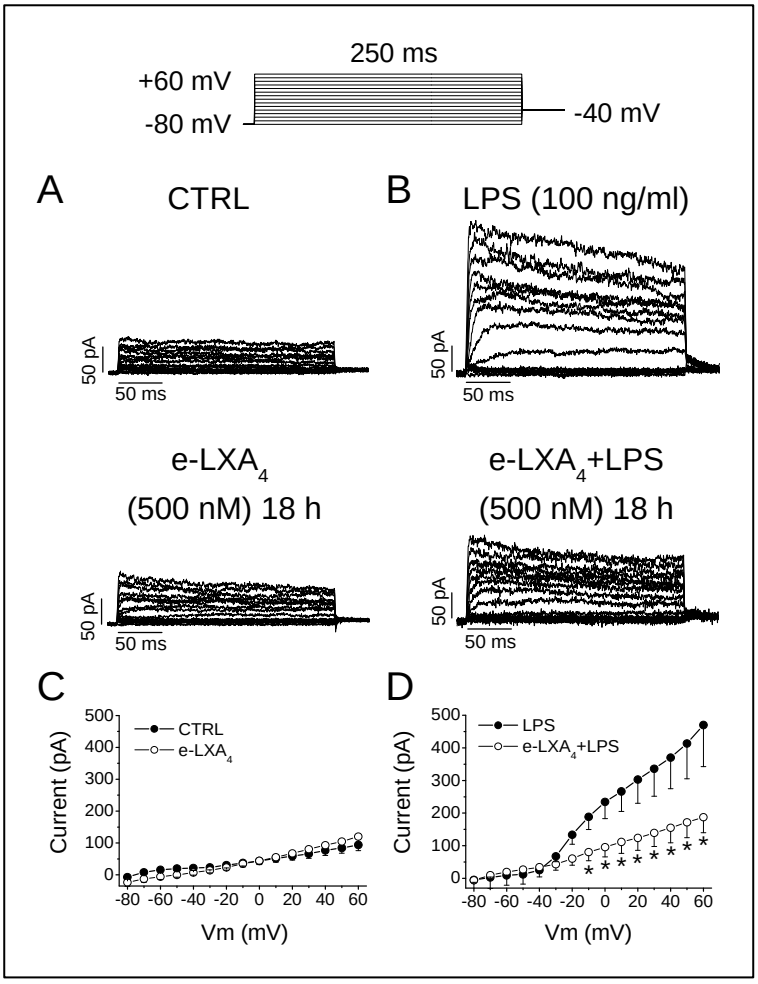

Figure 16. Effects of long-term treatment with e-LXA_4 on K_v currents. Representative traces of K_v currents recorded in non-stimulated and LPS-activated BMDM. Resting BMDM were incubated with e-LXA_4 (500 nM) for 18 h **(A)** or treated with LPS (100 ng/ml) and incubated with e-LXA_4+LPS for 18 h **(B).** Currents were elicited by applying depolarizing pulses from a holding potential of -80 mV to different depolarizing voltages from -80 to +60 mV in 10 mV steps (250 ms duration). IV relationships obtained in resting and LPS-stimulated BMDM after incubation with e-LXA_4 (500 nM) during 18 h **(C-D).** Results show the mean±SEM. *P<0.05 *vs.* control; n>10 cells per group.

As shown in Figure 17A-B, one of the characteristics of K_v recorded in LPS-activated BMDM is the use-dependent inactivation observed upon application of a train of stimuli. Figure 17A-B shows the chronic effects induced by e-LXA_4 (18 h) on the use-dependent inactivation of the K_v currents in resting and LPS-stimulated BMDM. e-LXA_4 did not modify the degree of use-dependent inactivation in resting BMDM (Figure 17B), as shown in the graphs representing the normalized peak K_v current during the application of train pulses. Interestingly, K_v generated by BMDM activated by e-LXA_4+LPS did not exhibit the use-dependent inactivation characteristic of K_v1.3 channels (Figure 17B). Similarly, incubation with e-LXA_4 did not modify the inactivation kinetics of resting BMDM, whereas it slowed this process in LPS-stimulated cells (1123±335 ms *vs.* 456±43 ms in cells incubated with e-LXA_4+LPS and LPS, respectively, P<0.05, n=6-11; Figure 17C-D).

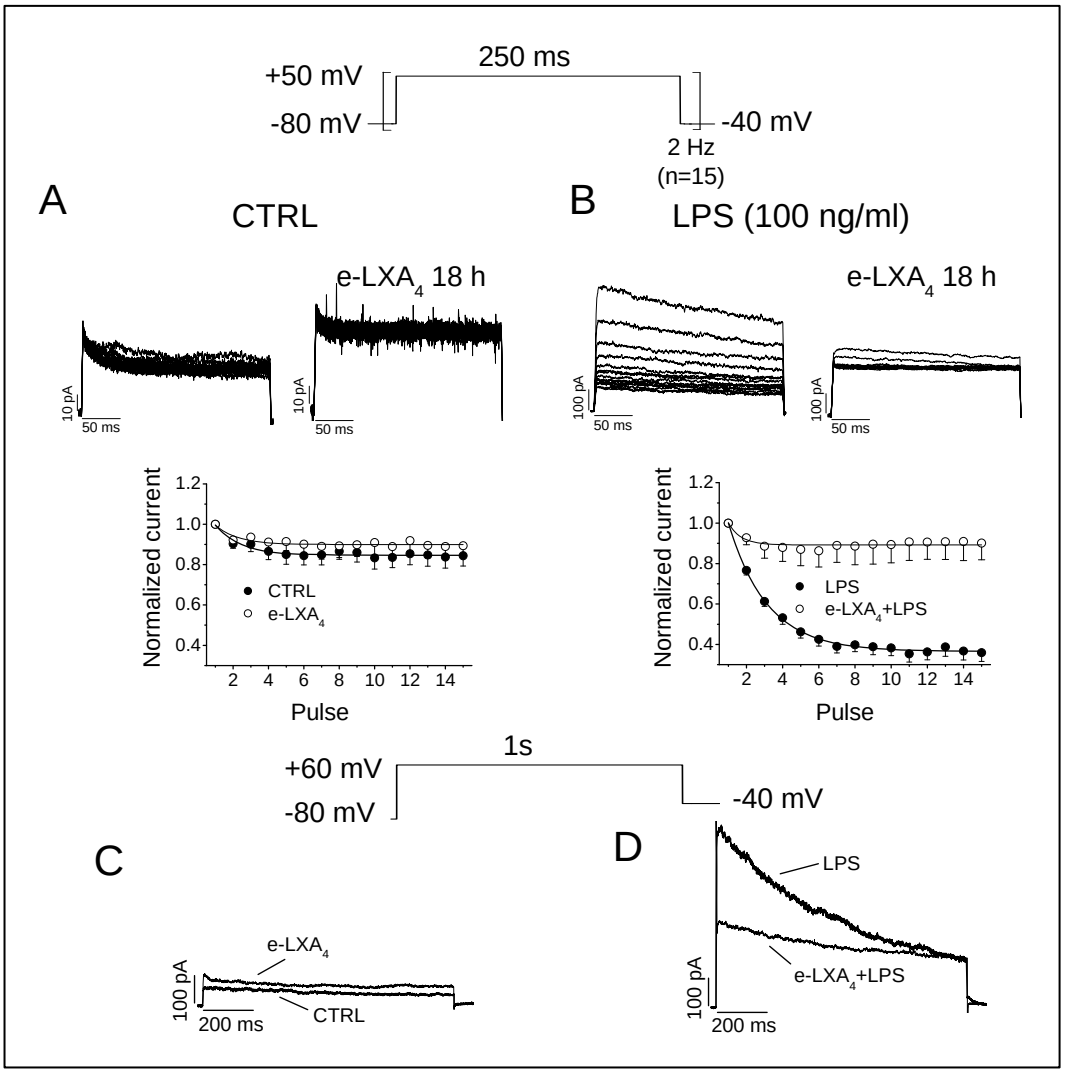

Figure 17. Effects of long-term treatment with e-LXA4 (500 nM) on K_v inactivation. Representative traces of K_v currents recorded in control or incubated with e-LXA4 (500 nM) **(A)** and in LPS-activated or incubated with e-LXA4 (500 nM)+LPS (100 ng/ml) BMDM cells **(B)** after applying the pulse protocol shown in the upper panel of the Figure. Plots show the normalized current measured at the maximum peak current during the application of a train of depolarizing pulses. Current records obtained after applying a depolarizing pulse of 1 s in cells not stimulated or incubated with e-LXA4 **(C)** and in LPS activated or incubated with e-LXA4 BMDM cells **(D)**. Note that incubation with e-LXA4 prevents the LPS-induced effects on use-dependent and kinetics of inactivation. Results show the mean±SEM. *P<0.05 *vs.* LPS; n>10 cells per group.

These results suggest that e-LXA4 prevents the LPS-induced changes in the stoichiometry of K_v channels, leading to the formation of heterotetramers with a lower K_v1.3:K_v1.5 ratio. Thus, the resulting phenotype closely resembles resting BMDM.

K_{ir} currents were recorded in BMDM by using the same pulse protocol described before and shown in the top of Figure 18A-B. Similarly to that observed in K_v currents, e-LXA4 did not modify K_{ir} current magnitude *vs.* resting BMDM (Figure 18A,C). However, in LPS-activated BMDM, e-LXA4 prevented LPS effects, increasing the K_{ir} current magnitude at membrane potentials negative to -90 mV (Figure18 B,D). Interestingly, in all the experiments in which cells were incubated with e-LXA4+LPS, e-LXA4 prevented the current biophysical characteristics towards the control situation. These results could be explained either by e-LXA4-induced changes

in the expression of both K_v and K_{ir} channels, or by post-translational channel protein modification. To address this question, the mRNA and protein levels were measured. Our data show an upregulation of the $K_v1.3$ mRNA by LPS that was impaired when cells were pre-treated with e-LXA_4 (Figure 19A). e-LXA_4 promoted a modest upregulation of

$K_v1.5$ mRNA that was suppressed by LPS or IL4/IL13. $K_{ir}2.1$ mRNA levels were downregulated by LPS, and to a lesser extent by IL4/IL13. Interestingly, when the protein levels were determined at 18 h (the time of evaluation of the biochemical and electrophysiological parameters), a significant increase of $K_v1.3$ and $K_{ir}2.1$ protein levels were

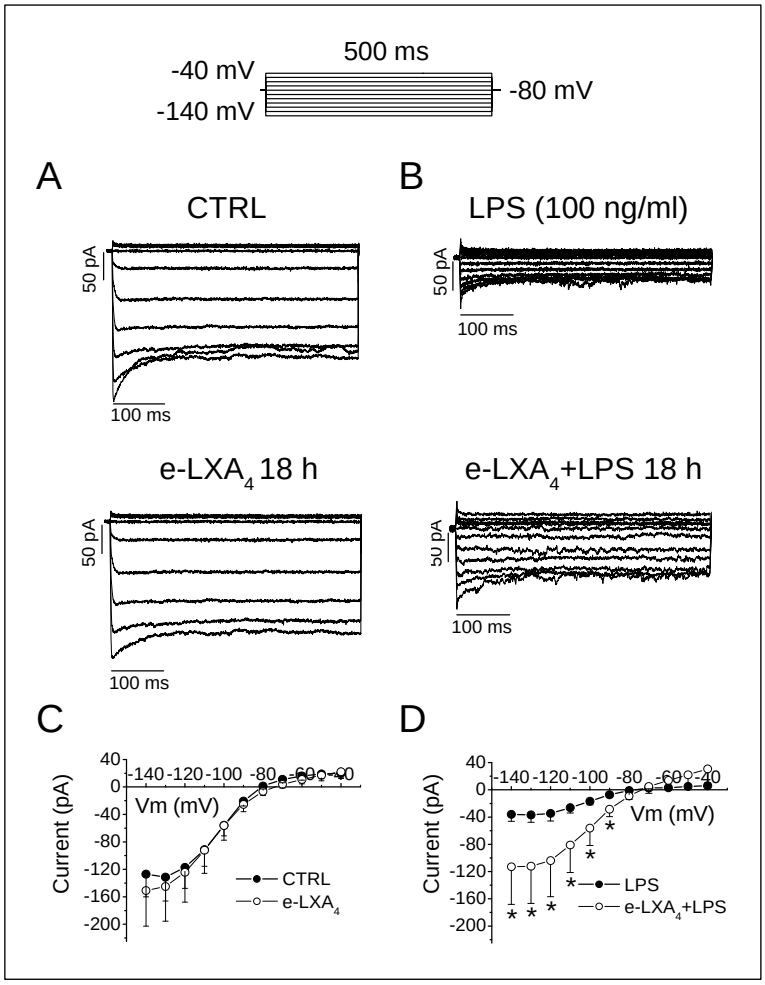

Figure 18. Effects of long-term treatment with e-LXA_4 (500 nM) on K_{ir} currents. Representative traces of Kir currents recorded in resting and LPS-activated (100 ng/ml) BMDM **(A-B, top panels)**. Resting and LPS-stimulated BMDM incubated with e-LXA4 for 18 h **(A-B, bottom panels)**. Currents were elicited by applying hyper- and depolarizing pulses from a holding potential of -80 mV to different depolarizing voltages from -140 to -40 mV in 10 mV steps (500 ms duration). IV relationships obtained in resting and LPS-stimulated BMDM cells after incubation with e-LXA4 during 18 h **(C-D)**. IV plots show the mean±SEM. *P<0.0 *vs.* control; n>10).

observed after challenge with LPS, an effect that was blunted by e-LXA_4 (Figure 19B). The mRNA and protein level changes of $K_v1.3$ and $K_v1.5$ are in agreement with the electrophysiological results shown above. However, there are controversial results for mRNA and protein levels of $K_{ir}2.1$. Moreover, the increase in the protein levels of $K_{ir}2.1$ does not correlate with the electrophysiological results observed, which could be attributed to posttranslational modifications as evidenced by the appearance of two adjacent bands in LPS-activated cells. Representative confocal microscopy images of the distribution of the fluorescence of $K_{ir}2.1$ show areas of aggregation, perhaps in specific intracellular environments (Figure 19C).

In another set of experiments we wanted to assess if the changes produced by e-LXA_4 in both resting BMDM and LPS-stimulated cells also modified either the endoplasmic reticulum release of Ca^{2+} or the influx via CRAC channels. Treatment of BMDM with thapsigargin (TG) induced in a transient increase in the $[Ca^{2+}]_i$ due to calcium

efflux from the intracellular stores. Subsequent addition of Ca^{2+} (1 mM) to the extracellular medium produced a further

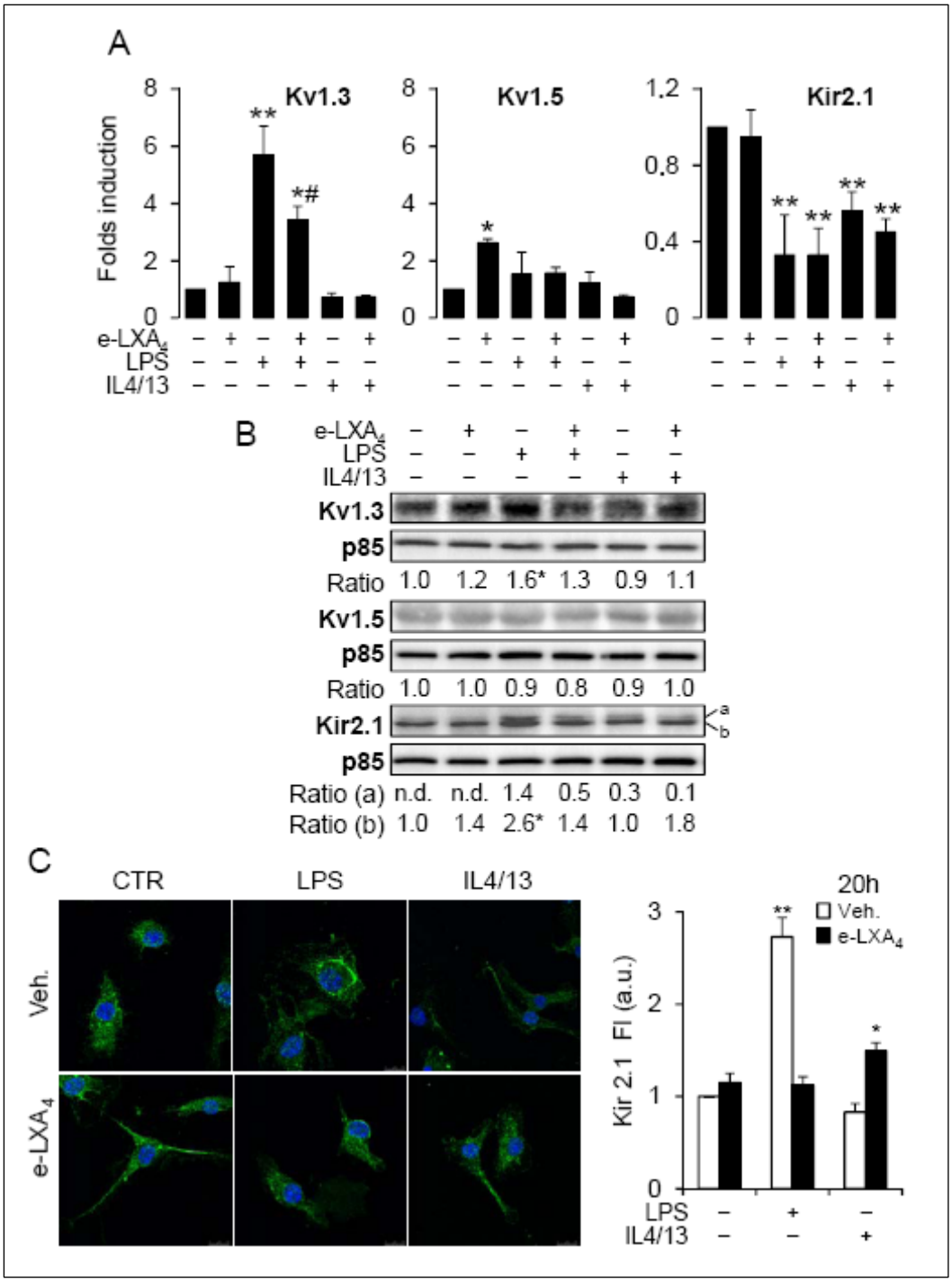

Figure 19. *Effects of e-LXA4 on K_v1.3, K_v1.5 and K_{ir}2.1 expression in activated BMDM.* Cells were incubated with 200 nM e-LXA_4 for 30 min prior to activation with LPS (100 ng/ml) or IL4/IL13 (20 ng/ml each). The mRNA levels of the channels were determined at 6 h after activation by real-time PCR **(A)**, and the protein levels of the channels were determined at 18 h by Western blot using specific Abs **(B)**. Immunolocalization of K_{ir}2.1 was determined by confocal microscopy after 20 h of stimulation with the indicated ligands and the intensity of the fluorescence was quantified using Image J software **(C)**. Data show the mean±SEM of three experiments **(A, C)**, representative blot out of three with indication of the relative band intensity (B) and representative immunocytochemistry images **(C).** *P<0.05, **P<0.01 *vs.* the control condition; #P<0.01 *vs*. the same condition in the absence of e-LXA_4. Veh: vehicle.

increase in $[Ca^{2+}]_i$ indicative of store-operated calcium entry. Figure 20 shows the effects produced by e-LXA_4 in

resting and LPS-stimulated BMDM on calcium release and calcium influx. Under all experimental conditions, Ca^{2+} release from intracellular stores was similar. When analyzing the Ca^{2+} influx mainly via CRAC channels, we observed that under resting conditions, e-LXA_4 did not produce significant changes in the fluorescence. The increase in fluorescence was greater in LPS-stimulated BMDM (P<0.01) and, interestingly, e-LXA_4 significant decreased fluorescence values in LPS-stimulated BMDM (P<0.01) (Figure 20).

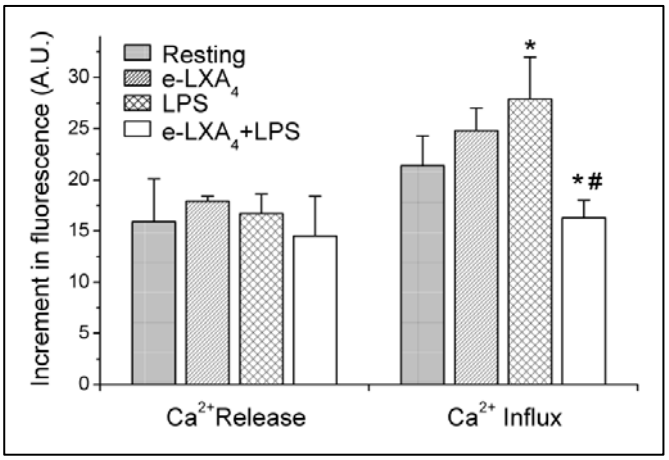

Figure 20. Effects induced by e-LXA_4 treatment on calcium handling. BMDM were resting or treated with e-LXA_4 (200 nM), LPS (100 ng/ml) or e-LXA_4 (200 nM) + LPS (100 ng/ml) during 18h. Then cells were loaded with FLUO4 and the calcium release (induced by thapsigargin) or calcium influx (induced by the addition of 1 mM $CaCl_2$) was detected using confocal microscopy. Results show the increment of fluorescence mean±SEM, *P<0.01*vs.* resting BMDM and #P<0.01 e-LXA_4+LPS *vs.* LPS BMDM n>8 cells per group.

4.1.5 e-LXA_4 produces its effects partially via ALX receptor

The biological effects of e-LXA_4 have been described to be mediated, at least in part, via ALX receptor (260,261). Using a selective ALX inhibitor (BocPLP; 1 μM) (262,263) >85% inhibition of the e-LXA_4 dependent

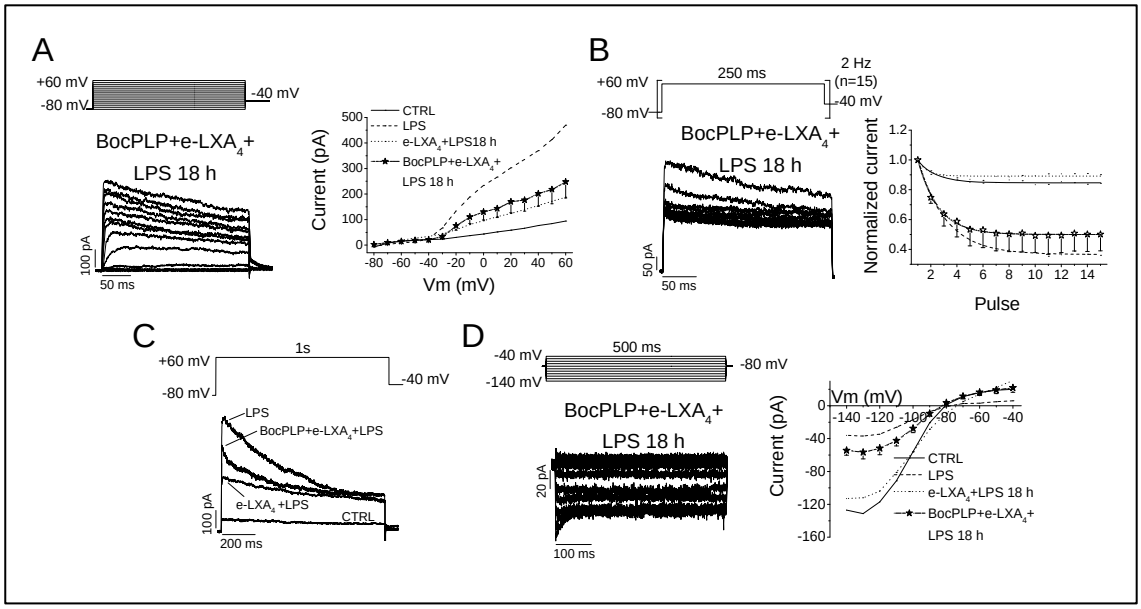

Figure 21. e-LXA_4 produces its effects partially via interaction with ALX. Effects of pre-treatment with e-LXA_4 on K_v currents recorded in LPS-activated BMDM in the presence of an ALX antagonist (BocPLP). K_v currents were slightly reverted *vs.* those recorded in LPS-activated BMDM pre-treated with e-LXA_4 **(A)**. Similar effects were observed on the use-dependent inactivation **(B)** and on the time course of inactivation observed after applying 1s-depolarizing pulses **(C).** K_{ir} currents were reverted versus K_{ir} currents recorded in LPS-activated BMDM pretreated with e-LXA_4 **(D)**. Note that the effects of e-LXA_4 on K_v were slightly receptor-dependent, whereas those produced on K_{ir} current are highly receptor-dependent. n>10 cells per group. IV plots show the mean±SEM. *P<0.05 *vs.* control; n>10.

ERK phosphorylation was observed (data not shown). Figure 21 shows the effects of BocPLP on K_v and K_{ir} currents and the IV relationships in different combinations of LPS and e-LXA_4 BMDM treatments, indicating that the effects of e-LXA_4, on both K_v and K_{ir}, appear to be partially mediated via ALX receptor. The biophysical characteristics of K_v currents were very similar to those recorded in cells activated with LPS and to a lesser extent to e-LXA_4+LPS. However, as shown in the K_v IV relationship (Figure 21A), the mean magnitude of the current resulted to be slightly smaller than that recorded in cells activated with LPS, and somewhat greater than that obtained after stimulating with e-LXA_4+LPS (Figure 21A).

In addition, K_v currents still exhibit cumulative inactivation as occurred in LPS stimulated cells in the absence of e-LXA_4 (Figure 21B). Regarding this effect, the K_v inactivation recorded in BMDM stimulated with e-LXA_4+LPS in the presence of BocPLP was intermediate between those observed in LPS and e-LXA_4+LPS stimulated cells (Figure 21B,C), suggesting that the effects of e-LXA_4 on K_v currents are partially ALX-receptor dependent. In agreement with this hypothesis is the fact that a significant reduction of K_v current was observed when LPS-stimulated BMDM were perfused with e-LXA_4. Concerning the effects of BocPLP on the K_{ir} current in BMDM stimulated with e-LXA_4+LPS, we observed that the inward current was similar to that recorded in LPS-activated BMDM (Figure 21D).

4.1.6 e-LXA_4 effects are dose-dependent

Finally, since antiinflammatory actions of e-LXA_4 have been also observed at very low concentrations, the effects of 100 nM e-LXA_4 were analyzed on K_v and K_{ir} currents recorded in BMDM activated with LPS (Figure 22). As shown in Figure 22, the effects of 100 nM e-LXA_4 on the magnitude of K_v currents were smaller than those induced by 500 nM e-LXA_4. Moreover, pre-treatment with 100 nM e-LXA_4 did not abolish the use-

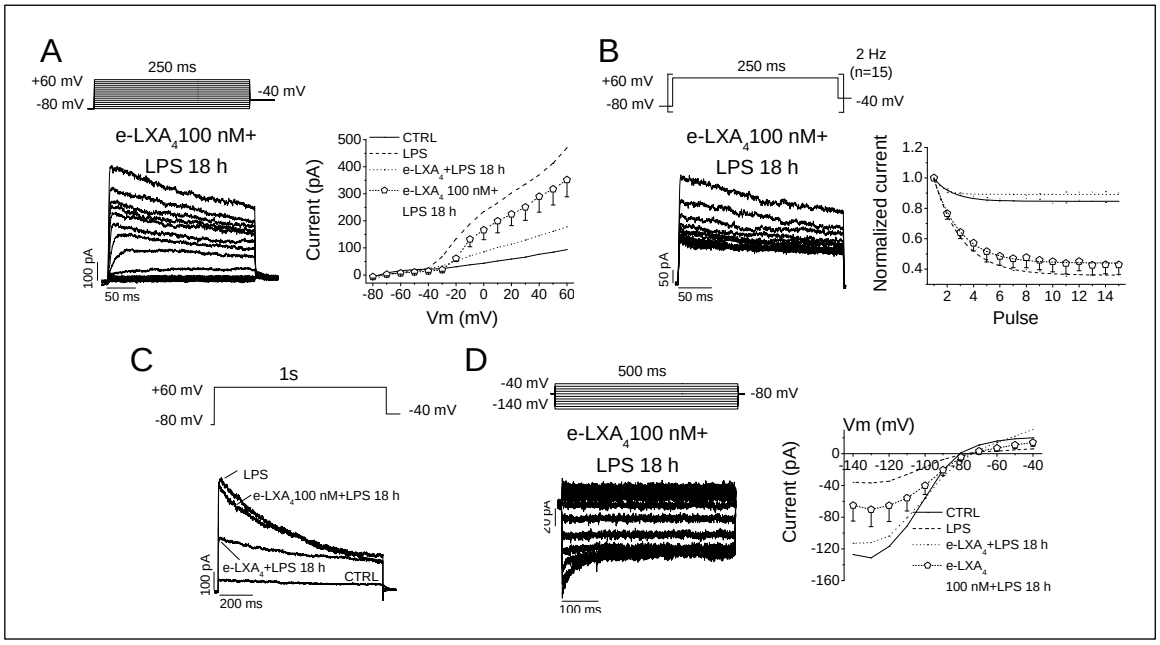

Figure 22. Effects produced by lower concentrations of e-LXA_4 (100 nM): On K_v magnitude. **(A)**, use dependent inactivation **(B)**, time course of inactivation of K_v currents **(C)** and K_{ir} current **(D)**. Note that the effects of e-LXA_4 were concentration dependent. Results show the mean±SEM, n>10 cells per group

dependent inactivation, as 500 nM did (Figure 22B). In addition, the time course of inactivation was very similar to that observed in BMDM activated with LPS (Figure 22C). Concerning to the action of 100 nM e-LXA_4 on K_{ir} channels, this lower concentration partially reverted the effects induced by LPS, but to a lesser extent than 500 nM e-LXA_4 (Figure 22 A,D). All these results suggest that the effects of e-LXA_4 are concentration-dependent.

.

4.2 EFFECTS OF n-3 PUFAs ON K_v7.1/KCNE1 CURRENT

4.2.1 EPA and DHA increase K_v7.1/KCNE1 current magnitude

The concentration of EPA or DHA (20 µM) used in this study was selected on the basis of the free fatty acid levels in the plasma of 6 patients included in the Study on Omega-3 Fatty Acids and Ventricular Arrhythmia (SOFA) trial (264) who were taking 2 g/day fish oil. In this clinical trial, plasma free fatty acids were measured by gas-liquid chromatography (265). From this study it was showed that the average concentration of free EPA and DHA was ~10 µM (range, 5.0 to 16.4 µM). Figure 23A shows original K_v7.1/KCNE1 records obtained after applying 12 s depolarizing pulses from a holding potential of -80 mV to +60 mV in the absence and in the presence of 20 µM EPA and DHA. Both PUFAs increased the current magnitude by 37.3±6.2% (P<0.05, n=13)

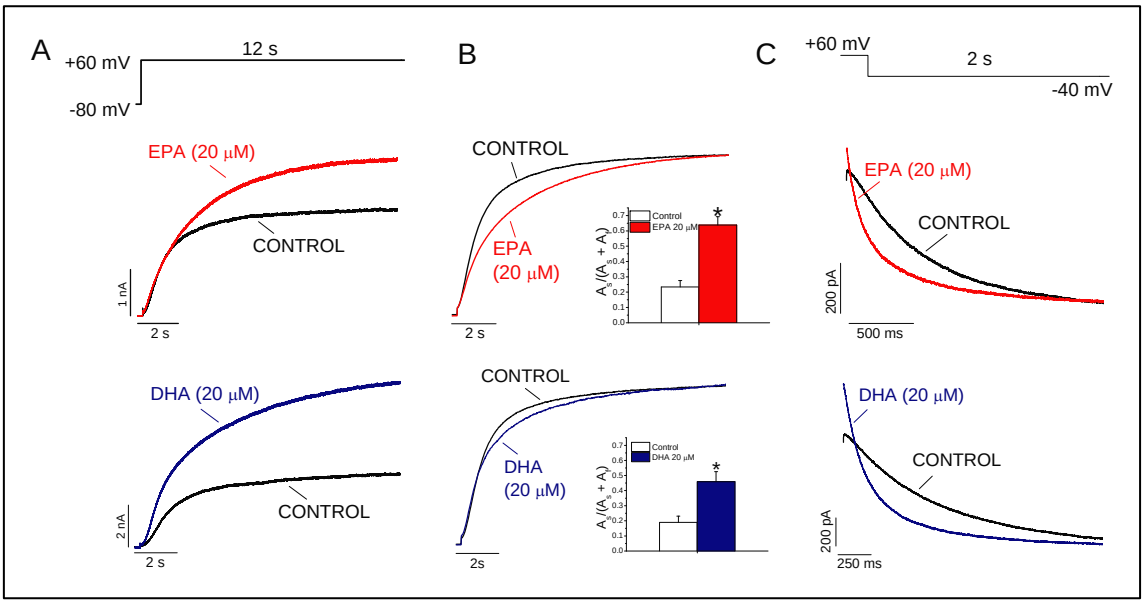

Figure 23. Acute effects of DHA and EPA on K_v7.1/KCNE1 current. Effects of EPA and DHA (20 µM) on the current elicited by the activation of K_v7.1/KCNE1 during depolarizing pulses from a holding potential of -80 mV to +60 during 12 s. **(A)**: Original traces of K_v7.1/KCNE1 obtained in the absence and in the presence of EPA (top) or DHA (bottom). **(B)**: Normalized traces to matching control. The inset represents the plot of the $A_s/(A_s+A_f)$ in control and in the presence of each PUFA. **(C)**: Tail currents recorded at -40 mV after the application of 5.5s depolarizing pulse to +60 mV in the absence and in the presence of each PUFA. Results show the mean±SEM. *P<0.05 *vs.* control; n=8-16 cells per group.

and 82.8±27.0% (P<0.05 n=13) for EPA and DHA respectively. The increase induced by EPA was time-dependent, being this effect greater when the current magnitude was measured after longer depolarizing pulses (3.6±6.2%, 28.4±5.3%* and 37.3±6.2%* after 1.5, 5.5 and 12 s, respectively, *P<0.05, n=5-13).

The onset of K_v7.1/KCNE1 activation, after 150 ms, is better described by a two exponential process. Figure 23B shows the normalized currents obtained under control conditions and after exposure to EPA (20 µM) and DHA (20 µM). This process followed a biexponential process. Under control conditions, the activation time constants arose mean values of τ_f=737±53 ms and τ_s=4604±542 ms (n=16). The most relevant effect produced by EPA was to slow the activation kinetics due to an increased contribution of the slow component to the to the

total activation process ($A_s/(A_s+A_f)$=0.23±0.04 *vs.* $A_s/(A_s+A_f)$=0.64±0.05 for control and acute EPA respectively, P<0.05, n=8) (Figure 23B inset). The time constants were not modified (τ_f =653±56 ms and τ_s=4106±796 ms, P>0.05, n=8). In the presence of DHA, the total activation process was also slowed due to an increased contribution of the slow component of activation ($A_s/(A_s+A_f)$=0.19±0.04 *vs.* $A_s/(A_s+A_f)$=0.46± 0.07, for control and acute DHA respectively P<0.05, n=8). However, DHA slightly accelerated the fast component of activation (τ_f=592±52* ms and τ_s=3506±560 ms, *P<0.05, n=8)**.** The increase of the current induced by DHA was not time when measured after 1.5, 5.5 or 12 s depolarizing pulses (91.8±19.3%, 92.7±23.8% and 82.8±26.9%, P>0.05, n=4-13, respectively).

Tail currents were elicited upon repolarization to -40 mV after each voltage step. An increase in the tail current magnitude of 12.6±5.2% (P<0.05, n=13) and 27.3±13.3% (P<0.05, n=9) after exposure to EPA and DHA, respectively was observed, being this increase similar for both PUFAs (Figure 23C). Under control conditions the deactivation exhibited monoexponential kinetics. EPA and DHA modified the deactivation kinetics, in such a way that in the presence of either PUFA the kinetics of the tail currents became biexponential (Table 3).

Table 3. Time-dependent effects of EPA and DHA (20 µM) on the deactivation process of K_v7.1/KCNE1 channels. Tail currents were recorded at -40mV pulses after a depolarizing pulse to +60mV of 5.5s in duration and were fitted to a monoexponential function or a biexponential funtion in the case of EPA.

CONTROL	Acute EPA 20 µM		CONTROL	Acute DHA 20 µM	
τ (ms)	τ_f (ms)	τ_s (ms)	τ (ms)	τ_f (ms)	τ_s (ms)
531.4±52.9	121.3±7.0	490.0±110.9	585.0±63.2	131.8±18.2	695.6±118.8

4.2.2 Voltage-dependent effects of acute EPA

Figure 24 shows the voltage-dependent effects produced by EPA on K_v7.1/KCNE1 current. Figure 24A shows current records obtained in the absence and in the presence of EPA when applying 5.5 s depolarizing pulses from -80 mV to +60 mV in 10 mV-steps from a holding potential of -80 mV. After the application of depolarization pulses, membrane potential was repolarized to -40 mV to record the tail currents. EPA (20 µM) increased the amplitude of the current at all membrane potentials tested positive to -10 mV (Figure 24B). EPA shifted the midpoint of the activation curve towards more negative potentials (+22.3±6.6 mV *vs.* +13.5±5.5 mV, before and after perfusion with EPA, P<0.05, n=5) without modifying the slope values (16.7±1.3 mV *vs.* 18.6±1.7 mV, P>0.05, n=5) (Figure 24C). In Figure 24D the relative current in the presence of EPA was plotted versus the membrane potential. The maximal increase occurred at ~10 mV. This effect might be due to the negative shift of the activation curve, suggesting that the primary mechanism of the increased magnitude of K_v7.1/KCNE1 might be due to an effect on channel gating. Similar qualitative effects were produced by DHA, although this PUFA did not significantly shift the midpoint of activation or the slope factor of the activation curve (Figure S2).

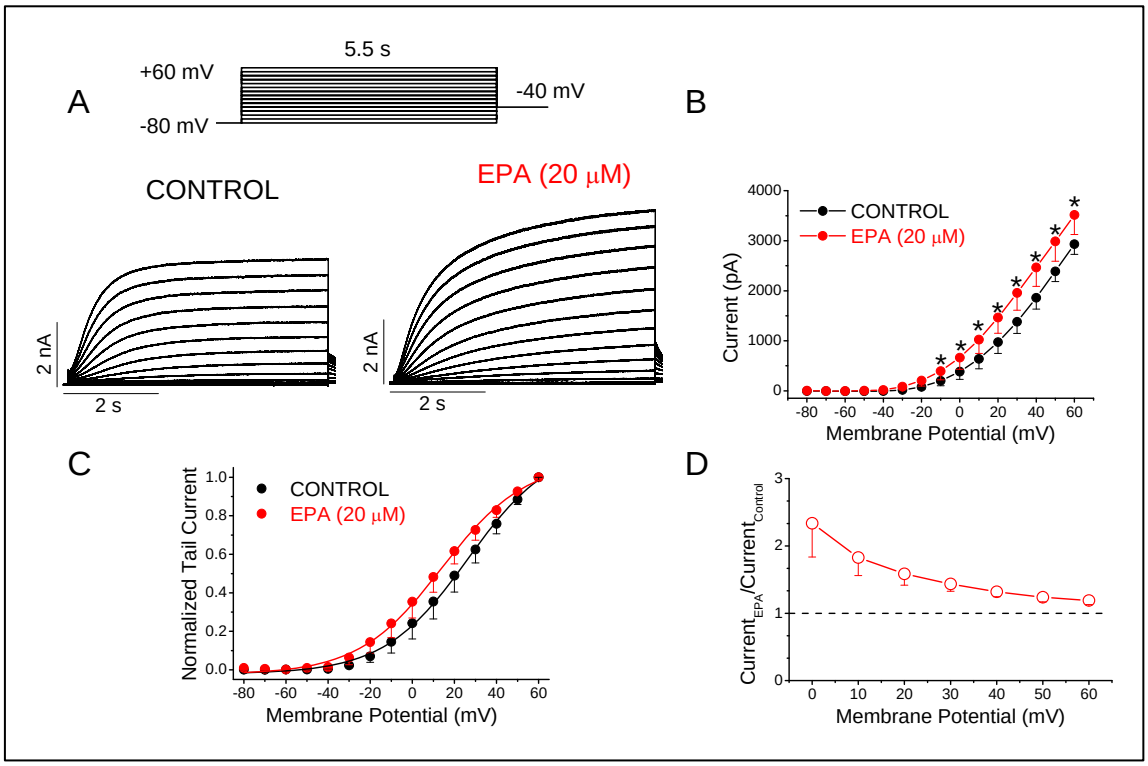

Figure 24. Voltage dependent effects of acute EPA on K_v7.1/KCNE1 current. **(A)**: Traces obtained after applying the pulse protocol shown in the top in the absence and in the presence of EPA. **(B)**: IV relationship obtained under control conditions and after perfusion with EPA. **(C)**: Activation curves obtained under control conditions and after perfusion with EPA. **(D)**: Graph showing the ratio between the current obtained in the presence of EPA and that under control conditions. Results show the mean±SEM. *P<0.05 *vs.* control; n=5 cells.

4.2.3 Acute *versus* chronic effects of EPA on K_v7.1/KCNE1 current

It has been described that increased consumption of n-3 PUFAs leads to increased blood levels of n-3 PUFAs (264,266) and n-3 PUFAs incorporation to various tissues (267). However, the relative contribution of acute versus long term administration on the electrophysiological effects on ion currents has not been determined. In order to differentiate the acute from the possible chronic effects of EPA and DHA, three different approaches were used. Firstly, the electrophysiological properties of K_v7.1/KCNE1 after incubation of COS7 cells for 48 h with EPA 20 μM in serum-free medium were assessed. Chronic incubation with EPA did not alter the activation kinetics of K_v7.1/KCNE1 (τ_f=737±53 ms and τ_s=4604±542 ms *vs.* τ_f=613±62 ms and τ_s=5376±1745 ms, P>0.05, n=5-16, for control conditions and chronic EPA respectively, Figure 24A, 25A). However, the activation process was slightly accelerated compared to acute EPA due to a reduced contribution of the slow component to this process ($A_s/(A_s+A_f)$=0.56±0.04 *vs.* $A_s/(A_s+A_f)$=0.30±0.06, for acute and chronic EPA respectively, P<0.05, n=5-8). The tail current kinetics was faster than under control conditions, becoming a biexponential process (τ_f=179±16 ms and τ_s=628±95 ms). However, the fast time constant of deactivation, was slower than when EPA was added acutely (τ_f=179±16 ms *vs.* τ_f=124±7 ms, for chronic and acute EPA respectively, P<0.05, n=5-18) (Figure 25C)

It is interesting to note that chronic EPA induced a more depolarized threshold of activation in

comparison with control values (-10 mV *vs.* 0 mV for control conditions and chronic EPA respectively) (Figure 25C).This effect was accompanied by a shift of the activation curve towards more positive potentials (V_{mid}=24.8±2.6 mV *vs.* V_{mid}=34.4±3.9 mV, P<0.05, n=14-5, for control conditions and chronic EPA respectively) (i.e. EPA induces opposite effects after incubating the cells with this PUFA during 48 h than when they were perfused acutely with this PUFA (Figure 25D).

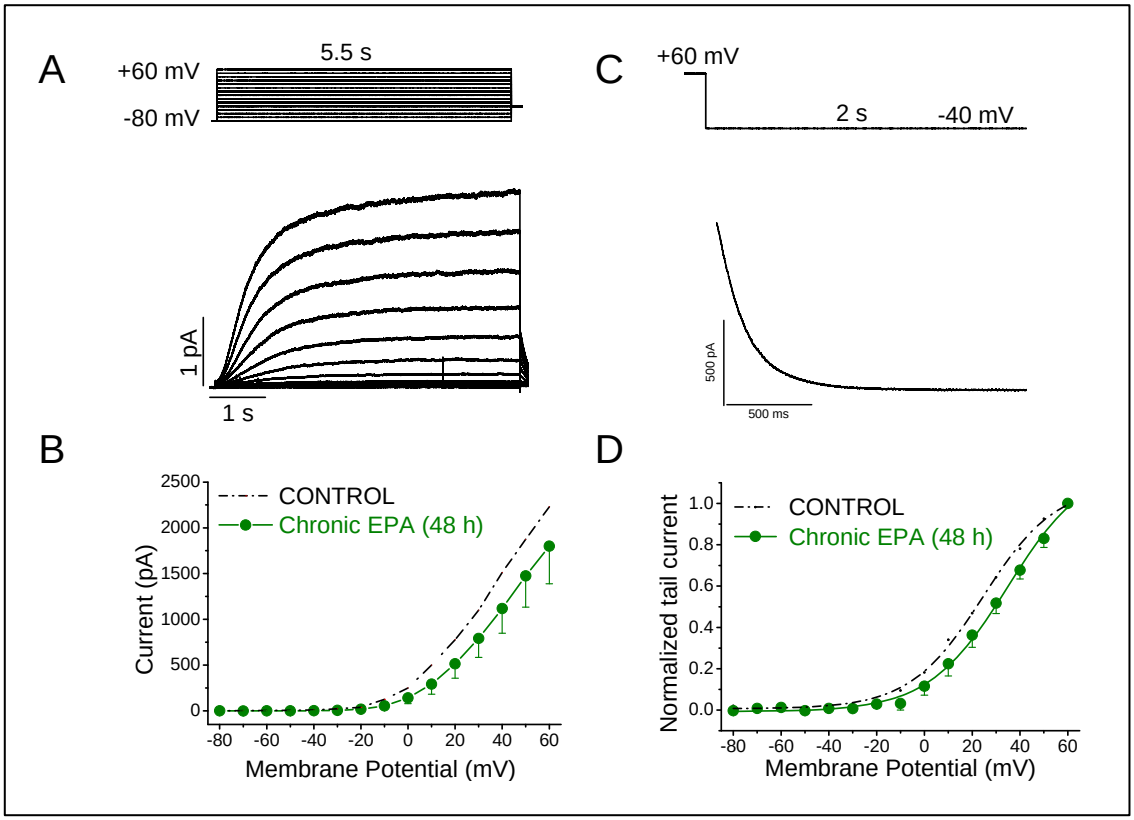

Figure 25. Electrophysiological effects of chronic incubation (48 h) with EPA on K_v7.1/KCNE1. (**A**): Currents are shown for depolarizations from -80 mV to voltages between -80 and +60 mV in steps of 10 mV. Tail currents were obtained on return to -40 mV. **(B)**: IV relationship obtained after measure the current after 5.5 s at all membrane potentials. **(C)**: Original tail records obtained during repolarization to -40 mV after a 5.5 s depolarization to +60 mV. **(D)**: Activation curves of K_v7.1/KCNE1 current obtained after representing the normalized tail current amplitude versus the previous step potential recorded in cells incubated for 48 h with EPA. Results show the mean±SEM of 4-8 cells per group.

4.2.4 Effects of EPA incubation on K_v7.1 and KCNE1 protein levels

In a previous study (212), it was reported that chronic treatment (48 h) with EPA and DHA, but not with α-linolenic acid, decreased protein levels of K_v1.5 in *Ltk*$^-$ cells. Thus, our second approach was to analyze if chronically applied EPA and DHA were able to modify the expression pattern of K_v7.1 and KCNE1 proteins. In order to asses this issue, COS7 cells were transfected with K_v7.1-YFP alone or together with KCNE1-CFP, and the levels of K_v7.1 and KCNE1 were measured by western blot. Under both experimental conditions, EPA (30 and 100 μM) reduced the levels of K_v7.1 protein in a concentration-dependent manner (Figure 26A) but not those of KCNE1 (Figure 26B). Since COS7 cells were transiently transfected with the cDNA encoding K_v7.1 was cloned

into a vector with a CMV promoter, it is unlikely that EPA would decrease the expression of $K_v7.1$. In addition, it has been demonstrated that internalization and stability of $K_v7.1$ is regulated by ubiquitylation (268) and that n-3

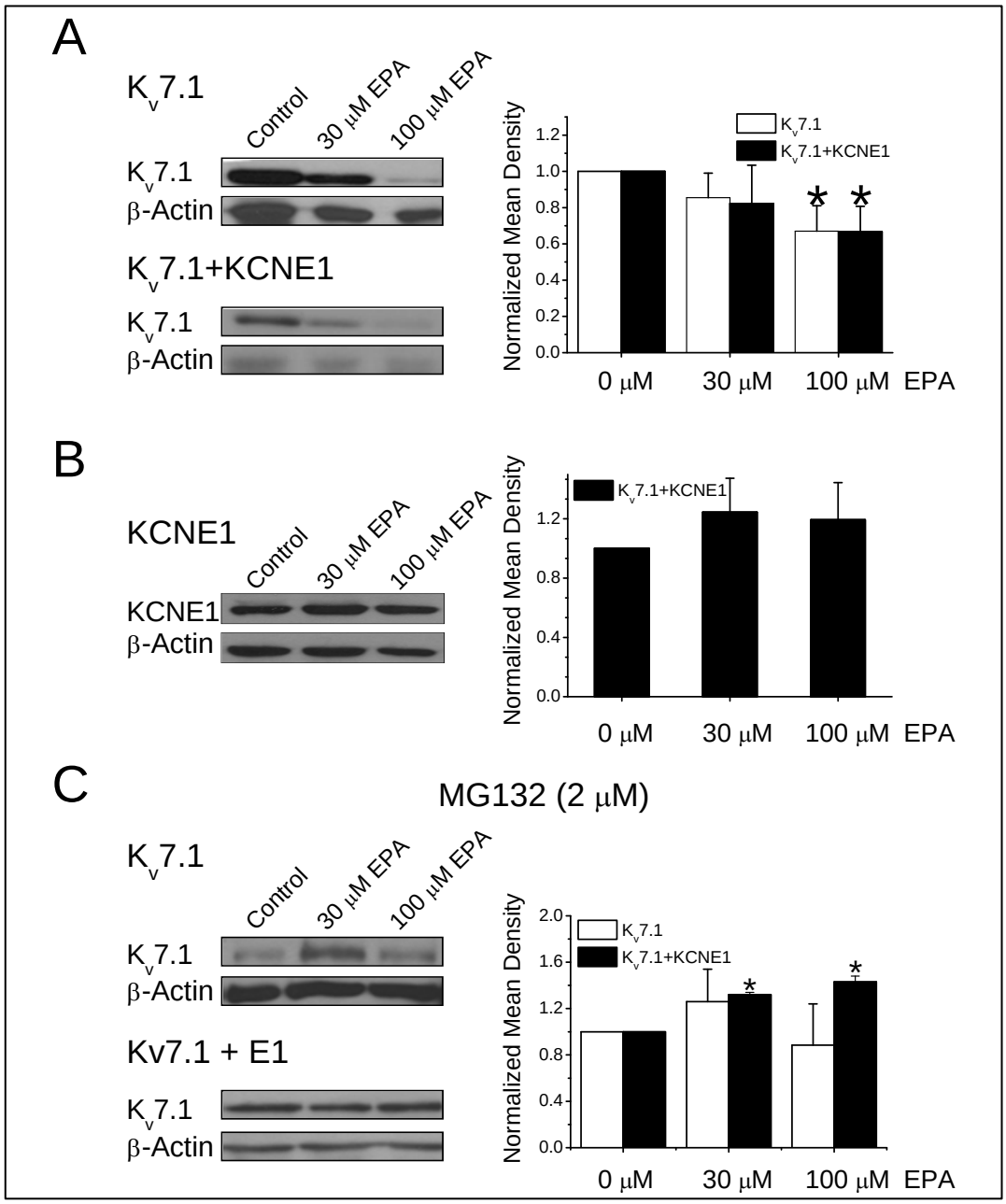

Figure 26. EPA decreases steady-state levels of $K_v7.1$ protein. **(A)**: Left: Shown are representative western blots that illustrate treatments with EPA. Note that EPA induces dose-dependent reductions of $K_v7.1$ protein. Cellular lysates were prepared from COS7 cells transiently expressing $K_v7.1$ and incubated for 48 h with EPA at two concentrations (30 and 100 µM). Right: Bar graph summarizing densitometry measurements used to compare protein levels for the treatments of EPA for 48 h. β-actin levels were used as a loading control (*P<0.05, n=3-4). **(B)**: Representative western blots and graph showing the effects of EPA (30 and 100 µM) on KCNE1 in cells transfected with $K_v7.1$/KCNE1. **(C)**: Representative western blots and graphs showing the effects of EPA (30 and 100 µM) on $K_v7.1$ in the presence of MG132 (proteasome inhibitor). Bar graphs shows the mean±SEM of 3-4 experiments per group. *P<0.05 *vs.* control

PUFAs are able to modify the activity of the proteasome. Therefore, the decrease in $K_v7.1$ protein level might be due to a higher degree of $K_v7.1$ degradation via proteosoma. Hence, a series of experiments in the presence of a proteasome inhibitor (MG132, 2 µM) were performed. Figure 26C shows western blots of these experiments as

well as the quantification of the images referred to the β-actin used as a load control. Under these experimental conditions, EPA did not produce any change in the protein levels of $K_v7.1$, thus suggesting that EPA induces degradation of $K_v7.1$ via proteasome. Similar results were obtained when the cells were treated with DHA (Figure S3).

4.2.5 Effects of EPA on the location of $K_v7.1$ and KCNE1 subunits in the plasma membrane

$K_v7.1$ channels and KCNE1 subunits target lipid rafts in eukaryotic cells (269). Lipid rafts are membrane microdomains enriched in cholesterol and sphingolipids. Because of their high lipid content, lipid rafts are detergent insoluble at 4ºC, allowing the identification and study of lipid rafts-associated molecules in density gradients after centrifugation. As mentioned before, dietary administration of n-3 PUFAs leads to the incorporation of these compounds into all membranes including myocardial membranes of the heart (195,213). Once incorporated, n-3 PUFAs alter the lipid composition and protein distribution of the membrane lipid raft and thus the environment of the ion channel, which could affect its function. Thus, the third approach we used was to analyze possible changes in the location of $K_v7.1$ and/or KCNE1 in lipid rafts. 48 h post-transfection, lipid rafts were purified from low density fractions (top fractions) of flotation gradients. Figure 27 shows the distribution of $K_v7.1$ and KCNE1 over the sucrose gradient under control conditions and after incubation with EPA for 48 h. As

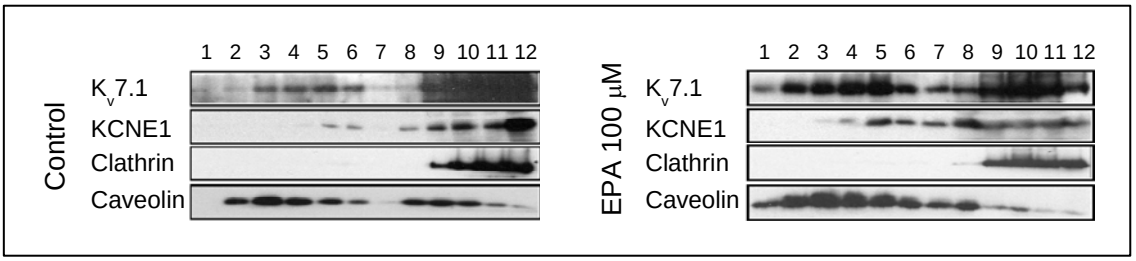

Figure 27. Chronic effects of EPA on $K_v7.1$ and KCNE1 location. Sucrose density gradient fractions of cells expressing $K_v7.1$ and KCNE1 in the absence **(A)** or in the presence of EPA **(B)**. Caveolin indicated floating lipid rafts with low density, clathrin labeled non-raft fractions. $K_v7.1$ and KCNE1 colocalized with caveolin in low-buoyant density fractions (fractions 2-6) in control experiments, whereas EPA triggered a wider distribution of proteins (fractions 1-12) and rafts. Pictures are representative images of at least 3 independent lipid rafts extractions analysed by western blot.

previously described, both channel subunits target lipid rafts. EPA triggered a wider distribution of $K_v7.1$ and KCNE1 that can account, at least in part, for some of the electrophysiological changes observed on $K_v7.1$/KCNE1. Similar results were obtained when the cells were treated with DHA (Figure S4).

4.2.6 Effects of cholesterol depletion on $K_v7.1$/KCNE1 current

Association with lipid rafts is an important mechanism for signaling protein and ion channel function. Changes in the composition of these microdomains or their complete disruption modify the activity of several ion channels. For example, it was found that lipid raft disruption increased the transient receptor potential cation channel subfamily M member 8 (TRPM8) current suggesting that channel activity is higher outside of these

microdomains (270).

As we found that n-3 PUFAs modifiy the association between these potassium channels and lipid rafts, we wanted to analyze the electrophysiological consequences of the disruption of these structures on K_v7.1/KCNE1. To that end, COS7 cells were perfused with different external solutions in the following order: 1) methyl-beta-cyclodextrin (MβCD, 10 mM), agent capable to deplete membrane cholesterol; 2) EPA 20 µM and 3)

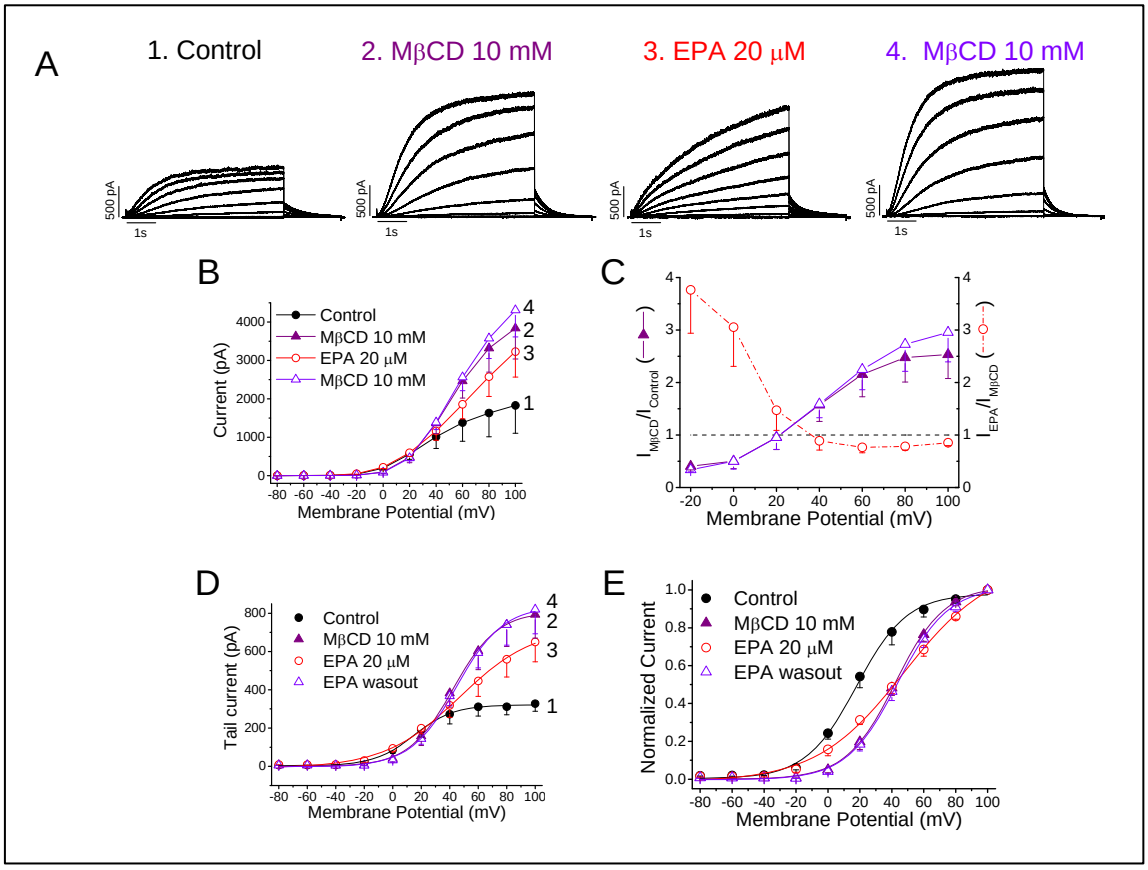

Figure 28. Effects of acute EPA in membrane cholesterol depleted cells. **(A)**: Representative traces of K_v7.1/KCNE1 current under control conditions, after perfusion with MβCD for 40 min, perfusion with EPA and washout with EPA-free external solution. All records were obtained from the same cell. **(B)**: IV relationships under these experimental conditions. **(C)**: Graph showing the ratio between the current magnitudes obtained after perfusion with MβCD divided by current under control conditions, as well as current recorded in the presence of EPA divided by current recorded after perfusion with MβCD. Activation curves obtained under all the experimental conditions before **(D)** and after normalization **(E)**. IV and activation curve plots showing the mean±SEM of 4 cells.

drug-free external solution. Upon perfusion of the cells with MβCD, an increase of the K_v7.1/KCNE1 was observed at membrane potentials positive to +30mV and a decrease of the current at membrane potentials negative to +30 mV (Figure 28A-E). These effects appeared in a parallel way to a positive shift of the activation curve ~+23 mV ($P<0.05$, n=4) (Table 4). Under these experimental conditions, perfusion with EPA produced similar effects than those observed in cells non-treated with MβCD. Indeed, EPA produced an increase of the current at membrane potentials negative to +40 mV and did not shift the midpoint of the activation curve in comparison to that obtained in the presence of MβCD, but it increased its slope factor (Table 4). The effects produced by EPA were accompanied by the typical slowing down of the activation kinetics that was due to the abolishment of the fast component of the activation process (Table S1A) and the appereance of a second

component of deactivation, becoming this process biexponential (Table S1B). EPA effects produced in cells cholesterol depleted with MβCD were reversible, not only in the magnitude of the current, but also in the kinetics and in the activation curve (Figure 28).

Table 4. Modulation of the gating properties of $K_V7.1$/KCNE1 channels by acute EPA in cholesterol depleted cells. Results show the mean±SEM of 4 cells. *P<0.05 *vs.* the control condition and #P<0.05 *vs.* MβCD 10 mM perffusion. Currents were elicited in 10-mV increments to test potentials ranging from -80 to +60 mV from a holding potential of −80 mV. Peak tail currents were measured, and the normalized data were fit to a Boltzmann function.

CONTROL		**MβCD 10 mM**		**EPA 20 µM**		**MβCD 10 mM**	
V_{mid} (mV)	s (mV)	V_{mid} (mV)	s (mV)	V_{mid} (mV)	s (mV)	V_{mid} (mV)	s (mV)
18.9±3.6	15.7±4.1	42.2±5.9*	15.2±4.1	48.3±2.8	26.8±5.1*#	43.9±6.8	15.6±1.2

4.3 A NEW MUTATION ON K_v7.1 ASSOCIATED WITH SHORT QT SYNDROME

4.3.1 Patient characteristics: clinical analysis and genetics

The index case of the family was a 37 years old man who dropped dead unexpectedly while working as a postman. Apparently, he had no history of syncopal episodes nor other cardiac symptoms prior to death, and the information obtained from relative's interview did not demonstrate the cause of the death. Full report from post-mortem study was not available to review.

His son, an athletic and healthy 23 years old was referred recently for cardiac evaluation. ECG showed sinus bradycardia of 55 bpm, normal PR, QRS, and a slightly short QTc interval of 356 ms with prominent T

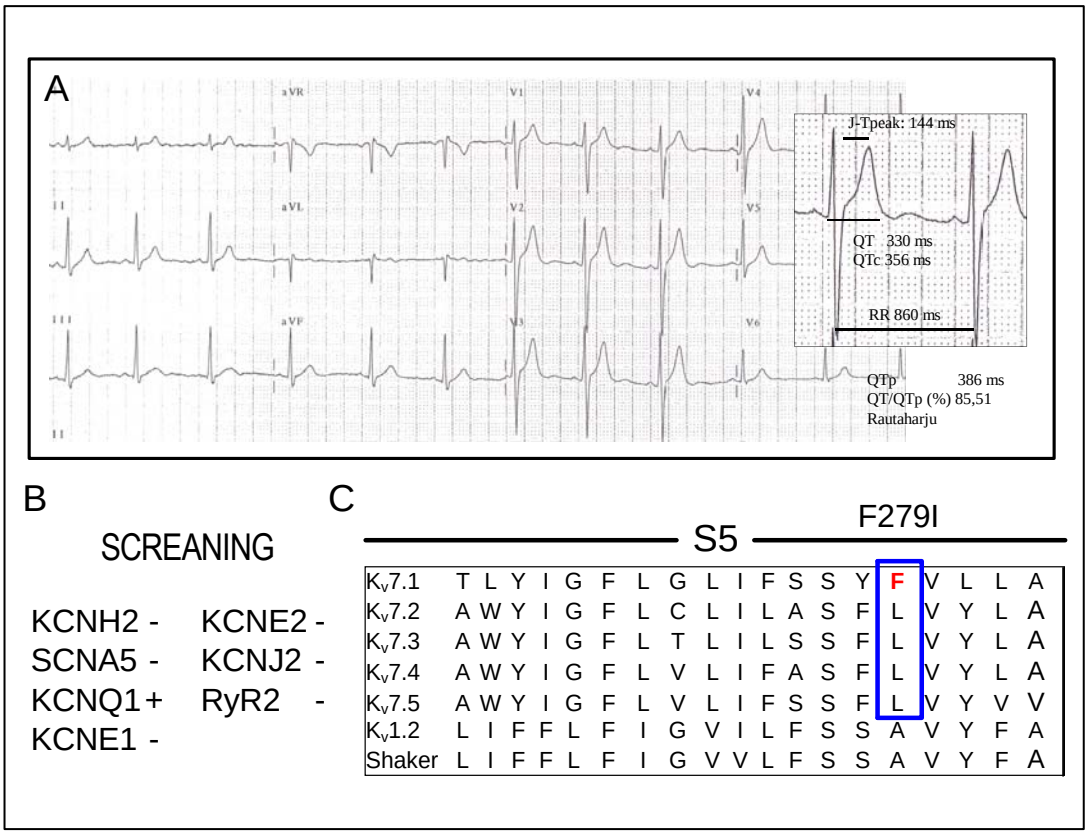

Figure 29. Electrocardiogram of the patient and genetic analysis. **(A)** Twelve-lead ECG of an affected individual (III-9). **(B)**. Screening of the genes more prominent for cardiac arrhythmias. **(C)** DNA and amino acid sequence of K_v7.1 missense mutation found in the patient and also in a blood sample of his sister and sequence alignment of the other members of the K_v7 family, K_v1.2 and shaker channels.

waves in V2-V4 (Figure 29A). Exercise test was normal of note; QTc was shortened with the exercise, measuring 350 ms at maximum workload. Echocardiogram and cardiac magnetic resonance demonstrated a normal heart, and 24-hours Holter monitoring showed no arrhythmias. Cardiac evaluation of the asymptomatic 13 years old daughter demonstrated normal ECG, Holter, exercise test, echocardiogram and cardiac magnetic resonance. In particular corrected, QTc was 400 ms. In the absence of DNA available from the deceased father, a blood sample from the patient and from his sister was sent for genetic study of most prevalent genes related to

channelopathies. Genetic studies on the patient's DNA excluded mutation in KCNH2, SCN5A, KCNE1, KCNE2, KCNJ2 and RyR2. Analysis of the KCNQ1 gene revealed a novel heterozygous mutation, a single-base substitution at nucleotide 127910 (g.127910T>A) in the exon 6 of the *KCNQ1* gene, resulting in an amino acid change from phenylalanine to isoleucine at 279 in K_v7.1 (p.F279I)) within the S5 transmembrane domain, which was not reported before (Figure 29B-C).

4.3.2 Characterization of F279I mutation on K_v7.1 channel function

The electrophysiological consequences of the F279I K_v7.1 mutation, located in the S5 region of the K_v7.1 channel, were characterized after heterologous expression in COS7 cells. Currents were elicited by 5.5 s pulses to potentials ranging from -80 mV to +100 mV from a holding potential of -80 mV in 20 mV steps. In response to membrane depolarization, both WT and F279I K_v7.1 generated outward rectifying potassium current that fully activate during the 5.5 s pulse with an exponential activation time course and a threshold for activation of approximately -20 mV for WT and -40 mV for F279I K_v7.1 channel (Figure 30A-B). Upon repolarization to -50 mV, WT K_v7.1 tail currents were characterized by an initial increase as channels recovered from inactivation,

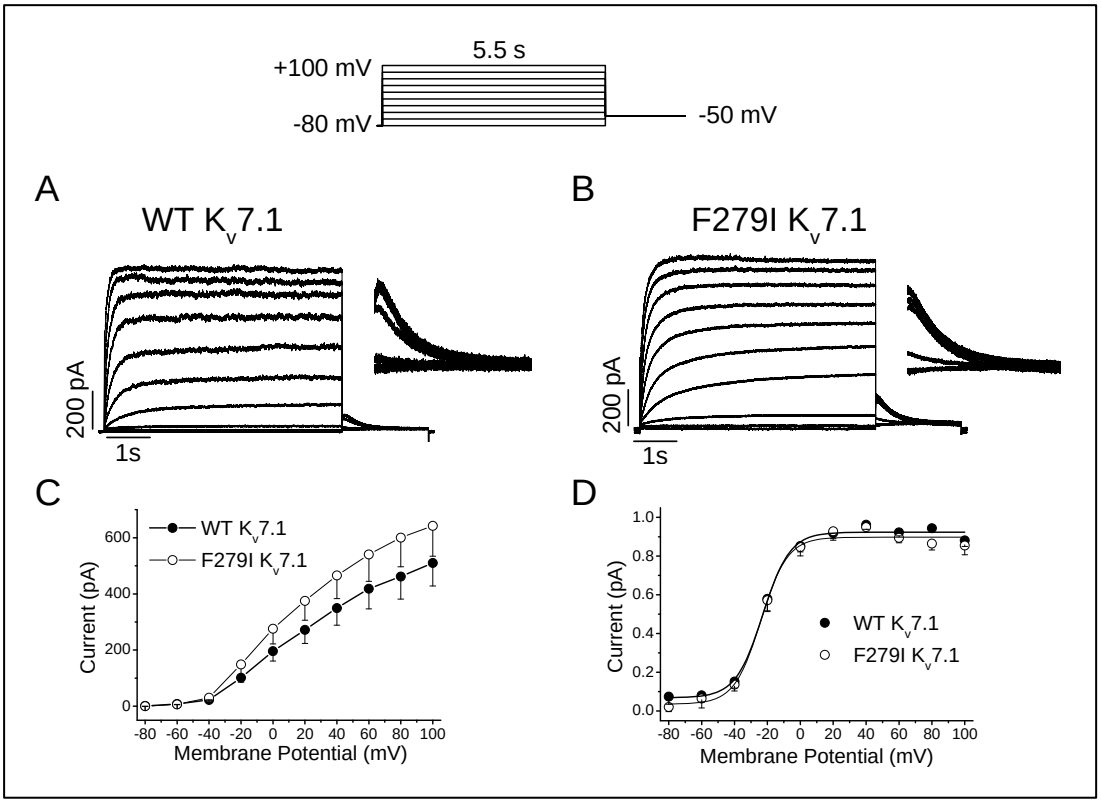

Figure 30. Current induced by expression of WT and mutant F279I K_v7.1 channels in COS7 cells. Representative currents for COS7 cells transfected with **(A)**: WT or **(B)**: F279I K_v7.1 mutant channels. The voltage protocol is shown on the top. **(C)**: IV relationships of measured at the end of a 5.5 depolarizing pulse for WT and F279I K_v7.1 channels. **(D)**: Voltage dependence of activation: activation curves were obtained by plotting the normalized tail currents versus the membrane potential. The fit with a Boltzmann equation is shown with a solid line. Results show the mean±SEM of 8-9 cells per group.

followed by a slow decay as channels deactivated (139,140). However, mutant tail currents did not display this

typical hooked configuration. The lack of a hook in the tail current suggested either these channels did not inactivate at positive potentials or that recovery from inactivation was very fast. The average IV relationships determined with 5.5 s pulses for WT and F279I $K_v7.1$ are plotted in Figure 30C. The current magnitude was increased by about 50% compared with WT $K_v7.1$ at potentials between +0 mV and +40 mV ($P<0.05$, n=8-9), but at positive potentials this increase was not statistically significant. Thus, a decrease in the side chain or the lack of an aromatic residue in the S5 transmembrane domain at F279 position altered the gating of $K_v7.1$. To determine the voltage dependence of activation, the peak amplitudes of tail currents recorded at -50 mV were plotted as a function of the test pulse potential, normalized and fitted to a Boltzmann equation (Figure 30D). The midpoint potential of the activation curve V_{mid} was -21.2±1.9 mV and the slope factor 9.9±1.9 mV for WT $K_v7.1$ channels. In the case of F279I $K_v7.1$channels the V_{mid} was -22.9±1.9 mV ($P<0.05$, n=9) and the slope factor 8.1±0.5 mV ($P>0.05$, n=9).

4.3.3 Inactivation is reduced by the F279I mutation

Inactivation of WT $K_v7.1$ channels is indirectly revealed by the hooked tail currents, which reflect recovery from the inactivation process (139,140,271). To investigate whether the apparent increase in the steady-state currents of the F279I $K_v7.1$ channel could be explained by an altered inactivation properties, we applied a triple pulse protocol to direct measure the channel inactivation (272-274) (Figure 31). The first depolarizing pulse opened and inactivated the channels. By applying a second pulse (4 ms and 20 ms) to -130 mV, a number of the inactivated channels will reenter the open state. Deactivation is minimized by the short pulse duration. If channels recovered from inactivation during the second pulse, then current inactivation was observable during a subsequent depolarization applied to the same potential as the first pulse (+40, +60, +80 or +100 mV). In Figure 31A-B, representative traces obtained with this triple pulse protocol are shown. We estimated the fraction of channels that inactivated during the third pulse. The degree of channel inactivation for WT channels was larger after a 20 than a 4 ms pulse, indicating that the 4 ms pulse to -130 mV was insufficient to allow adequate recovery of WT channels from inactivation and exhibited a linear relation with the increasing voltage, suggesting that this process is voltage independent. Compared to WT, F279I mutant channels exhibited a diminished fraction of channel inactivation at every voltage tested. F279I $K_v7.1$ channels were partially inactivated during pulses to +80 and +100 mV but not during pulses to +40 and +60 mV. These data indicate that F279I $K_v7.1$ channels can only inactivate at potentials far more positive than those observed for WT $K_v7.1$ channels. These data are consistent with the non hooked tails observed after repolarization at -50 mV (Figure 30).

It has been reported that mutations of residues within the pore region spanning S5 to S6 affect $K_v7.1$ inactivation (118,125), indicating a possible involvement of this region on this process. Furthermore, experiments performed with functional quimeras between the closely related channels $K_v7.1$ and $K_v7.2$ (a component of the neuronal non-inactivating M-current) indicated that the borders of the crucial region for inactivation could be assigned to the S5 transmembrane segment and parts of the P-loop (144). Similarly, the mutation V307L (responsible of short QT) located in the pore loop showed slightly slowed activation and deactivation kinetics

compared with WT, but again abolished inactivation (144). Therefore, a reduced level of inactivation could account for the bigger steady-state current amplitudes observed for the F279I K_v7.1 mutant channel.

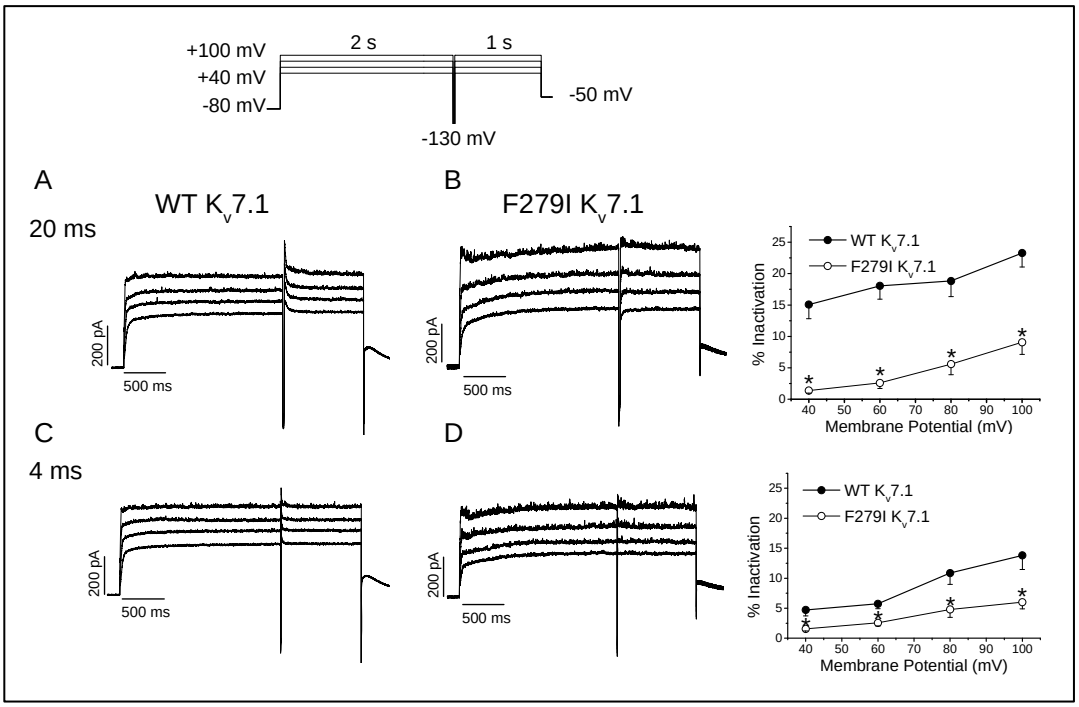

Figure 31. F279I mutation reduces K_v7.1 inactivation assessed with a three pulse protocol. The three pulse protocol is shown on the top. Currents were recorded from cells transfected with WT or F279I K_v7.1 cDNA. Cells were pulsed to a test potential of +40, +60, +80, or +100 mV for 2 s before applying a 20 ms **(A)** or 4-ms **(B)** interpulse to -130 mV to allow channels to recover from inactivation. The membrane potential was returned to the test potential after the interpulse to measure the extent of inactivation.*P<0.05, n=9-12

4.3.4 Properties of the WT and F279I K_v7.1/KCNE1 channel complexes

As reported previously (135,136), coexpression of WT K_v7.1 and KCNE1 subunits induce a large, slowly activating current similar to cardiac I_{Ks}. To investigate the effect of the F279I mutant in this more physiologically relevant channel configuration, either 0.5 µg WT K_v7.1 or the mutant F279I subunit were co-transfected with 0.5 µg KCNE1. The mutant channel complex F279I/KCNE1 displayed ~1.8 fold acceleration of the fast component of the activation kinetics in comparison to the WT K_v7.1/KCNE1 complex (794.1±36.0 ms *vs.* 445.7±27.9 ms, P<0.05, n=8-9) and was thus kinetically situated intermediate between WT K_v7.1 and WT K_v7.1/KCNE1 channel complexes. Furthermore, the initial sigmoidal activation, characteristic of WT K_v7.1 associated with KCNE1, was no longer obvious (Figure 32A-B). This acceleration might be indicative of an impaired alpha-beta interaction. In fact, it has been described that substitutions at this residue by the smaller amino acid alanine, strongly disturbed the KCNE1 gating modulation. In contrast, the deactivation kinetics of the mutant channel complex F279I/KCNE1 was similar to that of WT K_v7.1/KCNE1 complex. The deactivation process of F279I mutant channels was slighly faster compared with WT channel complexes but was not significantly different (Figure S5).

The average current induced by co-expression of F279I K_v7.1 and KCNE1 at the end of a 5.5 s depolarizing pulse was higher at potentials between -20 to +20 mV (which is physiologically relevant), but this

effect was reverted at potentials positive to +40 mV (Figure 32C). Furthermore, the mutant channel starts to display accumulate of the current amplitude at potentials at around +80 mV. This effect could be due to the presence of an inactivated state that according to the model of Silva and Rudy (146,275), is absent in WT K_v7.1 WT/KCNE1, suggesting again an impaired functional interaction with KCNE1 (Fig 32A-B). Mean current was also measured 300 ms after the step change in membrane potential to more accurately reflect the duration of a cardiac action potential (Figure 32D). The mutant current magnitude was higher at every potential tested positive to 0 mV, which could be explained by the faster activation kinetics of the mutant channel. As illustrated in Figure

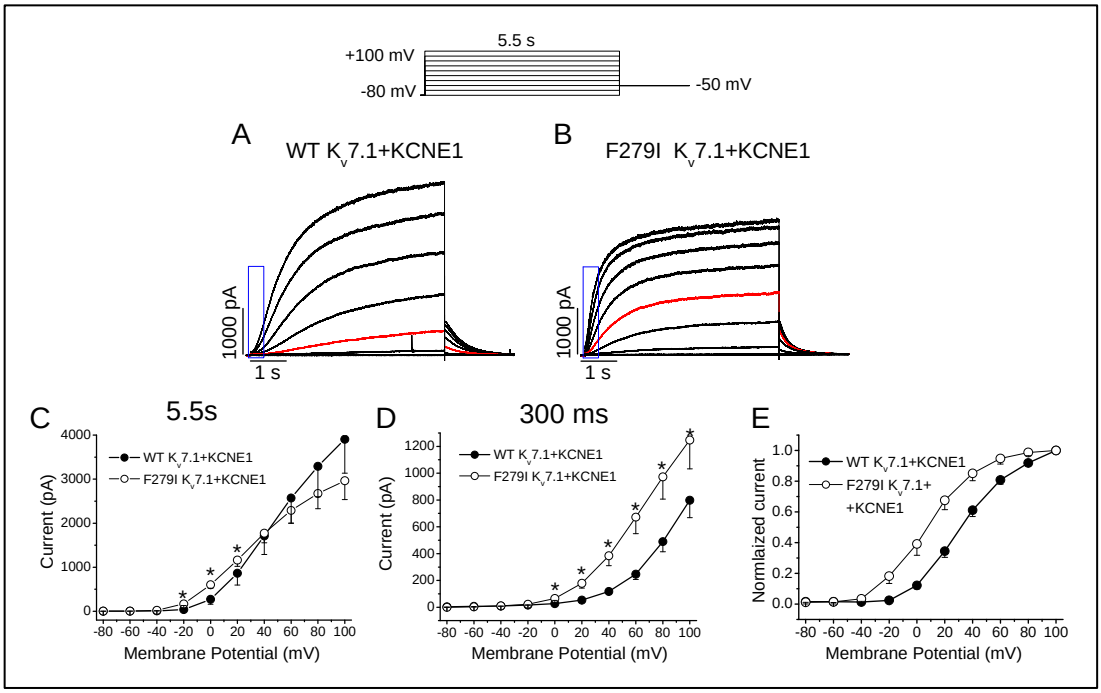

Figure 32. Currents induced by co-expression of KCNE1 with WT or F279I K_v7.1 mutant channels. Currents induced in COS7 cells transfected with K_v7.1 plus KCNE1 cDNA **(A)**. For panels A-B, pulses were applied from a holding potential of -80 mV to +100 mV in 20 mV steps. Tail currents were recorded at -50 mV. IV relationships obtained after plotting the current magnitude at the end of 5.5 depolarizing pulses **(C)** or after measuring the current at 300 ms **(D)**. Voltage dependence of activation **(E)** Activation curves were obtained by plotting the tail current versus the membrane potential normalized. Results show the mean±SEM of 8-9 cells per group.*P<0.05 *vs.*WT K_v7.1/KCNE1.

32E, the voltage dependence of channel opening for the mutant channel was shifted towards more negative potentials, as well as the threshold for channel opening, but the slope of the voltage sensitivity was unchanged (Figure 32C-E). Altogether, the shift in the activation curve and the faster activation kinetics indicate that mutant F279I K_v7.1/KCNE1 channels open faster and that more channels will be open at physiological relevant plateau potentials. These biophysical properties would therefore predict an increase of the repolarizing potassium current and thus, a gain of function.

4.3.5 Subcellular location of WT and F279I K_v7.1/KCNE1 channel complexes

The electrophysiological analysis of the F279I K_v7.1/KCNE1 channel complex revealed an altered interaction with the accessory subunit. Therefore, in order to test if this effect could be due to a reduced physical

interaction between both subunits we performed coimmunoprecipitation experiments in HEK293 cells. As it is shown in Figure 33A, there were no differences in the co assembly between F279I K_v7.1 channels and KCNE1 compared with the WT K_v7.1 channel. We also examined the effects of the point mutation F279I on the traffic of K_v7.1 protein using a cell surface biotinylation assay. These analyses revealed an increased surface expression of F279I K_v7.1 channels in HEK293 cells transfected cells in comparison to WT K_v7.1 channel (Figure 33B). There was no change in the protein expression levels of K_v7.1 channels as revealed by immunoblot analyses of the whole cell lysates (Figure 33). Analyses on K_v7.1 surface expression by biotinylation assay in the presence of KCNE1 reveal that F279I K_v7.1 channel gain of function is also mediated by an increase of its cell surface expression.

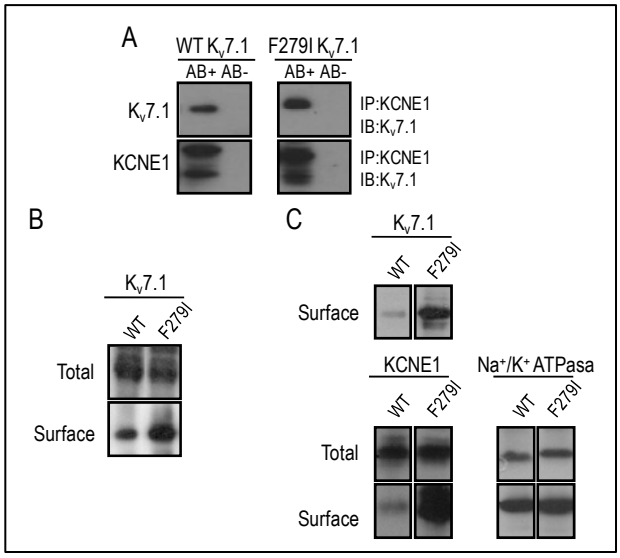

Figure 33. F279I K_v7.1 channels present an increased cell surface expression in HEK293 cells. **(A)** negative (*Ab-*) and positive (*Ab+*) immunoprecipitation of KCNE1 subunits blotted against K_v7.1 revealed the coimmunoprecipitation of both subunits for WT and mutant channel complexes indicating that the protein assembly is not decreased in mutant complexes. **(B)** Cell-surface biotinylation assay showing cell surface and total expression of K_v7.1 and KCNE1 in HEK293 cell transiently cotransfected with K_v7.1 and KCNE1. The Na^+/K^+ ATPasa protein was used as a loading control.

4.3.6 Rate-dependent increase in current upon depolarizing pulse trains

It has been shown that I_{KS} is important for both action potential repolarization and adaptation to changes in rate (276-279). Action potential duration shortens in response to elevated heart rate, which is a necessary accommodation in order to maintain a proper time spent in electrical systole to time spent in diastole (280,281). Slow activation ensures that I_{KS} activated by a single pulse (action potential) does not reach the maximal value and can be further increased. This increase in I_{KS} appears to be the result of pooling channels in open and mostly pre-open states leading to a shorter delay in the activation and increased amplitude upon a subsequent depolarization (146,275). Since the F279I mutant resulted in faster activation kinetics, we investigated how these altered electrophysiological properties affected the rate dependent effects of I_{KS}. To this end, we applied a stimulus train of 70 depolarizations to + 50 mV from a holding potential of -80 mV at different frequencies (1,2 and 2.5 Hz) mimicking normal and fast heart rates. For the WT K_v7.1/KCNE1 channel complex, no increase in current was observed at 1 Hz, but at faster rates (2 Hz and 2.5 Hz) a significant increase was observed (Figure 34A). This corresponds well to previously described rate-dependencies for WT K_v7.1/KCNE1 (282). To quantify this increase, the instantaneous current amplitude of each pulse was normalized to the steady state current amplitude reached with a single 5.5 s depolarization to +50 mV. This normalized current was plotted as a function of cycle

number and displayed a clear increase in current with shorter cycle lengths. When the same stimulus waveform was applied to cells expressing F279I K_v7.1/KCNE1 channels there was a notable increase in current even at 1 Hz. This indicated that the rate-dependent increase in current for the mutant F279I K_v7.1/KCNE1 channels occurred at every frequency and did not reach its maximum level (Figure 34B). Thus, the altered kinetics of the mutant might account for increased I_{KS} especially at elevated heart rates.

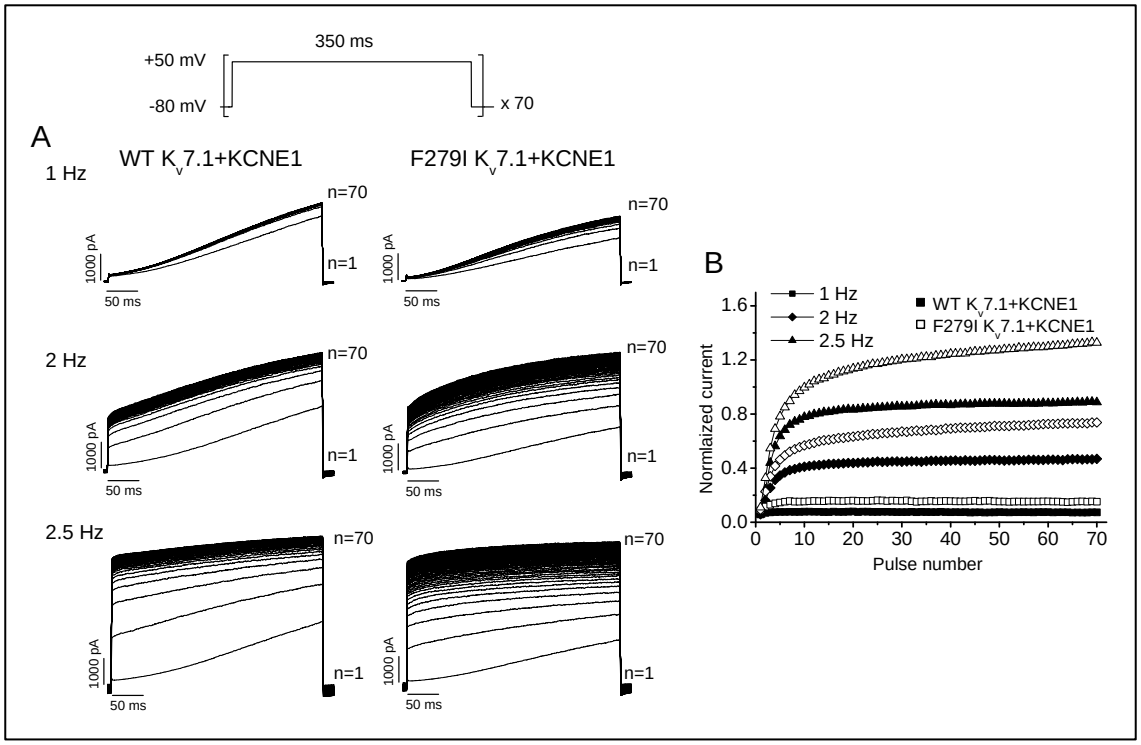

Figure 34. Rate dependent current increase for WT and F279I K_v7.1/KCNE1 channels. Panel **A** shows current recordings for WT and F279I K_v7.1/KCNE1 channels. On the top, it is shown the train protocol used and the corresponding current at different frequencies (1, 2 and 2.5 Hz). To normalize this increase in current, the instantaneous current amplitude was normalized to the steady-state current amplitude reached during a 5.5s depolarizing pulse to +50 mV and plotted as a function of the pulse number **(B)**. Results show the mean±SEM of 8-9 cells per group.

4.3.7 Heterozygous condition

To mimic the heterozygous condition occurring in the patient, co-expressions of the WT and F279I K_v7.1 mutant channels in a ratio (1:1) together with KCNE1 were performed. Figure 35A shows representative current traces. The WT/F279I K_v7.1/KCNE1 channel complexes, exhibited a faster activation kinetics compared with WT K_v7.1/KCNE1 (τ_f 616±70 ms *vs.* 794±36 ms for WT/F279I K_v7.1/KCNE1 and WT K_v7.1/KCNE1 channel complexes, P<0.05, n=4-9) but slower than F279I K_v7.1 /KCNE1 (τ_f 616±70 ms *vs.* 445±27 ms for WT/F279I K_v7.1/KCNE1 and F279I K_v7.1/KCNE1, P<0.05, n=4-8). Compared to WT K_v7.1/KCNE1 channels, the deactivation kinetics was faster for the heterozygous channel complex (Figure S5). The current amplitude for the heterozygous condition was also greater compared to WT K_v7.1/KCNE1 at the end of the 5.5 depolarizing pulse at potentials between 0 and +40 mV and at every potential positive to -20 mV when measured 300 ms after the

first voltage step (P<0.05; n=4-9) exhibiting an intermediate phenotype (Figure 35C) . The activation curve for the heterozygous was shifted towards more negative potentials compared to WT K_v7.1/KCNE1 exhibiting an

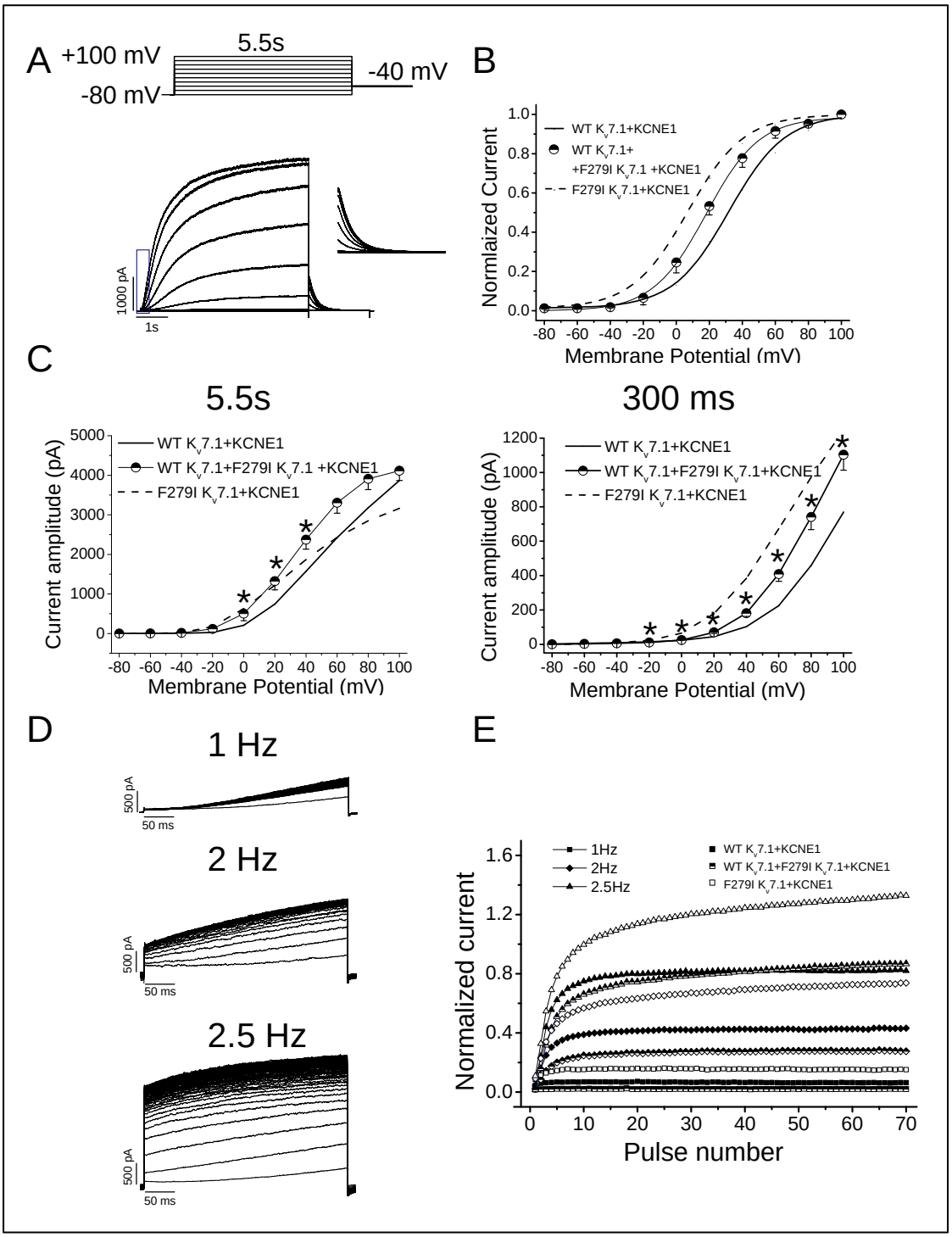

Figure 35. Electrophysiological properties of the heterozygous WT/F279 K_v7.1/KCNE1 channel complex. Current induced in COS7 cells transfected with WT and F279I K_v7.1 plus KCNE1 cDNA. **(A)**. Pulses were applied form a holding potential of -80 mV to +100 mV in 20 mV steps. Tail currents were measured at -50 mV. Activation curves were obtained by plotting the normalized tail current versus the membrane potential **(B).** IV relationships obtained at the end of a 5.5 depolarizing pulse or after 300 ms **(C)**. Rate dependent current increase for WT K_v7.1/F279I K_v7.1/KCNE1 channels **(D-E)**. The train pulse protocol applied was the same described in Figure x. The heterozygous channel complex exhibited an intermediate phenotype between WT K_v7.1 current and WT K_v7.1/KCNE1 current. Results show the mean±SEM of 4-9 cells per group. *P<0.05 *vs.* WT K_v7.1/KCNE1

intermediate phenotype between the F279I K_v7.1/KCNE1 and WT K_v7.1/KCNE1 channel complexes (Figure 35B). Finally, the rate-dependence increase of I_{Ks} was analyzed. At low frequencies, a decrease in the normalized current was observed compared to WT K_v7.1/KCNE1were observed between the heterozygous and WT K_v7.1/KCNE1 channel complexes and a slower kinetic of increase. However, at 2.5 Hz the rate-dependent increase in current for the WT/F279I K_v7.1/KCNE1 complexes was higher than those induce by WT K_v7.1/KCNE1 and it did not reach the steady-state as it was noticed for F279I K_v7.1KCNE1 channel complexes (Figure 36D-E). All these data indicate that co-expression of the WT K_v7.1 subunit together with the mutant F279I subunit mimicking the heterozygous inheritance, also results in a gain of function of I_{Ks}.

5 DISCUSSION

5.1 MODULATION OF K_v AND K_{ir} CURRENTS BY 15-EPI-LIPOXIN-A_4 IN ACTIVATED MACROPHAGES. IMPLICATIONS IN INNATE IMMUNITY

This study provides experimental evidence for new mechanisms of action by which e-LXA_4 contributes to inflammation resolution. On one hand, by directly attenuating NF-κB activity and, on the other hand, affecting the electrophysiological properties of the macrophage membrane. We have demonstrated that: 1) activation of BMDM with IL4/IL13 produces similar effects on potassium currents to those reported after glucocorticoid treatment; 2) when acutely administrated, e-LXA_4 decreases K_v currents in LPS-stimulated BMDM, and also K_{ir} currents in resting, LPS- and IL4/IL13-stimulated BMDM at potentials negative to -120 mV, suggesting receptor-independent effects; 3) after prolonged exposure of BMDM to e-LXA_4, the LPS-induced effects on K_v and K_{ir} were partially reverted, at the same time that the enhanced protein levels of K_v1.3 and K_{ir}2.1 were downregulated; 4) long term exposure to e-LXA_4 reverted the LPS-induced calcium influx; and 5) the effects of e-LXA_4 on K_v and K_{ir} channels in LPS-activated BMDM were partially mediated via ALX receptor.

Potassium channels play a critical role in maintaining the electrochemical gradient required for sustained calcium entry in the time frame required for activation and effector functions of immune cells (86). We previously reported that LPS-activated RAW 264.7 macrophages exhibited a 1.6-fold elevation in functional K_v1.3 channels *vs.* their non-stimulated counterparts (69). We also described that heteromeric K_v1.3/K_v1.5 channel expression and their biophysical and pharmacological properties changed differentially upon activation and immunosuppression: LPS induced K_v1.3 protein expression, whereas treatment with dexamethasone resulted in the opposite effect (69). This enhanced K_v1.3 expression is likely to promote calcium signaling necessary for co-activation/effector functions of macrophages. Indeed, blockade of K_v1.3 channels suppresses antigen-driven proliferation and cytokine production in T cells, and ameliorate experimental allergic encephalomyelitis in rats induced by the adoptive transfer of myelin specific activated effectors memory T cells (283-286). Moreover, several groups have described that K_v1.3 is expressed in macrophages and microglia (67,69,287-292). Indeed, K_v1.3 channels, together with K_{ir}2.1, K_v1.5, K_{Ca}3.1 and BK_{Ca} channels modulate macrophage and microglia function and therefore, immunotherapy with channels blockers may have effects on the immune response (67,288,293-295). Our data add new insights on the fine-tuning of these channels by lipoxins.

The effects of e-LXA_4 were analyzed in resting, LPS-stimulated (innate response) or IL4/IL13-stimulated (alternatively response) BMDM. In resting cells, the outward K_v current exhibited small amplitude, fast activation and very slow inactivation kinetics. Most of the K_v current seems to be due to the activation of heterotetramers of K_v1.5+K_v1.3 subunits in which K_v1.5 predominates (67,69). Under these conditions, e-LXA_4 did not produce significant effects on the magnitude of the K_v current, the use-dependent decrease or the slow inactivation of the current. These results suggest that e-LXA_4 does not produce significant direct effects on K_v1.5 channels, and experiments performed on stably transfected *Ltk*$^-$ cells expressing K_v1.5 channels confirmed it (data not shown).

As previously reported, LPS increases K_v and decreases K_{ir} currents (63,67,69). The increase in K_v current induced by LPS appeared concomitantly with a use-dependent decay and a C-type inactivation, both characteristics of $K_v1.3$ channels. In agreement, LPS upregulated both the mRNA and protein levels of $K_v1.3$. On LPS-stimulated macrophages, e-LXA_4 decreased the magnitude of the K_v current but did not modify the use-dependent decrease or the C-type inactivation of the current. Thus, some of the effects of e-LXA_4 in LPS-stimulated cells are probably due to a direct interaction with the $K_v1.3$ channels. Finally, after stimulation of BMDM with IL4/IL13, K_v currents exhibited similar magnitude than those recorded in resting cells. Interestingly, although activation of BMDM with IL4/IL13 did not modify the amplitude of the current, it decreased the use-dependent effects, resembling the actions of dexamethasone (69). These results suggest that alternative activation can change the stoichiometry of K_v, leading to the formation of channels with a decreased $K_v1.3$:$K_v1.5$ ratio, which is supported by a slight increase in the mRNA for $K_v1.5$ after IL4/IL13 activation. In BMDM stimulated with IL4/IL13, e-LXA_4 did not produce significant effects on the magnitude nor the electrophysiological properties of K_v currents. In resting and alternatively activated BMDM, K_{ir} current exhibited the typical characteristics of the inward rectifying potassium current. As it was previously reported, LPS decreased K_{ir} current, consistent with a downregulation of the mRNA for $K_{ir}2.1$ (67). e-LXA_4 decreased the amplitude of the K_{ir} current at negative membrane potentials under the three experimental conditions tested. In resting BMDM, but not in LPS- or IL4/IL13-stimulated BMDM, the reversal potential became more positive, which leads to a depolarization of the membrane potential, thus avoiding Ca^{2+} entry into the cell.

Since the early inhibitory effects of e-LXA_4 on NF-κB and pro-inflammatory signaling are extended at later periods (>10h), the electrophysiological effects of long-term incubation with e-LXA_4 were studied. Long term treatment with e-LXA_4 did not modify the magnitude of the K_v or the K_{ir} currents in resting BMDM. On the contrary, it was able to partially prevent the electrophysiological effects produced by LPS, decreasing the amplitude, the use-dependent decrease and the C-type inactivation of the K_v current. In a parallel way, chronic e-LXA_4 diminished the decrease of the K_{ir} current induce by LPS. Using the selective inhibitor of ALX, BocPLP (254) we have shown that the actions of long term incubation with e-LXA_4 on K_v currents are, at least in part, dependent on the interaction with ALX receptor. Indeed, in LPS-stimulated BMDM, $K_v1.5$ protein level was not modified by e-LXA_4, whereas $K_v1.3$ was upregulated by LPS and downregulated by e-LXA_4. Since K_v currents recorded in BMDM stimulated with LPS are the consequence of the activation of heterotetramers of $K_v1.5$+$K_v1.3$ with different stoichiometry, the contribution of $K_v1.5$ to the total of this current can explain the apparently low dependency of the effects of e-LXA_4 on K_v. On the contrary, the K_{ir} current measured in the presence of BocPLP in cells treated with e-LXA_4+LPS was much more similar to that recorded in BMDM activated with LPS, suggesting that the e-LXA_4 effects on K_{ir} channels involves the interaction with the ALX receptor. The influx of extracellular Ca^{2+} is an essential requirement for the activity of many cellular processes (84,235,296). Therefore, $K_v1.3$ channels and the Ca^{2+}-activated K^+ channel $K_{Ca}3.1$ regulate Ca^{2+} influx through the calcium release activated Ca^{2+} channel, which consists of the Ca^{2+}-sensor stromal interaction molecule 1 (STIM1) and the pore-forming protein CRACM1 (Orai1) (244,245,297,298). In T cells, this crucial influx of Ca^{2+} is only possible if they can keep its membrane potential negative by a

counterbalance of K^+ efflux through $K_v1.3$ and/or $K_{Ca}3.1$ (86,299) and both channels are regarded as targets for immunosuppression (86). In the present study, we have demonstrated that e-LXA_4 inhibits $K_v1.3$ in LPS-stimulated cells. This inhibition would lead to a depolarization of the membrane potential and, as a consequence, to an inhibition of the Ca^{2+} influx through CRAC channels, which is a critical event in the activation of macrophages (300). Indeed, we have reported that in cells activated with LPS, e-LXA_4 is able to decrease extracellular entry of Ca^{2+}. Therefore, e-LXA_4 may produce its antiinflammatory effects through this new mechanism of action.

Lipoxins were the first mediators exhibiting both antiinflammatory and proresolving actions. The beneficial actions of aspirin in the cardiovascular system have been attributed to its capability to block prostaglandin and prothrombotic thromboxane (TXA_2) generation via acetylation of COX. Aspirin acetylation of COX-2 not only inhibits prostanoid formation but also alters the active site of COX-2 and thereby permits conversion of arachidonic acid into 15*R*-HETE in vascular endothelial cells. This intermediate compound can be further transformed to epimeric lipoxins by leukocytes and other immune cells contributing to the fine tuning of the inflammatory response. Our data describe a direct inhibition of e-LXA_4 on IKKβ activity, a broad inhibition of NF-κB activity and a cytoprotective mechanism of macrophages during resolution. In addition to this, Ca^{2+} fluxes are negatively modulated by e-LXA_4 through the inhibition of $K_v1.3$ channels in LPS-stimulated cells; all these mechanisms concur on the attenuation of the inflammatory response as far as e-LXA_4 accumulates in the medium.

5.2 EFFECTS OF n-3 PUFAs ON K_v7.1/KCNE1 CURRENT

In this section of the present Doctoral Thesis we have investigated the effects of EPA and DHA, two n-3 PUFAs from marine origin on K_v7.1/KCNE1 channels expressed in COS7 cells. We have demonstrated that: 1) At physiological concentrations, both PUFAs increase the magnitude of K_v7.1/KCNE1 current after acute but not after chronic exposition, DHA being more potent than EPA. 2) Acute and chronic effects of PUFAs were time- and voltage-dependent. 3) Both PUFAs reduced the expression of K_v7.1, but not that of KCNE1 due to an enhanced degradation of K_v7.1 via proteasome. 4) Both PUFAs delocalized K_v7.1 channels from lipid rafts and 5) EPA effects on K_v7.1/KCNE1 current recorded in cholesterol depleted cells were similar to those observed after acute exposition, consistent with a direct interaction with the channel.

In this study we have demonstrated that acute perfusion of EPA or DHA increased to a different extent the magnitude of K_v7.1/KCNE1 current. However, their effects on the electrophysiological properties of this current exhibited some differences. Thus, EPA increased K_v7.1/KCNE1 current in a time- and voltage-dependent manner. The midpoint of the activation curve in the presence of EPA was shifted towards more negative membrane potentials and the increase in the magnitude of the current was also voltage dependent, being greater at 0 than at +60 mV. EPA slowed the activation time course and speeded up the deactivation process. This slowing of the activation time course was due to an increased contribution of the slow component of activation to the total process, and not to changes in the time constants. Therefore, EPA effects on the activation kinetics can be the consequence, at least in part, of the shift in the activation curve. On the other hand, DHA increased the K_v7.1/KCNE1 current to a greater extent than EPA in a time-dependent but voltage-independent manner: The midpoint of the activation curve was not modified in the presence of DHA. DHA slowed the total process of activation but to a lesser extent than EPA, despite it accelerated the initial fast component of activation. Similarly to EPA, DHA accelerated the deactivation kinetics. As previously described, neither EPA nor DHA modified the properties of K_v7.1 channels when expressed alone. Thus, the presence of KCNE1 subunits is essential for the observed electrophysiological effects of acutely applied PUFAs.

Dietary administration of fish oil leads to the incorporation of n-3 PUFAs into the cell membrane including membranes from myocytes of the heart (213,301). During the last decade, it has been reported that long term n-3 PUFAs intake also modulate the activity of several cardiac ion channels. However, the effects of long term administration of n-3 PUFAs on several ion currents in some cases differ from those observed by acutely administered n-3 PUFAs (302). When acutely applied, n-3 PUFAs decrease I_{Na} (207,214,303-305) $I_{Ca,L}$ (208), I_{To} (210,306,307), I_{Kur} (206,212) and I_{Kr} (211), whereas when chronically applied they have no effect on I_{Na}, (195,213) I_{To}, (213) and I_{Kr} (213) but decrease $I_{Ca,L}$ (213) and I_{Kur} (212). According to this, when the effects of long term administration of EPA (48 h) on COS7 cells expressing K_v7.1/KCNE1 channels were analyzed, we observed some differences compared to the effects produced by acute perfusion with the fatty acid. Chronically applied

EPA did not increase the current magnitude; however, it accelerated the activation process and, surprisingly, shifted the activation curve towards more positive potentials, suggesting that the mechanism by which acute or chronic n-3 PUFAs modulate the electrophysiological properties of $K_v7.1$ channels is different.

Several hypothesis have been proposed to explain the electrophysiological differences between acute and of long term administration of n-3 PUFAs. Some authors explain n-3 PUFAs effects by a direct interaction between n-3 fatty acid and the ion channel. This hypothesis is supported by the observation that substitution of a single amino acid in the human $Na_v1.5$ channel diminished the inhibitory effect of acutely administered EPA (304).The results from this Doctoral Thesis showing that such similar compounds (EPA and DHA) exert different effects on $K_v7.1$/KCNE1 current, are in agreement with a direct interaction between the n-3 PUFA and the ion channel, at least when they are acutely applied. However, other authors suggest that n-3 PUFAs effects are the result of an alteration of the membrane properties rather than a direct interaction with the ion channel. It has been reported that n-3 PUFAs alter the composition and order of the plasmalema (302). In this line of evidence, it has been proposed that the potency of n-3 PUFAs to block cardiac sodium currents is correlated with their ability to increase membrane fluidity measured by steady-state fluorescence anisotropy (308). In addition to these two mechanisms, changes in cellular redox status, metabolism of phospholipids and modulation of gene expression are other processes in which n-3 PUFAs participate that might modulate ion channel function (309).

In order to further explore the mechanisms by which acute and chronic n-3 PUFAs exert their actions on $K_v7.1$/KCNE1 channels, three different approaches were used: The effects of long-term administration of EPA were analyzed on: 1) $K_v7.1$ and KCNE1 expression, 2) their target to lipid rafts, and finally, 3) the effects of cholesterol depletion with MβCD on $K_v7.1$/KCNE1 current followed by the acute application of EPA on cholesterol depleted cells.

In addition to their ability to modulate the electrophysiological properties of ion channels, it has been reported that n-3 PUFAs can modify their protein levels as was the case of $K_v1.5$ (212). Our data showed that long term administration (48 h) of n-3 PUFAs also decreased the protein levels of $K_v7.1$, but not those of KCNE1, in a concentration-dependent manner. It was established that one mechanism that modulates $K_v7.1$ protein stability involves its ubiquitination by the Nedd4-2 ubiquitin ligase and posterior degradation in the proteasome (268). Since this decrease was prevented by the MG132 proteasome inhibitor; these data suggest that n-3 PUFAs promote $K_v7.1$ degradation via proteasome.

$K_v7.1$ channels target lipid rafts in eukaryotic cells, whereas KCNE1 does it only when $K_v7.1$ subunit is present (269). Cell incubation with EPA delocalized both $K_v7.1$ and KCNE1 subunits. On the contrary, DHA induced a delocalization of $K_v7.1$ channels from these membrane structures, whereas KCNE1 remained targeted to lipid rafts. It has been proposed that ion channels located in lipid rafts form signaling complexes and that they represent the locus of the cell membrane in which the ion channel, regulatory subunits, scaffolding proteins,

kinases and other modulatory proteins interact (310). Differential targeting of K_v7.1 and KCNE1 subunits to lipid rafts represents an important mechanism that regulate this current properties as it has been described for several ion channels (270,311-316).

The importance of K_v7.1 and KCNE1 location on specific microdomains for their function was confirmed in experiments in which lipid rafts structures were disrupted. Our results showed that membrane cholesterol depletion with MβCD and, consequently, lipid raft disruption, markedly increased the current magnitude of K_v7.1/KCNE1 at potentials positive to +30 mV and shifted the activation curve towards more positive potentials. Although the current magnitude did not increase after incubating COS7 cells with EPA for 48 h, the shift of the activation curve was very similar to that obtained after MβCD treatment. Hence, at least some of the electrophysiological changes on K_v7.1/KCNE1 current might be due to a different location of both subunits on the plasma membrane induced by the chronic treatment with the fatty acid. The precise mechanism involved in lipid raft modulation of channel activity is not fully understood. Three different explanations have been proposed: i) by affecting the biophysical properties of the membrane. Because of its high content on cholesterol and sphingolipids, lipid rafts represent thicker and less fluid parts of the membrane than nonrafts domains. Changes in the membrane fluidity may modulate ion channel activity through a hydrophobic mismatch between the transmembrane domains of the protein and the lipid bilayer. According to this, it has been described that TRPM8 channels agonists, such as menthol, geraniol and monoterpenes enhance the membrane fluidity and increase the ion current (270). Conversely, increasing the order of the membrane after enrichment with cholesterol inhibits K_v11.1 and K_v7 currents (315). We can speculate that the location of K_v7.1 and KCNE1 subunits in a thicker and less deformable membrane will increase the energy required for the transition from the closed to the open state. ii) By specific lipid-protein interactions occurring at rafts microdomains. A growing number of studies have demonstrated that cholesterol and PIP_2, major components of the lipid rafts, modulate the activity of several ion channels (103,111,150). Supporting this hypothesis it was described that an increase in cholesterol strongly suppresses K_{ir}2.1 current (317). In fact, point mutations on specific region of the C-terminus of the cytosolic domain of the channel, called CD-loop, abrogated the sensitivity of K_{ir}2 channels to cholesterol (317). Moreover, it has been recently reported the binding site for fatty acids in the cavity of the prokaryotic potassium channel KcsA (318). iii) By protein-protein interactions. It is known that lipid rafts are enriched in multiple signaling molecules such as G-proteins, protein kinases, phosphatases, Ca^{2+} binding proteins, etc. Lee and co-workers reported that inhibition of K_v7 channels by cholesterol involves the activity of PKC. Following a similar reasoning, the interaction between K_v7.1/KCNE1 with adjacent proteins could destabilize the closed conformation of the ion channel within less ordered domains of the membrane than lipid rafts. It is important to note that these mechanisms are not mutually exclusive. Finally, in cholesterol depleted cells, posterior perfusion with EPA produced similar effects on K_v7.1/KCNE1 current than those observed in acute conditions. EPA slowed the activation kinetics and increased the magnitude of the current at potentials negative to +30 mV. These effects were reversible when cells were washed with EPA-free external solution. The functional analysis from our data in cells lacking lipid rafts domains revealed two different effects of EPA on K_v7.1/KCNE1. Compared with acute EPA, a very similar pattern of

current increase (higher at negative potentials) and a change in the slope factor of the activation curve, which was fully reversed, were observed. This fact strongly suggests a direct interaction between the fatty acid and the channel protein. On the other hand, after MβCD treatment, EPA was not able to shift the activation curve toward more negative potentials indicating that other mechanisms such as specific protein-protein interactions or the composition of the lipid environment could be also involved in the modulation of K_v7.1+KCNE1 by PUFAs.

5.3 A NEW MUTATION ON K_V7.1 RESPONSIBLE OF SHORT QT SYNDROME

As mentioned before, K_v7.1 is the alpha subunit of the ion channel complex underlying the slow component of the cardiac delayed rectifier I_{Ks} (135,136). I_{Ks}, together with I_{Kr}, are the major repolarizing currents of ventricular myocytes (257). Gain of function mutations on K_v7.1 cause QT shortening and thus, the type 2 short QT syndrome. Until date, three mutations associated with short QT2 have been found: two located in the S1 and another one in the S6 transmembrane segment of K_v7.1. In this Doctoral Thesis we have characterized the functional effects of the new missense mutation F279I on K_v7.1 found in a patient with a QTc interval of 356 ms at resting and a family history of SCD. This mutation, located in the S5 transmembrane segment, modifies the gating of WT K_v7.1/KCNE1 complexes. As it is shown in Figure 29, among the K_v7 family, and also in other potassium channels, K_v7.1 is the unique channel carrying a phenylalanine at the equivalent position; suggesting that this residue might be important for the exceptional properties of the cardiac I_{Ks}

The mutant F279I K_v7.1 channel compared with WT K_v7.1, showed a slower activation kinetics and a reduced degree of inactivation, a characteristic that is exclusively observed in the absence of KCNE1 (140). Tail currents decay of WT K_v7.1 channels were preceded by a relatively rapid increase, due to recovery of channels from an inactivated state. In contrast, deactivation currents of F279I K_v7.1 were not preceded by any increase. The lack of the initial hook in the tail current suggested that mutant channels did not inactivate at potentials as positive as +80 mV. This was confirmed using a three-pulse protocol designed to determine the degree of inactivation. These experiments confirmed that F279I K_v7.1 channels inactivated to a lesser extent than WT K_v7.1 channels at every potential tested. Structural basis of K_v7.1 for inactivation is not fully understood, but several reports indicate that mutations in the S5, were the F279I lies, have a profound effect on the voltage dependence of this process (125,144,319) and therefore, on the channel gating.

Co-assembly of F279I K_v7.1 with KCNE1 had a big impact on K_v7.1/KCNE1 current properties. The functional effects of KCNE1 are to modulate K_v7.1 kinetics (slower activation and slightly slower deactivation), to remove inactivation (135,136) and to increase current magnitude by enhancing the single channel conductance (121,127,128). Compared with K_v7.1/KCNE1, the F279I K_v7.1/KCNE1 current exhibited faster activation kinetics, increased current magnitude at potentials between -20 and 20 mV, and a more negative midpoint for activation. In addition, it showed a small degree of inactivation, revealed by the fact that F279I K_v7.1/KCNE1 reached the steady state at potentials positive to +80 mV. Therefore, the electrophysiological properties of the F279I Kv7.1/KCNE1 current seem to be intermediate between K_v7.1 and K_v7.1/KCNE1 current. Taken together, all these results suggest that the underlying mechanism by which this mutation modifies the gating of F279I K_v7.1/KCNE1 current seem to be due to an abnormal interaction of F279I K_v7.1 with the accessory KCNE1 subunit. All these effects lead to a gain of function, which likely will result in an enhanced I_{Ks} repolarizing current during the AP.

The interaction between KCNE1 and K_v7.1 appears to involve interactions between residues located extracellularly (320,321), specific elements in the intracellular C-termini regions (282) and residues in the transmembrane segments (322-325). These data argue for a multi-point interaction between KCNE1 and the voltage sensing and pore-domain of neighboring K_v7.1 subunits (326). Furthermore, it appears that these interactions are dynamic and that KCNE1 reorients with respect to K_v7.1 during channel gating (320,321). According to this hypothesis, there have been reported three substitutions on K_v7.1 located in close proximity to 279 residue (L266W, F275W, and Y278A) and another one at the exact position of the mutation of the present suty but to a different amino acid F279A, which impaired KCNE1 modulation of channel gating. Mapping these residues onto the K_v1.2 structure shows that F275, F278 and F279 are located at the interface between the voltage-sensor and the pore domain. It is possible that the interaction sites between KCNE1 and the pore region of K_v7.1 are state-dependent. KCNE1 transmembrane domain most likely undergoes cooperative movement upon channel opening. As a consequence, different residues in S5 are closer to the neighboring KCNE1 subunit at the closed and open states. KCNE1 is most likely in close contact with L266 at the closed state, whereas F275, Y278, F279 at the open state. Since these mutations do not affect K_v7.1 gating properties when expressed alone, this study together with the results presented in the present Doctoral Thesis suggest that these residues are determinant for K_v7.1-KCNE1 interaction. F279I K_v7.1 mutation results in a substitution of a phenylalanine for an isoleucine. Both aminoacids are hydrophobic, however, the former is larger and posses an aromatic ring that could establish π-π interactions with another aminoacids carrying an aromatic ring (Phe, Tyr and Trp). Therefore, we can speculate that a larger amino acid or an aromatic ring is necessary to achieve a correct interaction between the alpha and the beta subunits. In fact, and supporting this hypothesis, it was reported that replacement of the phenylalanine by a tryptophan at the same position induced the opposite effect, a shift of the activation curve towards more positive potentials. In addition to these findings, biotinylation assays showed an increased protein expression of F279I compared to WT K_v7.1 channels on the cell membrane. However, it has been suggest that KCNE1 subunit would probably directly interact with the S6 segment of K_v7.1 channels but not with the S5 segment. Then, the effects of al these mutations at the S5 on the electrophysiological properties of K_v7.1 might be due to an impaired coupling of the gating modulation of K_v7.1 induced by KCNE1 and not to an altered physical interaction with the β subunit.

An enhanced translocation of K_v7.1 channels to the membrane would predict an increased current density that correlates with the electrophysiological analysis of our data and again points out to a gain of function of K_v7.1/KCNE1 current when the complexes incorporate F279I K_v7.1 subunits.

It has been shown that the contribution of I_{Ks} to repolarization is rate dependent (276,277). At slow heart rates, there is no accumulated activation of I_{Ks} because diastole is sufficiently long to allow for complete deactivation. As heart rate speeds up, the diastolic interval becomes shorter and the deactivation of I_{Ks} is incomplete between beats. This results in an accumulation of the channels in the pre-open closed states, which leads to a rate-dependent increase of current, which causes action potential shortening (146,275). To compare

the effects of repetitive stimulation between WT K_v7.1/KCNE1 and F279I K_v7.1/KCNE1 channels train pulses at variable cycle lengths in order to simulate a condition of rest (1 Hz) and exercise (2 Hz, 2.5 Hz). Even at 1 Hz, the F279I K_v7.1/KCNE1 channel complex already displayed steady-state current amplitude that was larger compared to WT K_v7.1/KCNE1. At every frequencies(1 Hz, 2 Hz and 2.5 Hz), the overall current amplitude was also higher compared to WT and, importantly, it did not reach the steady state. All these data suggest that the enhanced accumulation of activation of I_{Ks} in response to increased heart rate would be more pronounced in F279I K_v7.1/KCNE1 channels, likely because its activation kinetics is faster and its deactivation kinetics slower and hence will exhibit a different response to changes in rate.

Since patients are heterozygous for the F279I mutation, co-expression experiments of the WT and F279I K_v7.1 together with KCNE1 were performed to mimic the *in vivo* situation. The voltage dependence of activation for WT/F279I K_v7.1/KCNE1 was intermediate to those of WT K_v7.1/KCNE1 and F279I K_v7.1/KCNE1 complexes, as it was the activation kinetics and the current magnitude. As mentioned before, these biophysical characteristics would point out to an enhanced function of the heterozygous channel complex. Regarding to the rate-dependent effects, it was observed that at slow rates (1-2 Hz), there were no differences compared with the WT K_v7.1/KCNE1 situation. However, at faster rates (2.5 Hz), although there was just a slight increase in the accumulation of current, it did not reach the steady state, as the WT K_v7.1/KCNE1 complex did. Taken together, the results of our experiments are indicative of a significantly greater contribution of I_{Ks} to net AP repolarization when WT K_v7.1/KCNE1 channels complexes incorporate F279I K_v7.1 subunits

There is little information in the literature on the short QT syndrome, and this is based on small series of cases or isolated case reports. Recently, a revision of 61 cases has set the QTc cut-off for the diagnosis of the syndrome in 370 ms, although variability of this interval in different ECGs from the same patients varied significantly and in 2 cases the interval was constantly above this value (188). Compared to long QT and Brugada syndrome, there is no drug challenge test to help in the diagnosis. Both the son and the daughter of the index case were carriers of the F279I K_v7.1 mutation. A recent study from Schimpf and colleagues analysed the response of the QTc on exercise in patients with short QT syndrome compared to a control group (327). QTc of normal individuals in this study shortened to a greater extent the QTc more than short QT syndrome patients (327). The patient showing F279I mutation had a baseline ECG QTc of 356 ms and shortened with exercise up to 350 ms.

According to short QT syndrome diagnostic criteria (188), to begin to implement the diagnostic algorithm the QTc interval has to be shorter than 370 ms. The patient had a QTc interval of 356 ms (1 point), a Jpoint-T peak interval of 144 ms (no point), a first-degree relative with autopsy-negative who suffered SCD (1 point), and after the electrophysiological characterization of the F279I K_v7.1 realized in the present study, a genotype positive (2 points). Within this criteria, the patient would obtained in summary 4 points (high probability of short QT).

Although the present study does not definitely prove an association between the short QT interval and the $K_v7.1$ mutation, our data provide clear evidence for a causal relationship based on several findings. This residue is unique among the equivalent amino acid in the K_v7 family, and it appears to be an important residue for the $K_v7.1$-KCNE1 interaction. The electrophysiological characteristics associated with the mutation are expected to lead an enhanced repolarization with shortening of the QT interval (leftward shift of the activation curve, faster activation kinetics, and increased accumulation of current in response to changes in rate). F279I $K_v7.1$ protein expression is enhanced compared to WT, which further contribute to the increased repolarization of I_{Ks} when channels incorporate F279I subunits. And finally, no additional mutation was found among the genes that might be responsible of the short QT phenotype.

6 CONCLUSIONS

1. e-LXA_4 contributes to inflammation resolution by directly attenuating NF-κB activity and affecting the electrophysiological properties of the macrophage. e-LXA_4 partially reverts the effects produced by LPS on K_v and K_{ir} currents in BMDM. In addition, Ca^{2+} fluxes are negatively modulated by e-LXA_4 in LPS-stimulated cells. All these mechanisms converge in the attenuation of the inflammatory response.

2. The effects of n-3 PUFAs on K_v7.1/KCNE1 current depend on their way of administration. EPA and DHA increase K_v7.1/KCNE1 current magnitude when acutely applied. However, after long term incubation of cells expressing K_v7.1/KCNE1 with EPA, the magnitude of the current was not modified, although the kinetics and voltage-dependent characteristics were changed. The electrophysiological effects of acute EPA seem to be due to a direct interaction with the K_v7.1/KCNE1 channels. However, the modulation of K_v7.1/KCNE1 channels after chronic incubation with EPA seems to be due mainly to a delocalization of K_v7.1 channels from lipid rafts.

3. The functional analysis of the novel F279I mutation in K_v7.1 provide clear evidence for a causal relationship for the appearance of short QT syndrome. The electrophysiological characteristics associated with the mutation are expected to lead to an enhanced repolarization with shortening of the QT interval: leftward shift of the activation curve of K_v7.1/KCNE1 channels, faster activation kinetics, and an impaired adaptation to change in response to changes in rate. Presumably due to an impaired gating modulation of K_v7.1 induced by KCNE1.

1. La e-LXA_4 contribuye a la resolución de la inflamación directamente atenuando la actividad de NF-κB y afectando a las propiedades electrofisiológicas de los macrófagos. La e-LXA_4 revierte parcialmente los efectos producidos por el LPS en las corrientes K_v y K_{ir} de BMDM. Además, los flujos de Ca^{2+} en las células estimuladas con LPS están regulados negativamente por la e-LXA_4. Todos estos mecanismos convergen en la atenuación de la respuesta inflamatoria.

2. Los efectos de los AGPIs n-3 en la corriente K_v7.1/KCNE1 dependen del modo de administración. EPA y DHA aumentan la magnitud de la corriente K_v7.1/KCNE1 cuando son administrados agudamente. Sin embargo, tras la incubación prolongada de células que expresan K_v7.1/KCNE1 con EPA, la magnitud de la corriente no se modificó, a pesar de que las características cinéticas y dependientes de voltaje cambiaron. Los efectos electrofisiológicos agudos de EPA parecen estar debidos a una interacción directa con los canales K_v7.1/KCNE1. Sin embargo, la modulación de los canales K_v7.1/KCNE1 tras la incubación prolongada con EPA parece estar debida principalmente a una deslocalización de los canales K_v7.1 de las balsas lipídicas.

3. El análisis funcional de la nueva mutación F279I de K_v7.1 proporciona evidencias claras de una relación causal para la aparición de síndrome de QT corto. Las características electrofisiológicas de la mutación producirían una repolarización aumentada y un acortamiento del intevalo QT: desplazamiento hacia la izquierda de la curva de activación de los canales K_v7.1/KCNE1, cinética de activación más rápida y una adaptación a los cambios en frecuencia alterada. Presumiblemente debido a una modulación del *gating* de K_v7.1 inducido por KCNE1 alterada.

7 REFERENCES

1. Huang, C.L., Feng, S., Hilgemann, D.W. (1998) Direct activation of inward rectifier potassium channels by PIP2 and its stabilization by Gbetagamma. **Nature** 391:803-806.

2. Hille, B., Armstrong, C.M., MacKinnon, R. (1999) Ion channels: from idea to reality. **Nat. Med.** 5:1105-1109.

3. Yu, F.H., Yarov-Yarovoy, V., Gutman, G.A., Catterall, W.A. (2005) Overview of molecular relationships in the voltage-gated ion channel superfamily. **Pharmacol. Rev.** 57:387-395.

4. Choe, S. (2002) Potassium channel structures. **Nat. Rev. Neurosci.** 3:115-121.

5. Papazian, D.M., Schwarz, T.L., Tempel, B.L., Jan, Y.N., Jan, L.Y. (1987) Cloning of genomic and complementary DNA from *Shaker*, a putative potassium channels gene from Drosophila. **Science** 237:749-753.

6. Heginbotham, L., Lu, Z., Abramson, T., MacKinnon, R. (1994) Mutations in the K^+ channel signature sequence. **Biophys. J.** 66:1061-1067.

7. Marty, A. (1981) Ca-dependent K channels with large unitary conductance in chromaffin cell membranes. **Nature** 291:497-500.

8. Wickman, K. Clapham, D.E. (1995) Ion channel regulation by G proteins. **Physiol. Rev.** 75:865-885.

9. Bezanilla, F. (2000) The voltage sensor in voltage-dependent ion channels. **Physiol Rev.** 80:555-592.

10. Sigworth, F.J. (1994) Voltage gating of ion channels. **Quarterly Reviews of Biophysics** 27:1-40.

11. Catterall, W.A. (1988) Structure and function of voltage-sensitive ion channels. **Science** 242:50-61.

12. Snyders, D.J. (1999) Structure and function of cardiac potassium channels. **Cardiovasc. Res.** 42:377-390.

13. Swartz, K.J. (2004) Towards a structural view of gating in potassium channels. **Nat. Rev. Neurosci.** 5:905-916.

14. Roden, D.M. George, A.L., Jr. (1997) Structure and function of cardiac sodium and potassium channels. **Am J Physiol** 273:H511-H525.

15. Hille, B. (2001) *Ion channels of excitable membranes*, 3rd Ed., Sinauer Associates, Inc., Sunderland

16. Goldstein, S.A., Bockenhauer, D., O'Kelly, I., Zilberberg, N. (2001) Potassium leak channels and the KCNK family of two-P-domain subunits. **Nat. Rev. Neurosci.** 2:175-184.

17. Gutman, G.A., Chandy, K.G., Grissmer, S., Lazdunski, M., McKinnon, D., Pardo, L.A., Robertson, G.A., Rudy, B., Sanguinetti, M.C., Stuhmer, W., Wang, X. (2005) International Union of Pharmacology. LIII. Nomenclature and molecular relationships of voltage-gated potassium channels. **Pharmacol. Rev.** 57:473-508.

18. Deal, K.K., England, S.K., Tamkun, M.M. (1996) Molecular physiology of cardiac potassium channels. **Physiol. Rev.** 76:49-76.

19. Yellen, G. (2002) The voltage-gated potassium channels and their relatives. **Nature** 419:35-42.

20. Barros, F., Dominguez, P., de la Pena, P. (2012) Cytoplasmic domains and voltage-dependent potassium channel gating. **Front Pharmacol.** 3:49.

21. Doyle, D.A., Cabral, J.M., Pfuetzner, R.A., Kuo, A., Gulbis, J.M., Cohen, S.L., Chait, B.T., MacKinnon, R. (1998) The structure of the potassium channel: molecular basis of K^+ conduction and selectivity. **Science** 280:69-77.

22. Zhou, Y., Morais-Cabral, J.H., Kaufman, A., MacKinnon, R. (2001) Chemistry of ion coordination and hydration revealed by a K+ channel-Fab complex at 2.0 A resolution. **Nature** 414:43-48.

23. MacKinnon, R. (2003) Potassium channels. **FEBS Lett.** 555:62-65.

24. Zhou, Y. MacKinnon, R. (2003) The occupancy of ions in the K+ selectivity filter: charge balance and coupling of ion binding to a protein conformational change underlie high conduction rates. **J Mol. Biol.** 333:965-975.

25. del Camino, D., Holmgren, M., Liu, Y., Yellen, G. (2000) Blocker protection in the pore of a voltage-gated K+ channel and its structural implications. **Nature** 403:321-325.

26. Hodgkin, A.L. Huxley, A.F. (1952) A quantitative description of membrane current and its application to conduction and excitation in nerve. **J. Physiol. (Lond)** 117:500-544.

27. Papazian, D.M., Timpe, L.C., Jan, Y.N., Jan, L.Y. (1991) Alteration of voltage-dependence of Shaker potassium channel by mutations in the S4 sequence. **Nature** 349:305-310.

28. Long, S.B., Campbell, E.B., MacKinnon, R. (2005) Crystal structure of a mammalian voltage-dependent Shaker family K+ channel. **Science** 309:897-903.

29. Bezanilla, F. Stefani, E. (1998) Gating currents. **Methods Enzymol.** 293:331-352.

30. Mannuzzu, L.M., Moronne, M.M., Isacoff, E.Y. (1996) Direct physical measure of conformational rearrangement underlying potassium channel gating. **Science** 271:213-216.

31. Tao, X., Lee, A., Limapichat, W., Dougherty, D.A., MacKinnon, R. (2010) A gating charge transfer center in voltage sensors. **Science** 328:67-73.

32. Jiang, Y., Ruta, V., Chen, J., Lee, A., MacKinnon, R. (2003) The principle of gating charge movement in a voltage-dependent K+ channel. **Nature** 423:42-48.

33. Jiang, Y., Lee, A., Chen, J., Ruta, V., Cadene, M., Chait, B.T., MacKinnon, R. (2003) X-ray structure of a voltage-dependent K+ channel. **Nature** 423:33-41.

34. Zhou, M., Morais-Cabral, J.H., Mann, S., MacKinnon, R. (2001) Potassium channel receptor site for the inactivation gate and quaternary amine inhibitors. **Nature** 411:657-661.

35. Long, S.B., Campbell, E.B., MacKinnon, R. (2005) Voltage sensor of Kv1.2: structural basis of electromechanical coupling. **Science** 309:903-908.

36. Kuo, A., Gulbis, J.M., Antcliff, J.F., Rahman, T., Lowe, E.D., Zimmer, J., Cuthbertson, J., Ashcroft, F.M., Ezaki, T., Doyle, D.A. (2003) Crystal structure of the potassium channel KirBac1.1 in the closed state. **Science** 300:1922-1926.

37. Liu, Y., Holmgren, M., Jurman, M.E., Yellen, G. (1997) Gated access to the pore of a voltage-dependent K^+ channel. **Neuron** 19:175-184.

38. Holmgren, M., Shin, K.S., Yellen, G. (1998) The activation gate of a voltage-gated K+ channel can be trapped in the open state by an intersubunit metal bridge. **Neuron** 21:617-621.

39. del Camino, D. Yellen, G. (2001) Tight steric closure at the intracellular activation gate of a voltage-gated K(+) channel. **Neuron** 32:649-656.

40. Webster, S.M., del Camino, D., Dekker, J.P., Yellen, G. (2004) Intracellular gate opening in Shaker K+ channels defined by high-affinity metal bridges. **Nature** 428:864-868.

41. Isacoff, E.Y., Jan, Y.N., Jan, L.Y. (1991) Putative receptor for the cytoplasmic inactivation gate in the *Shaker* K^+ channel. **Nature** 353:86-90.

42. McCormack, K., Tanouye, M.A., Iverson, L.E., Lin, J.W., Ramaswami, M., McCormack, T., Campanelli, J.T., Mathew, M.K., Rudy, B. (1991) A role for hydrophobic residues in the voltage-dependent gating of Shaker K^+ channels. **Proc. Natl. Acad. Sci. U. S. A.** 88:2931-2935.

43. Sanguinetti M.C. Xu Q.P. (1999) Mutations of the S4-S5 linker alter activation properties of HERG potassium channels expressed in Xenopus oocytes. **J Physiol Lond** -Physiol-Lond. 1999 F.

44. Chen, H., Kurennyi, D.E., Smith, P.A. (2001) Modulation of M-channel conductance by adenosine 5' triphosphate in bullfrog sympathetic B-neurones. **J. Auton. Pharmacol.** 21:57-62.

45. Decher, N., Chen, J., Sanguinetti, M.C. (2004) Voltage-dependent gating of hyperpolarization-activated, cyclic nucleotide-gated pacemaker channels: molecular coupling between the S4-S5 and C-linkers. **J Biol. Chem** 279:13859-13865.

46. Caprini, M., Fava, M., Valente, P., Fernandez-Ballester, G., Rapisarda, C., Ferroni, S., Ferrer-Montiel, A. (2005) Molecular compatibility of the channel gate and the N terminus of S5 segment for voltage-gated channel activity. **J. Biol. Chem.** 280:18253-18264.

47. Lu, Z., Klem, A.M., Ramu, Y. (2001) Ion conduction pore is conserved among potassium channels. **Nature** 413:809-813.

48. Lu, Z., Klem, A.M., Ramu, Y. (2002) Coupling between voltage sensors and activation gate in voltage-gated K+ channels. **J. Gen. Physiol** 120:663-676.

49. Smith-Maxwell, C.J., Ledwell, J.L., Aldrich, R.W. (1998) Role of the S4 in cooperativity of voltage-dependent potassium channel activation. **J. Gen. Physiol** 111:399-420.

50. Ledwell, J.L. Aldrich, R.W. (1999) Mutations in the S4 region isolate the final voltage-dependent cooperative step in potassium channel activation. **J. Gen. Physiol.** 113:389-414.

51. Pathak, M., Kurtz, L., Tombola, F., Isacoff, E. (2005) The cooperative voltage sensor motion that gates a potassium channel. **J. Gen. Physiol** 125:57-69.

52. Stuhmer, W., Ruppersberg, J.P., Schroter, K.H., Sakmann, B., Stocker, M., Giese, K.P., Perschke, A., Baumann, A., Pongs, O. (1989) Molecular basis of functional diversity of voltage-gated potassium channels in mammalian brain. **EMBO J.** 8:3235-3244.

53. Swanson, R., Marshall, J., Smith, J.S., Williams, J.B., Boyle, M.B., Folander, K., Luneau, C.J., Antanavage, J., Oliva, C., Buhrow, S.A., Bennett, C., Stein, R.B., Kaczmarek, L.K. (1990) Cloning and expression of cDNA and genomic clones encoding three delayed rectifier potassium channels in rat brain. **Neuron** 4:929-939.

54. Christie, M.J., North, R.A., Osborne, P.B., Douglass, J., Adelman, J.P. (1990) Heteropolymeric potassium channels expressed in Xenopus oocytes from cloned subunits. **Neuron** 4:405-411.

55. Grissmer, S., Dethlefs, B., Wasmuth, J.J., Goldin, A.L., Gutman, G.A., Cahalan, M.D., Chandy, K.G. (1990) Expression and chromosomal localization of a lymphocyte K^+ channel gene. **Proc. Natl. Acad. Sci. U. S. A.** 87:9411-9415.

56. Chandy, K.G., Cahalan, M.D., Grissmer, S. (1990) Autoimmune diseases linked to abnormal K+ channel expression in double-negative CD4-CD8- T cells. **Eur. J. Immunol.** 20:747-751.

57. Douglass, J., Osborne, P.B., Cai, Y.C., Wilkinson, M., Christie, M.J., Adelman, J.P. (1990) Characterization and functional expression of a rat genomic DNA clone encoding a lymphocyte potassium channel. **J. Immunol.** 144:4841-4850.

58. Attali, B., Romey, G., Honoré, E., Schmid-Alliana, A., Mattei, M.G., Lesage, F., Ricard, P., Barhanin, J., Lazdunski, M. (1992) Cloning, functional expression, and regulation of two K^+ channels in human T lymphocytes. **J. Biol. Chem.** 267:8650-8657.

59. Biju, K.C., Marks, D.R., Mast, T.G., Fadool, D.A. (2008) Deletion of voltage-gated channel affects glomerular refinement and odorant receptor expression in the mouse olfactory system. **J. Comp Neurol.** 506:161-179.

60. Fadool, D.A., Tucker, K., Perkins, R., Fasciani, G., Thompson, R.N., Parsons, A.D., Overton, J.M., Koni, P.A., Flavell, R.A., Kaczmarek, L.K. (2004) Kv1.3 channel gene-targeted deletion produces "Super-Smeller Mice" with altered glomeruli, interacting scaffolding proteins, and biophysics. **Neuron** 41:389-404.

61. Li, Y., Wang, P., Xu, J., Desir, G.V. (2006) Voltage-gated potassium channel Kv1.3 regulates GLUT4 trafficking to the plasma membrane via a Ca2+-dependent mechanism. **Am. J. Physiol Cell Physiol** 290:C345-C351.

62. Xu, J., Wang, P., Li, Y., Li, G., Kaczmarek, L.K., Wu, Y., Koni, P.A., Flavell, R.A., Desir, G.V. (2004) The voltage-gated potassium channel Kv1.3 regulates peripheral insulin sensitivity. **Proc. Natl. Acad. Sci. U. S. A** 101:3112-3117.

63. Vicente, R., Escalada, A., Villalonga, N., Texido, L., Roura-Ferrer, M., Martin-Satue, M., Lopez-Iglesias, C., Soler, C., Solsona, C., Tamkun, M.M., Felipe, A. (2006) Association of Kv1.5 and Kv1.3 contributes to the major voltage-dependent K+ channel in macrophages. **J Biol. Chem** 281:37675-37685.

64. Wulff, H., Calabresi, P.A., Allie, R., Yun, S., Pennington, M., Beeton, C., Chandy, K.G. (2003) The voltage-gated Kv1.3 K(+) channel in effector memory T cells as new target for MS. **J. Clin. Invest** 111:1703-1713.

65. DeCoursey, T.E., Chandy, K.G., Gupta, S., Cahalan, M.D. (1984) Voltage-gated K+ channels in human T lymphocytes: a role in mitogenesis? **Nature** 307:465-468.

66. Matteson, D.R. Deutsch, C. (1984) K channels in T lymphocytes: a patch clamp study using monoclonal antibody adhesion. **Nature** 307:468-471.

67. Vicente, R., Escalada, A., Coma, M., Fuster, G., Sanchez-Tillo, E., Lopez-Iglesias, C., Soler, C., Solsona, C., Celada, A., Felipe, A. (2003) Differential voltage-dependent K+ channel responses during proliferation and activation in macrophages. **J. Biol. Chem.** 278:46307-46320.

68. Villalonga, N., Escalada, A., Vicente, R., Sanchez-Tillo, E., Celada, A., Solsona, C., Felipe, A. (2007) Kv1.3/Kv1.5 heteromeric channels compromise pharmacological responses in macrophages. **Biochem. Biophys. Res. Comm.** 352:913-918.

69. Villalonga, N., David, M., Bielánska, J., Vicente, R., Comes, N., Valenzuela, C., Felipe, A. (2010) Immunomodulation of voltage-dependent K^+ channels in macrophages: molecular and biophysical consequences. **J. Gen. Physiol** 135:135-147.

70. Beeton, C., Wulff, H., Standifer, N.E., Azam, P., Mullen, K.M., Pennington, M.W., Kolski-Andreaco, A., Wei, E., Grino, A., Counts, D.R., Wang, P.H., LeeHealey, C.J., Andrews, S., Sankaranarayanan, A., Homerick, D., Roeck, W.W., Tehranzadeh, J., Stanhope, K.L., Zimin, P., Havel, P.J., Griffey, S., Knaus, H.G., Nepom, G.T., Gutman, G.A., Calabresi, P.A., Chandy, K.G. (2006) Kv1.3 channels are a therapeutic target for T cell-mediated autoimmune diseases. **Proc. Natl. Acad. Sci. U. S. A** 103:17414-17419.

71. Tang, Q., Jin, M.W., Xiang, J.Z., Dong, M.Q., Sun, H.Y., Lau, C.P., Li, G.R. (2007) The membrane permeable calcium chelator BAPTA-AM directly blocks human ether a-go-go-related gene potassium channels stably expressed in HEK 293 cells. **Biochem. Pharmacol.** 74:1596-1607.

72. Grissmer, S. Cahalan, M.D. (1989) TEA prevents inactivation while blocking open K^+ channels in human T lymphocytes. **Biophys. J.** 55:203-206.

73. Panyi, G., Sheng, Z., Deutsch, C. (1995) C-type inactivation of a voltage-gated K+ channel occurs by a cooperative mechanism. **Biophys. J.** 69:896-903.

74. Nguyen, A., Kath, J.C., Hanson, D.C., Biggers, M.S., Canniff, P.C., Donovan, C.B., Mather, R.J., Bruns, M.J., Rauer, H., Aiyar, J., Lepple Wienhues, A., Gutman, G.A., Grissmer, S., Cahalan, M.D., Chandy, K.G. (1996) Novel nonpeptide agents potently block the C-type inactivated conformation of Kv1.3 and suppress T cell activation. **Mol. Pharmacol.** 50:1672-1679.

75. Grissmer, S. Cahalan, M.D. (1989) Divalent ion trapping inside potassium channels of human T lymphocytes. **J. Gen. Physiol.** 93:609-630.

76. Autieri, M.V., Belkowski, S.M., Constantinescu, C.S., Cohen, J.A., Prystowsky, M.B. (1997) Lymphocyte-specific inducible expression of potassium channel beta subunits. **J. Neuroimmunol.** 77:8-16.

77. Vicente, R., Escalada, A., Soler, C., Grande, M., Celada, A., Tamkun, M.M., Solsona, C., Felipe, A. (2005) Pattern of Kv beta subunit expression in macrophages depends upon proliferation and the mode of activation. **J. Immunol.** 174:4736-4744.

78. Toth, B., Sarang, Z., Vereb, G., Zhang, A., Tanaka, S., Melino, G., Fesus, L., Szondy, Z. (2009) Over-expression of integrin beta3 can partially overcome the defect of integrin beta3 signaling in transglutaminase 2 null macrophages. **Immunol. Lett.** 126:22-28.

79. Schilling, T. Eder, C. (2003) Effects of kinase inhibitors on TGF-beta induced upregulation of Kv1.3 K+ channels in brain macrophages. **Pflugers Arch.** 447:312-315.

80. Kuras, Z., Kucher, V., Gordon, S.M., Neumeier, L., Chimote, A.A., Filipovich, A.H., Conforti, L. (2012) Modulation of Kv1.3 channels by protein kinase A I in T lymphocytes is mediated by the disc large 1-tyrosine kinase Lck complex. **Am. J. Physiol Cell Physiol** 302:C1504-C1512.

81. Sands, S.B., Lewis, R.S., Cahalan, M.D. (1989) Charybdotoxin blocks voltage-gated K^+ channels in human and murine T lymphocytes. **J. Gen. Physiol.** 93:1061-1074.

82. Ghanshani, S., Wulff, H., Miller, M.J., Rohm, H., Neben, A., Gutman, G.A., Cahalan, M.D., Chandy, K.G. (2000) Up-regulation of the IKCa1 potassium channel during T-cell activation. Molecular mechanism and functional consequences. **J. Biol. Chem.** 275:37137-37149.

83. Panyi, G., Possani, L.D., Rodriguez de la Vega RC, Gaspar, R., Varga, Z. (2006) K+ channel blockers: novel tools to inhibit T cell activation leading to specific immunosuppression. **Curr. Pharm. Des** 12:2199-2220.

84. Cahalan, M.D. Chandy, K.G. (2009) The functional network of ion channels in T lymphocytes. **Immunol. Rev.** 231:59-87.

85. Felix, J.P., Bugianesi, R.M., Schmalhofer, W.A., Borris, R., Goetz, M.A., Hensens, O.D., Bao, J.M., Kayser, F., Parsons, W.H., Rupprecht, K., Garcia, M.L., Kaczorowski, G.J., Slaughter, R.S. (1999) Identification and biochemical characterization of a novel nortriterpene inhibitor of the human lymphocyte voltage-gated potassium channel, Kv1.3. **Biochem.** 38:4922-4930.

86. Chandy, K.G., Wulff, H., Beeton, C., Pennington, M., Gutman, G.A., Cahalan, M.D. (2004) K+ channels as targets for specific immunomodulation. **Trends Pharmacol. Sci.** 25:280-289.

87. Tamkun, M.M., Knoth, K.M., Walbridge, J.A., Kroemer, H., Roden, D.M., Glover, D.M. (1991) Molecular cloning and characterization of two voltage-gated K+ channel cDNAs from human ventricle. **FASEB J** 5:331-337.

88. Fedida, D., Wible, B., Wang, Z., Fermini, B., Faust, F., Nattel, S., Brown, A.M. (1993) Identity of a novel delayed rectifier current from human heart with a cloned K^+ channel current. **Circ. Res.** 73:210-216.

89. Mays, D.J., Foose, J.M., Philipson, L.H., Tamkun, M.M. (1995) Localization of the Kv1.5 K^+ channel protein in explanted cardiac tissue. **J. Clin. Invest.** 96:282-292.

90. Wang, J., Juhaszova, M., Rubin, L.J., Yuan, X.J. (1997) Hypoxia inhibits gene expression of voltage-gated K+ channel alpha subunits in pulmonary artery smooth muscle cells. **J. Clin. Invest.** 100:2347-2353.

91. Matsubara, H., Liman, E.R., Hess, P., Koren, G. (1994) Pretranslational mechanisms determine the type of potassium channels expressed in the rat skeletal and cardiac muscles. **J. Biol. Chem.** 266:13324-13328.

92. Jou, I., Pyo, H., Chung, S., Jung, S.Y., Gwag, B.J., Joe, E.H. (1998) Expression of Kv1.5 K+ channels in activated microglia in vivo. **GLIA** 24:408-414.

93. Macias, A., Moreno, C., Moral-Sanz, J., Cogolludo, A., David, M., Alemanni, M., Perez-Vizcaino, F., Zaza, A., Valenzuela, C., Gonzalez, T. (2010) Celecoxib blocks cardiac Kv1.5, Kv4.3 and Kv7.1 (KCNQ1) channels: effects on cardiac action potentials. **J. Mol. Cell Cardiol.** 49:984-992.

94. Valenzuela, C., Delpon, E., Franqueza, L., Gay, P., Perez, O., Tamargo, J., Snyders, D.J. (1996) Class III antiarrhythmic effects of zatebradine. Time-, state-, use-, and voltage-dependent block of hKv1.5 channels. **Circulation** 94:562-570.

95. Amos, G.J., Wettwer, E., Metzger, F., Li, Q., Himmel, H.M., Ravens, U. (1996) Differences between outward currents of human atrial and subepicardial ventricular myocytes. **J. Physiol** 491 (Pt 1):31-50.

96. Wang, Z., Fermini, B., Nattel, S. (1993) Sustained depolarization-induced outward current in human atrial myocytes. Evidence for a novel delayed rectifier K^+ current similar to Kv1.5 cloned channel currents. **Circ. Res.** 73:1061-1076.

97. Snyders, D.J., Tamkun, M.M., Bennett, P.B. (1993) A rapidly activating and slowly inactivating potassium channel cloned from human heart. Functional analysis after stable mammalian cell culture expression. **J. Gen. Physiol.** 101:513-543.

98. Uebele, V.N., England, S.K., Chaudhary, A., Tamkun, M.M., Snyders, D.J. (1996) Functional differences in Kv1.5 currents expressed in mammalian cell lines are due to the presence of endogenous Kvβ2.1 subunits. **J. Biol. Chem.** 271:2406-2412.

99. Uebele, V.N., England, S.K., Gallagher, D.J., Snyders, D.J., Bennett, P.B., Tamkun, M.M. (1998) Distinct domains of the voltage-gated K^+ channel Kvβ1.3 β-subunit affect voltage-dependent gating. **Am. J. Physiol** 274:C1485-C1495.

100. Gonzalez, T., Navarro-Polanco, R., Arias, C., Caballero, R., Moreno, I., Delpon, E., Tamargo, J., Tamkun, M.M., Valenzuela, C. (2002) Assembly with the Kvβ1.3 subunit modulates drug block of hKv1.5 channels. **Mol. Pharmacol.** 62:1456-1463.

101. Decher, N., Kumar, P., Gonzalez, T., Renigunta, V., Sanguinetti, M.C. (2005) Structural basis for competition between drug binding and Kvbeta1.3 accessory subunit-induced N-type inactivation of Kv1.5 channels. **Mol. Pharmacol.** 68:995-1005.

102. Arias, C., Guizy, M., David, M., Marzian, S., Gonzalez, T., Decher, N., Valenzuela, C. (2007) Kvβ1.3 reduces the degree of stereoselective bupivacaine block of Kv1.5 channels. **Anesthesiol.** 107:641-651.

103. Decher, N., Gonzalez, T., Streit, A.K., Sachse, F.B., Renigunta, V., Soom, M., Heinemann, S.H., Daut, J., Sanguinetti, M.C. (2008) Structural determinants of Kvbeta1.3-induced channel inactivation: a hairpin modulated by PIP2. **EMBO J.** 27:3164-3174.

104. England, S.K., Uebele, V.N., Shear, H., Kodali, J., Bennett, P.B., Tamkun, M.M. (1995) Characterization of a voltage-gated K^+ channel β subunit expressed in human heart. **Proc. Natl. Acad. Sci. U. S. A** 92:6309-6313.

105. Li, H., Guo, W., Mellor, R.L., Nerbonne, J.M. (2005) KChIP2 modulates the cell surface expression of Kv 1.5-encoded K^+ channels. **J Mol. Cell Cardiol** 39:121-132.

106. Li, G.R., Feng, J., Wang, Z., Fermini, B., Nattel, S. (1996) Adrenergic modulation of ultrarapid delayed rectifier K+ current in human atrial myocytes. **Circ. Res.** 78:903-915.

107. Kwak, Y.G., Navarro-Polanco, R., Grobaski, T., Gallagher, D.J., Tamkun, M.M. (1999) Phosphorylation is required for alteration of Kv1.5 K^+ channel function by the Kvβ1.3 subunit. **J. Biol. Chem.** 274:25355-25361.

108. Kwak, Y.G., Hu, N., Wei, J., George, A.L., Jr., Grobaski, T.D., Tamkun, M.M., Murray, K.T. (1999) Protein kinase A phosphorylation alters Kvβ1.3 subunit- mediated inactivation of the Kv1.5 potassium channel. **J. Biol. Chem.** 274:13928-13932.

109. Murray, K.T., Fahrig, S.A., Deal, K.K., Po, S.S., Hu, N.N., Snyders, D.J., Tamkun, M.M., Bennett, P.B. (1994) Modulation of an inactivating human cardiac K^+ channel by protein kinase C. **Circ. Res.** 75:999-1005.

110. Williams, C.P., Hu, N., Shen, W., Mashburn, A.B., Murray, K.T. (2002) Modulation of the human Kv1.5 channel by protein kinase C activation: role of the Kvbeta1.2 subunit. **J Pharmacol. Exp. Ther.** 302:545-550.

111. David, M., Macias, A., Moreno, C., Prieto, A., Martinez-Marmol, R., Vicente, R., Felipe, A., Gonzalez, T., Tamkun, M.M., Valenzuela, C. (2012) PKC activity regulates functional effects of K_Vβ1.3 on K_V1.5 channels. Identification of a cardiac Kv1.5 channelosome. **J. Biol. Chem.** 287:21416-21428.

112. Nunez, L., Vaquero, M., Gomez, R., Caballero, R., Mateos-Caceres, P., Macaya, C., Iriepa, I., Galvez, E., Lopez-Farre, A., Tamargo, J., Delpon, E. (2006) Nitric oxide blocks hKv1.5 channels by S-nitrosylation and by a cyclic GMP-dependent mechanism. **Cardiovasc. Res.** 72:80-89.

113. Franqueza, L., Valenzuela, C., Delpon, E., Longobardo, M., Caballero, R., Tamargo, J. (1998) Effects of propafenone and 5-hydroxy-propafenone on hKv1.5 channels. **Br. J. Pharmacol.** 125:969-978.

114. Delpon, E., Valenzuela, C., Perez, O., Franqueza, L., Gay, P., Snyders, D.J., Tamargo, J. (1996) Mechanisms of block of a human cloned potassium channel by the enantiomers of a new bradycardic agent: S-16257-2 and S-16260-2. **Br. J. Pharmacol.** 117:1293-1301.

115. Carmeliet, E. Mubagwa, K. (1998) Antiarrhythmic drugs and cardiac ion channels: mechanisms of action. **Prog. Biophys. Mol. Biol.** 70:1-72.

116. Snyders, D.J., Knoth, K.M., Roberds, S.L., Tamkun, M.M. (1992) Time-, voltage-, and state-dependent block by quinidine of a cloned human cardiac potassium channel. **Mol. Pharmacol.** 41:322-330.

117. Grissmer, S., Nguyen, A.N., Aiyar, J., Hanson, D.C., Mather, R.J., Gutman, G.A., Karmilowicz, M.J., Auperin, D.D., Chandy, K.G. (1994) Pharmacological characterization of five cloned voltage-gated K^+ channels, types Kv1.1, 1.2, 1.3, 1.5, and 3.1, stably expressed in mammalian cell lines. **Mol. Pharmacol.** 45:1227-1234.

118. Wang, Q., Curran, M.E., Splawski, I., Burn, T.C., Millholland, J.M., VanRaay, T.J., Shen, J., Timothy, K.W., Vincent, G.M., De Jager, T., Schwartz, P.J., Toubin, J.A., Moss, A.J., Atkinson, D.L., Landes, G.M., Connors, T.D., Keating, M.T. (1996) Positional cloning of a novel potassium channel gene: KVLQT1 mutations cause cardiac arrhythmias. **Nat. Genet.** 12:17-23.

119. Jespersen, T., Grunnet, M., Olesen, S.P. (2005) The KCNQ1 potassium channel: from gene to physiological function. **Physiology. (Bethesda.)** 20:408-416.

120. Demolombe, S., Lande, G., Charpentier, F., van Roon, M.A., van den Hoff, M.J., Toumaniantz, G., Baro, I., Guihard, G., Le Berre, N., Corbier, A., de Bakker, J., Opthof, T., Wilde, A., Moorman, A.F., Escande, D. (2001) Transgenic mice overexpressing human KvLQT1 dominant-negative isoform. Part I: Phenotypic characterisation. **Cardiovasc. Res.** 50:314-327.

121. Pusch, M. (1998) Increase of the single-channel conductance of KvLQT1 potassium channels induced by the association with minK. **Pflugers Arch.** 437:172-174.

122. Splawski, I., Tristani Firouzi, M., Lehmann, M.H., Sanguinetti, M.C., Keating, M.T. (1997) Mutations in the hminK gene cause long QT syndrome and suppress IKs function. **Nature Genetics** 17:338-340.

123. Wang, W., Xia, J., Kass, R.S. (1998) MinK-KvLQT1 fusion proteins, evidence for multiple stoichiometries of the assembled IsK channel. **J Biol. Chem.** 273:34069-34074.

124. Seebohm, G., Sanguinetti, M.C., Pusch, M. (2003) Tight coupling of rubidium conductance and inactivation in human KCNQ1 potassium channels. **J. Physiol** 552:369-378.

125. Seebohm, G., Westenskow, P., Lang, F., Sanguinetti, M.C. (2005) Mutation of colocalized residues of the pore helix and transmembrane segments S5 and S6 disrupt deactivation and modify inactivation of KCNQ1 K+ channels. **J. Physiol** 563:359-368.

126. Romey, G., Attali, B., Chouabe, C., Abitbol, I., Guillemare, E., Barhanin, J., Lazdunski, M. (1997) Molecular mechanism and functional significance of the MinK control of the KvLQT1 channel activity. **J. Biol. Chem.** 272:16713-16716.

127. Sesti, F. Goldstein, S.A. (1998) Single-channel characteristics of wild-type IKs channels and channels formed with two minK mutants that cause long QT syndrome. **J. Gen. Physiol** 112:651-663.

128. Yang, Y. Sigworth, F.J. (1998) Single-channel properties of IKs potassium channels. **J. Gen. Physiol** 112:665-678.

129. Dong, M.Q., Lau, C.P., Gao, Z., Tseng, G.N., Li, G.R. (2006) Characterization of recombinant human cardiac KCNQ1/KCNE1 channels (I (Ks)) stably expressed in HEK 293 cells. **J. Membr. Biol.** 210:183-192.

130. Busch, A.E., Busch, G.L., Ford, E., Suessbrich, H., Lang, H.J., Greger, R., Kunzelmann, K., Attali, B., Stuhmer, W. (1997) The role of the IsK protein in the specific pharmacological properties of the IKs channel complex. **Br. J. Pharmacol.** 122:187-189.

131. Heitzmann, D., Grahammer, F., von, H.T., Schmitt-Graff, A., Romeo, E., Nitschke, R., Gerlach, U., Lang, H.J., Verrey, F., Barhanin, J., Warth, R. (2004) Heteromeric KCNE2/KCNQ1 potassium channels in the luminal membrane of gastric parietal cells. **J. Physiol** 561:547-557.

132. Sesti, F., Tai, K.K., Goldstein, S.A. (2000) MinK endows the I(Ks) potassium channel pore with sensitivity to internal tetraethylammonium. **Biophys. J.** 79:1369-1378.

133. Melman, Y.F., Domenech, A., de la Luna, S., McDonald, T.V. (2001) Structural determinants of KvLQT1 control by the KCNE family of proteins. **J. Biol. Chem.** 276:6439-6444.

134. Sanguinetti, M.C. Jurkiewicz, N.K. (1990) Two components of cardiac delayed rectifier K^+ current. Differential sensitivity to block by class III antiarrhythmic agents. **J. Gen. Physiol.** 96:195-215.

135. Barhanin, J., Lesage, F., Guillemare, E., Fink, M., Lazdunski, M., Romey, G. (1996) K(V)LQT1 and IsK (minK) proteins associate to form the I(Ks) cardiac potassium current [see comments]. **Nature** 384:78-80.

136. Sanguinetti, M.C., Curran, M.E., Zou, A., Shen, J., Spector, P.S., Atkinson, D.L., Keating, M.T. (1996) Coassembly of K(V)LQT1 and minK (IsK) proteins to form cardiac I(Ks) potassium channel. **Nature** 384:80-83.

137. Bendahhou, S., Marionneau, C., Haurogne, K., Larroque, M.M., Derand, R., Szuts, V., Escande, D., Demolombe, S., Barhanin, J. (2005) In vitro molecular interactions and distribution of KCNE family with KCNQ1 in the human heart. **Cardiovasc. Res.** 67:529-538.

138. Wu, D.M., Jiang, M., Zhang, M., Liu, X.S., Korolkova, Y.V., Tseng, G.N. (2006) KCNE2 is colocalized with KCNQ1 and KCNE1 in cardiac myocytes and may function as a negative modulator of I(Ks) current amplitude in the heart. **Heart Rhythm.** 3:1469-1480.

139. Pusch, M., Magrassi, R., Wollnik, B., Conti, F. (1998) Activation and inactivation of homomeric KvLQT1 potassium channels. **Biophys. J.** 75:785-792.

140. Tristani Firouzi, M. Sanguinetti, M.C. (1998) Voltage-dependent inactivation of the human K+ channel KvLQT1 is eliminated by association with minimal K+ channel (minK) subunits. **J. Physiol. Lond.** 510:37-45.

141. Lerche, C., Seebohm, G., Wagner, C.I., Scherer, C.R., Dehmelt, L., Abitbol, I., Gerlach, U., Brendel, J., Attali, B., Busch, A.E. (2000) Molecular impact of MinK on the enantiospecific block of I(Ks) by chromanols. **Br. J Pharmacol.** 131:1503-1506.

142. Seebohm, G., Lerche, C., Busch, A.E., Bachmann, A. (2001) Dependence of I(Ks) biophysical properties on the expression system. **Pflugers Arch.** 442:891-895.

143. Seebohm, G., Lerche, C., Pusch, M., Steinmeyer, K., Bruggemann, A., Busch, A.E. (2001) A kinetic study on the stereospecific inhibition of KCNQ1 and I(Ks) by the chromanol 293B. **Br. J Pharmacol.** 134:1647-1654.

144. Seebohm, G., Scherer, C.R., Busch, A.E., Lerche, C. (2001) Identification of specific pore residues mediating KCNQ1 inactivation. A novel mechanism for long QT syndrome. **J Biol. Chem** 276:13600-13605.

145. Seebohm, G., Chen, J., Strutz, N., Culberson, C., Lerche, C., Sanguinetti, M.C. (2003) Molecular determinants of KCNQ1 channel block by a benzodiazepine. **Mol. Pharmacol.** 64:70-77.

146. Terrenoire, C., Clancy, C.E., Cormier, J.W., Sampson, K.J., Kass, R.S. (2005) Autonomic control of cardiac action potentials: role of potassium channel kinetics in response to sympathetic stimulation. **Circ. Res.** 96:e25-e34.

147. Potet, F., Scott, J.D., Mohammad-Panah, R., Escande, D., Baro, I. (2001) AKAP proteins anchor cAMP-dependent protein kinase to KvLQT1/IsK channel complex. **Am J Physiol Heart Circ. Physiol** 280:H2038-H2045.

148. Marx, S.O., Kurokawa, J., Reiken, S., Motoike, H., D'Armiento, J., Marks, A.R., Kass, R.S. (2002) Requirement of a macromolecular signaling complex for beta adrenergic receptor modulation of the KCNQ1-KCNE1 potassium channel. **Science** 295:496-499.

149. Kurokawa, J., Motoike, H.K., Rao, J., Kass, R.S. (2004) Regulatory actions of the A-kinase anchoring protein Yotiao on a heart potassium channel downstream of PKA phosphorylation. **Proc. Natl. Acad. Sci. U. S. A** 101:16374-16378.

150. Loussouarn, G., Park, K.H., Bellocq, C., Baro, I., Charpentier, F., Escande, D. (2003) Phosphatidylinositol-4,5-bisphosphate, PIP2, controls KCNQ1/KCNE1 voltage-gated potassium channels: a functional homology between voltage-gated and inward rectifier K+ channels. **EMBO J** 22:5412-5421.

151. Park, K.H., Piron, J., Dahimene, S., Merot, J., Baro, I., Escande, D., Loussouarn, G. (2005) Impaired KCNQ1-KCNE1 and phosphatidylinositol-4,5-bisphosphate interaction underlies the long QT syndrome. **Circ. Res.** 96:730-739.

152. Ho, K., Nichols, C.G., Lederer, W.J., Lytton, J., Vassilev, P.M., Kanazirska, M.V., Hebert, S.C. (1993) Cloning and expression of an inward rectifying ATP-regulated potassium channel. **Nature** 362:31-38.

153. Kubo, Y., Baldwin, T.J., Jan, Y.N., Jan, L.Y. (1993) Primary structure and functional expression of a mouse inward rectifier potassium channel. **Nature** 362:127-133.

154. Kubo, Y., Adelman, J.P., Clapham, D.E., Jan, L.Y., Karschin, A., Kurachi, Y., Lazdunski, M., Nichols, C.G., Seino, S., Vandenberg, C.A. (2005) International Union of Pharmacology. LIV. Nomenclature and molecular relationships of inwardly rectifying potassium channels. **Pharmacol. Rev.** 57:509-526.

155. Doupnik, C.A., Davidson, N., Lester, H.A. (1995) The inward rectifier potassium channel family. **Curr. Opin. Neurobiol.** 5:268-277.

156. Hibino, H., Inanobe, A., Furutani, K., Murakami, S., Findlay, I., Kurachi, Y. (2010) Inwardly rectifying potassium channels: their structure, function, and physiological roles. **Physiol Rev.** 90:291-366.

157. Karschin, C., Dissmann, E., Stuhmer, W., Karschin, A. (1996) IRK(1-3) and GIRK(1-4) inwardly rectifying K+ channel mRNAs are differentially expressed in the adult rat brain. **J. Neurosci.** 16:3559-3570.

158. Fang, Y., Schram, G., Romanenko, V.G., Shi, C., Conti, L., Vandenberg, C.A., Davies, P.F., Nattel, S., Levitan, I. (2005) Functional expression of Kir2.x in human aortic endothelial cells: the dominant role of Kir2.2. **Am. J. Physiol Cell Physiol** 289:C1134-C1144.

159. Tinker, A., Jan, Y.N., Jan, L.Y. (1996) Regions responsible for the assembly of inwardly rectifying potassium channels. **Cell** 87:857-868.

160. Preisig-Muller, R., Schlichthorl, G., Goerge, T., Heinen, S., Bruggemann, A., Rajan, S., Derst, C., Veh, R.W., Daut, J. (2002) Heteromerization of Kir2.x potassium channels contributes to the phenotype of Andersen's syndrome. **Proc. Natl. Acad. Sci. U. S. A** 99:7774-7779.

161. Lopez-Izquierdo, A., Ponce-Balbuena, D., Ferrer, T., Rodriguez-Menchaca, A.A., Sanchez-Chapula, J.A. (2010) Thiopental inhibits function of different inward rectifying potassium channel isoforms by a similar mechanism. **Eur. J. Pharmacol.** 638:33-41.

162. Matsuda, H., Saigusa, A., Irisawa, H. (1987) Ohmic conductance through the inwardly rectifying K channel and blocking by internal Mg^{2+}. **Nature** 325:156-159.

163. Vandenberg, C.A. (1987) Inward rectification of a potassium channel in cardiac ventricular cells depends on internal magnesium ions. **Proc. Natl. Acad. Sci. U. S. A.** 84:2560-2564.

164. Lopatin, A.N., Makhina, E.N., Nichols, C.G. (1994) Potassium channel block by cytoplasmic polyamines as the mechanism of intrinsic rectification. **Nature** 372:366-369.

165. Minor, D.L., Jr., Masseling, S.J., Jan, Y.N., Jan, L.Y. (1999) Transmembrane structure of an inwardly rectifying potassium channel. **Cell** 96:879-891.

166. Hilgemann, D.W., Feng, S., Nasuhoglu, C. (2001) The complex and intriguing lives of PIP2 with ion channels and transporters. **Sci. STKE.** 2001:re19.

167. Takano, M. Kuratomi, S. (2003) Regulation of cardiac inwardly rectifying potassium channels by membrane lipid metabolism. **Prog. Biophys. Mol. Biol.** 81:67-79.

168. Dart, C. Leyland, M.L. (2001) Targeting of an A kinase-anchoring protein, AKAP79, to an inwardly rectifying potassium channel, Kir2.1. **J. Biol. Chem.** 276:20499-20505.

169. Rapedius, M., Soom, M., Shumilina, E., Schulze, D., Schonherr, R., Kirsch, C., Lang, F., Tucker, S.J., Baukrowitz, T. (2005) Long chain CoA esters as competitive antagonists of phosphatidylinositol 4,5-bisphosphate activation in Kir channels. **J. Biol. Chem.** 280:30760-30767.

170. Soom, M., Schonherr, R., Kubo, Y., Kirsch, C., Klinger, R., Heinemann, S.H. (2001) Multiple PIP2 binding sites in Kir2.1 inwardly rectifying potassium channels. **FEBS Lett.** 490:49-53.

171. Alagem, N., Dvir, M., Reuveny, E. (2001) Mechanism of Ba(2+) block of a mouse inwardly rectifying K+ channel: differential contribution by two discrete residues. **J. Physiol** 534:381-393.

172. Abrams, C.J., Davies, N.W., Shelton, P.A., Stanfield, P.R. (1996) The role of a single aspartate residue in ionic selectivity and block of a murine inward rectifier K+ channel Kir2.1. **J. Physiol. (Lond)** 493:643-649.

173. Hagiwara, S., Miyazaki, S., Rosenthal, N.P. (1976) Potassium current and the effect of cesium on this current during anomalous rectification of the egg cell membrane of a starfish. **J. Gen. Physiol** 67:621-638.

174. Oonuma, H., Iwasawa, K., Iida, H., Nagata, T., Imuta, H., Morita, Y., Yamamoto, K., Nagai, R., Omata, M., Nakajima, T. (2002) Inward rectifier K(+) current in human bronchial smooth muscle cells: inhibition with antisense oligonucleotides targeted to Kir2.1 mRNA. **Am. J. Respir. Cell Mol. Biol.** 26:371-379.

175. Nerbonne, J.M. (2000) Molecular basis of functional voltage-gated K+ channel diversity in the mammalian myocardium. **J. Physiol** 525 Pt 2:285-298.

176. Coetzee, W.A., Amarillo, Y., Chiu, J., Chow, A., Lau, D., McCormack, T., Moreno, H., Nadal, M.S., Ozaita, A., Pountney, D., Saganich, M., Vega Saenz de Miera, E., Rudy, B. (1999) Molecular diversity of K+ channels. **Ann. N. Y. Acad. Sci.** 868:233-285.

177. Ravens, U. Cerbai, E. (2008) Role of potassium currents in cardiac arrhythmias. **Europace.** 10:1133-1137.

178. Cerrone, M., Napolitano, C., Priori, S.G. (2012) Genetics of ion-channel disorders. **Curr. Opin. Cardiol.** 27:242-252.

179. Martin, C.A., Matthews, G.D., Huang, C.L. (2012) Sudden cardiac death and inherited channelopathy: the basic electrophysiology of the myocyte and myocardium in ion channel disease. **Heart** 98:536-543.

180. Bastiaenen, R. Behr, E.R. (2011) Sudden death and ion channel disease: pathophysiology and implications for management. **Heart** 97:1365-1372.

181. Gussak, I., Brugada, P., Brugada, J., Wright, R.S., Kopecky, S.L., Chaitman, B.R., Bjerregaard, P. (2000) Idiopathic short QT interval: a new clinical syndrome? **Cardiology** 94:99-102.

182. Gaita, F., Giustetto, C., Bianchi, F., Wolpert, C., Schimpf, R., Riccardi, R., Grossi, S., Richiardi, E., Borggrefe, M. (2003) Short QT Syndrome: a familial cause of sudden death. **Circulation** 108:965-970.

183. Brugada, R., Hong, K., Dumaine, R., Cordeiro, J., Gaita, F., Borggrefe, M., Menendez, T.M., Brugada, J., Pollevick, G.D., Wolpert, C., Burashnikov, E., Matsuo, K., Wu, Y.S., Guerchicoff, A., Bianchi, F., Giustetto, C., Schimpf, R., Brugada, P., Antzelevitch, C. (2004) Sudden death associated with short-QT syndrome linked to mutations in HERG. **Circulation** 109:30-35.

184. Bellocq, C., van Ginneken, A.C., Bezzina, C.R., Alders, M., Escande, D., Mannens, M.M., Baro, I., Wilde, A.A. (2004) Mutation in the KCNQ1 gene leading to the short QT-interval syndrome. **Circulation** 109:2394-2397.

185. Priori, S.G., Pandit, S.V., Rivolta, I., Berenfeld, O., Ronchetti, E., Dhamoon, A., Napolitano, C., Anumonwo, J., di Barletta, M.R., Gudapakkam, S., Bosi, G., Stramba-Badiale, M., Jalife, J. (2005) A novel form of short QT syndrome (SHORT QT3) is caused by a mutation in the KCNJ2 gene. **Circ Res** 96:800-807.

186. El, H.A., Zhang, H., Hancox, J.C. (2010) The S140G KCNQ1 atrial fibrillation mutation affects 'I(KS)' profile during both atrial and ventricular action potentials. **J. Physiol Pharmacol.** 61:759-764.

187. Hong, K., Piper, D.R., Diaz-Valdecantos, A., Brugada, J., Oliva, A., Burashnikov, E., Santos-de-Soto, J., Grueso-Montero, J., Diaz-Enfante, E., Brugada, P., Sachse, F., Sanguinetti, M.C., Brugada, R. (2005) De novo KCNQ1 mutation responsible for atrial fibrillation and short QT syndrome in utero. **Cardiovasc. Res.** 68:433-440.

188. Gollob, M.H., Redpath, C.J., Roberts, J.D. (2011) The short QT syndrome: proposed diagnostic criteria. **J. Am. Coll. Cardiol.** 57:802-812.

189. Leaf, A., Kang, J.X., Xiao, Y.F., Billman, G.E. (2003) Clinical prevention of sudden cardiac death by n-3 polyunsaturated fatty acids and mechanism of prevention of arrhythmias by n-3 fish oils. **Circulation** 107:2646-2652.

190. Leaf, A., Xiao, Y.F., Kang, J.X., Billman, G.E. (2003) Prevention of sudden cardiac death by n-3 polyunsaturated fatty acids. **Pharmacol. Ther.** 98:355-377.

191. Sinclair, H.M. (1953) The diet of Canadian Indian Eskimos. **Proc. Nutr. Soc.** 12:69-82.

192. Sinclair, H.M. (1956) Deficiency of essential fatty acids and atherosclerosis, etcetera. **Lancet** 270:381-383.

193. Billman, G.E., Kang, J.X., Leaf, A. (1997) Prevention of ischemia-induced cardiac sudden death by n-3 polyunsaturated fatty acids in dogs. **Lipids** 32:1161-1168.

194. Billman, G.E., Kang, J.X., Leaf, A. (1999) Prevention of sudden cardiac death by dietary pure omega-3 polyunsaturated fatty acids in dogs. **Circulation** 99:2452-2457.

195. Leifert, W.R., Jahangiri, A., Saint, D.A., McMurchie, E.J. (2000) Effects of dietary n-3 fatty acids on contractility, Na+ and K+ currents in a rat cardiomyocyte model of arrhythmia. **J. Nutr. Biochem.** 11:382-392.

196. Burr, M.L., Fehily, A.M., Gilbert, J.F., Rogers, S., Holliday, R.M., Sweetnam, P.M., Elwood, P.C., Deadman, N.M. (1989) Effects of changes in fat, fish, and fibre intakes on death and myocardial reinfarction: diet and reinfarction trial (DART). **Lancet** 2:757-761.

197. GISSI-Prevenzione Investigators (1999) Dietary supplementation with n-3 polyunsaturated fatty acids and vitamin E after myocardial infarction: results of the GISSI-Prevenzione trial. Gruppo Italiano per lo Studio della Sopravvivenza nell'Infarto miocardico. **Lancet** 354:447-455.

198. Tanaka, K., Ishikawa, Y., Yokoyama, M., Origasa, H., Matsuzaki, M., Saito, Y., Matsuzawa, Y., Sasaki, J., Oikawa, S., Hishida, H., Itakura, H., Kita, T., Kitabatake, A., Nakaya, N., Sakata, T., Shimada, K., Shirato, K. (2008) Reduction in the recurrence of stroke by eicosapentaenoic acid for hypercholesterolemic patients: subanalysis of the JELIS trial. **Stroke** 39:2052-2058.

199. Tavazzi, L., Maggioni, A.P., Marchioli, R., Barlera, S., Franzosi, M.G., Latini, R., Lucci, D., Nicolosi, G.L., Porcu, M., Tognoni, G. (2008) Effect of n-3 polyunsaturated fatty acids in patients with chronic heart failure (the GISSI-HF trial): a randomised, double-blind, placebo-controlled trial. **Lancet** 372:1223-1230.

200. Marchioli, R., Barzi, F., Bomba, E., Chieffo, C., Di, G.D., Di, M.R., Franzosi, M.G., Geraci, E., Levantesi, G., Maggioni, A.P., Mantini, L., Marfisi, R.M., Mastrogiuseppe, G., Mininni, N., Nicolosi, G.L., Santini, M., Schweiger, C., Tavazzi, L., Tognoni, G., Tucci, C., Valagussa, F. (2002) Early protection against sudden death by n-3 polyunsaturated fatty acids after myocardial infarction: time-course analysis of the results of the Gruppo Italiano per lo Studio della Sopravvivenza nell'Infarto Miocardico (GISSI)-Prevenzione. **Circulation** 105:1897-1903.

201. Coronel, R., Wilms-Schopman, F.J., Den Ruijter, H.M., Belterman, C.N., Schumacher, C.A., Opthof, T., Hovenier, R., Lemmens, A.G., Terpstra, A.H., Katan, M.B., Zock, P. (2007) Dietary n-3 fatty acids promote arrhythmias during acute regional myocardial ischemia in isolated pig hearts. **Cardiovasc. Res** 73:386-394.

202. Kromhout, D., Giltay, E.J., Geleijnse, J.M. (2010) n-3 fatty acids and cardiovascular events after myocardial infarction. **N. Engl. J. Med.** 363:2015-2026.

203. Rauch, B., Schiele, R., Schneider, S., Diller, F., Victor, N., Gohlke, H., Gottwik, M., Steinbeck, G., Del, C.U., Sack, R., Worth, H., Katus, H., Spitzer, W., Sabin, G., Senges, J. (2010) OMEGA, a randomized, placebo-controlled trial to test the effect of highly purified omega-3 fatty acids on top of modern guideline-adjusted therapy after myocardial infarction. **Circulation** 122:2152-2159.

204. Burr, M.L., Ashfield-Watt, P.A., Dunstan, F.D., Fehily, A.M., Breay, P., Ashton, T., Zotos, P.C., Haboubi, N.A., Elwood, P.C. (2003) Lack of benefit of dietary advice to men with angina: results of a controlled trial. **Eur. J Clin. Nutr.** 57:193-200.

205. Raitt, M.H., Connor, W.E., Morris, C., Kron, J., Halperin, B., Chugh, S.S., McClelland, J., Cook, J., MacMurdy, K., Swenson, R., Connor, S.L., Gerhard, G., Kraemer, D.F., Oseran, D., Marchant, C., Calhoun, D., Shnider, R., McAnulty, J. (2005) Fish oil supplementation and risk of ventricular tachycardia and ventricular fibrillation in patients with implantable defibrillators: a randomized controlled trial. **JAMA** 293:2884-2891.

206. Honoré, E., Barhanin, J., Attali, B., Lesage, F., Lazdunski, M. (1994) External blockade of the major cardiac delayed-rectifier K^+ channel (Kv1.5) by polyunsaturated fatty acids. **Proc. Natl. Acad. Sci. U. S. A** 91:1937-1941.

207. Xiao, Y.F., Kang, J.X., Morgan, J.P., Leaf, A. (1995) Blocking effects of polyunsaturated fatty acids on Na^+ channels of neonatal rat ventricular myocytes. **Proc. Natl. Acad. Sci. U. S. A** 92:11000-11004.

208. Xiao, Y.F., Gomez, A.M., Morgan, J.P., Lederer, W.J., Leaf, A. (1997) Suppression of voltage-gated L-type Ca2+ currents by polyunsaturated fatty acids in adult and neonatal rat ventricular myocytes. **Proc. Natl. Acad. Sci. U. S. A** 94:4182-4187.

209. Doolan, G.K., Panchal, R.G., Fonnes, E.L., Clarke, A.L., Williams, D.A., Petrou, S. (2002) Fatty acid augmentation of the cardiac slowly activating delayed rectifier current (IKs) is conferred by hminK. **FASEB J.** 16:1662-1664.

210. Jude, S., Bedut, S., Roger, S., Pinault, M., Champeroux, P., White, E., Le Guennec, J.Y. (2003) Peroxidation of docosahexaenoic acid is responsible for its effects on I TO and I SS in rat ventricular myocytes. **Br. J. Pharmacol.** 139:816-822.

211. Guizy, M., Arias, C., David, M., Gonzalez, T., Valenzuela, C. (2005) ω-3 and ω-6 polyunsaturated fatty acids block *HERG* channels. **Am J Physiol Cell Physiol** 289:C1251-C1260.

212. Guizy, M., David, M., Arias, C., Zhang, L., Cofan, M., Ruiz-Gutierrez, V., Ros, E., Lillo, M.P., Martens, J.R., Valenzuela, C. (2008) Modulation of the atrial specific Kv1.5 channel by the n-3 polyunsaturated fatty acid, alpha-linolenic acid. **J. Mol. Cell Cardiol.** 44:323-335.

213. Verkerk, A.O., van Ginneken, A.C., Berecki, G., Den Ruijter, H.M., Schumacher, C.A., Veldkamp, M.W., Baartscheer, A., Casini, S., Opthof, T., Hovenier, R., Fiolet, J.W., Zock, P.L., Coronel, R. (2006) Incorporated sarcolemmal fish oil fatty acids shorten pig ventricular action potentials. **Cardiovasc. Res** 70:509-520.

214. Dujardin, K.S., Dumotier, B., David, M., Guizy, M., Valenzuela, C., Hondeghem, L.M. (2008) Ultrafast sodium channel block by dietary fish oil prevents dofetilide-induced ventricular arrhythmias in rabbit hearts. **Am. J. Physiol Heart Circ. Physiol** 295:H1414-H1421.

215. Das, U.N. (2006) Hypertension as a low-grade systemic inflammatory condition that has its origins in the perinatal period. **J. Assoc. Physicians India** 54:133-142.

216. Luc, G., Bard, J.M., Juhan-Vague, I., Ferrieres, J., Evans, A., Amouyel, P., Arveiler, D., Fruchart, J.C., Ducimetiere, P. (2003) C-reactive protein, interleukin-6, and fibrinogen as predictors of coronary heart disease: the PRIME Study. **Arterioscler. Thromb. Vasc. Biol.** 23:1255-1261.

217. Das, U.N. (2001) Is obesity an inflammatory condition? **Nutrition** 17:953-966.

218. Das, U.N. (2007) Is depression a low-grade systemic inflammatory condition? **Am. J. Clin. Nutr.** 85:1665-1666.

219. Dougan, M. Dranoff, G. (2008) Inciting inflammation: the RAGE about tumor promotion. **J. Exp. Med.** 205:267-270.

220. Lawrence, T., Hageman, T., Balkwill, F. (2007) Cancer. Sex, cytokines, and cancer. **Science** 317:51-52.

221. Rao, A.A., Sridhar, G.R., Das, U.N. (2007) Elevated butyrylcholinesterase and acetylcholinesterase may predict the development of type 2 diabetes mellitus and Alzheimer's disease. **Med. Hypotheses** 69:1272-1276.

222. Das, U.N. (2011) Influence of polyunsaturated fatty acids and their metabolites on stem cell biology. **Nutrition** 27:21-25.

223. Weber, C. Noels, H. (2011) Atherosclerosis: current pathogenesis and therapeutic options. **Nat. Med.** 17:1410-1422.

224. Pena, J.M., MacFadyen, J., Glynn, R.J., Ridker, P.M. (2012) High-sensitivity C-reactive protein, statin therapy, and risks of atrial fibrillation: an exploratory analysis of the JUPITER trial. **Eur. Heart J.** 33:531-537.

225. Sobirin, M.A., Kinugawa, S., Takahashi, M., Fukushima, A., Homma, T., Ono, T., Hirabayashi, K., Suga, T., Azalia, P., Takada, S., Taniguchi, M., Nakayama, T., Ishimori, N., Iwabuchi, K., Tsutsui, H. (2012) Activation of natural killer T cells ameliorates postinfarct cardiac remodeling and failure in mice. **Circ. Res.** 111:1037-1047.

226. Bench, T.J., Jeremias, A., Brown, D.L. (2011) Matrix metalloproteinase inhibition with tetracyclines for the treatment of coronary artery disease. **Pharmacol. Res.** 64:561-566.

227. Serhan, C.N., Clish, C.B., Brannon, J., Colgan, S.P., Chiang, N., Gronert, K. (2000) Novel functional sets of lipid-derived mediators with antiinflammatory actions generated from omega-3 fatty acids via cyclooxygenase 2-nonsteroidal antiinflammatory drugs and transcellular processing. **J. Exp. Med.** 192:1197-1204.

228. Serhan, C.N., Hong, S., Gronert, K., Colgan, S.P., Devchand, P.R., Mirick, G., Moussignac, R.L. (2002) Resolvins: a family of bioactive products of omega-3 fatty acid transformation circuits initiated by aspirin treatment that counter proinflammation signals. **J. Exp. Med.** 196:1025-1037.

229. Serhan, C.N. (2002) Lipoxins and aspirin-triggered 15-epi-lipoxin biosynthesis: an update and role in anti-inflammation and pro-resolution. **Prostaglandins Other Lipid Mediat.** 68-69:433-455.

230. Samuelsson, B., Dahlen, S.E., Lindgren, J.A., Rouzer, C.A., Serhan, C.N. (1987) Leukotrienes and lipoxins: structures, biosynthesis, and biological effects. **Science** 237:1171-1176.

231. Serhan, C.N. Savill, J. (2005) Resolution of inflammation: the beginning programs the end. **Nat. Immunol.** 6:1191-1197.

232. Gordon, S. Martinez, F.O. (2010) Alternative activation of macrophages: mechanism and functions. **Immunity.** 32:593-604.

233. Pasare, C. Medzhitov, R. (2005) Control of B-cell responses by Toll-like receptors. **Nature** 438:364-368.

234. Eder, C. (1998) Ion channels in microglia (brain macrophages). **Am. J. Physiol.** 275:C327-C342.

235. Cahalan, M.D. Chandy, K.G. (1997) Ion channels in the immune system as targets for immunosuppression. **Curr. Opin. Biotechnol.** 8:749-756.

236. Panyi, G., Vamosi, G., Bodnar, A., Gaspar, R., Damjanovich, S. (2004) Looking through ion channels: recharged concepts in T-cell signaling. **Trends Immunol.** 25:565-569.

237. Gordon, S. (2007) The macrophage: past, present and future. **Eur. J. Immunol.** 37 Suppl 1:S9-17.

238. Mantovani, A., Garlanda, C., Locati, M. (2009) Macrophage diversity and polarization in atherosclerosis: a question of balance. **Arterioscler. Thromb. Vasc. Biol.** 29:1419-1423.

239. Bottazzi, B., Doni, A., Garlanda, C., Mantovani, A. (2010) An integrated view of humoral innate immunity: pentraxins as a paradigm. **Annu. Rev. Immunol.** 28:157-183.

240. Rodriguez-Prados, J.C., Traves, P.G., Cuenca, J., Rico, D., Aragones, J., Martin-Sanz, P., Cascante, M., Bosca, L. (2010) Substrate fate in activated macrophages: a comparison between innate, classic, and alternative activation. **J. Immunol.** 185:605-614.

241. Coma, M., Vicente, R., Busquets, S., Carbo, N., Tamkun, M.M., Lopez-Soriano, F.J., Argiles, J.M., Felipe, A. (2003) Impaired voltage-gated K+ channel expression in brain during experimental cancer cachexia. **FEBS Lett.** 536:45-50.

242. Zhang, S.L., Yu, Y., Roos, J., Kozak, J.A., Deerinck, T.J., Ellisman, M.H., Stauderman, K.A., Cahalan, M.D. (2005) STIM1 is a Ca2+ sensor that activates CRAC channels and migrates from the Ca2+ store to the plasma membrane. **Nature** 437:902-905.

243. Liou, J., Kim, M.L., Heo, W.D., Jones, J.T., Myers, J.W., Ferrell, J.E., Jr., Meyer, T. (2005) STIM is a Ca2+ sensor essential for Ca2+-store-depletion-triggered Ca2+ influx. **Curr. Biol.** 15:1235-1241.

244. Feske, S., Gwack, Y., Prakriya, M., Srikanth, S., Puppel, S.H., Tanasa, B., Hogan, P.G., Lewis, R.S., Daly, M., Rao, A. (2006) A mutation in Orai1 causes immune deficiency by abrogating CRAC channel function. **Nature** 441:179-185.

245. Vig, M., Peinelt, C., Beck, A., Koomoa, D.L., Rabah, D., Koblan-Huberson, M., Kraft, S., Turner, H., Fleig, A., Penner, R., Kinet, J.P. (2006) CRACM1 is a plasma membrane protein essential for store-operated Ca2+ entry. **Science** 312:1220-1223.

246. Penna, A., Demuro, A., Yeromin, A.V., Zhang, S.L., Safrina, O., Parker, I., Cahalan, M.D. (2008) The CRAC channel consists of a tetramer formed by Stim-induced dimerization of Orai dimers. **Nature** 456:116-120.

247. Grissmer, S., Nguyen, A.N., Cahalan, M.D. (1993) Calcium-activated potassium channels in resting and activated human T lymphocytes. Expression levels, calcium dependence, ion selectivity, and pharmacology. **J. Gen. Physiol.** 102:601-630.

248. Fanger, C.M., Ghanshani, S., Logsdon, N.J., Rauer, H., Kalman, K., Zhou, J., Beckingham, K., Chandy, K.G., Cahalan, M.D., Aiyar, J. (1999) Calmodulin mediates calcium-dependent activation of the intermediate conductance KCa channel, IKCa1. **J Biol. Chem** 274:5746-5754.

249. Chen, M., Divangahi, M., Gan, H., Shin, D.S., Hong, S., Lee, D.M., Serhan, C.N., Behar, S.M., Remold, H.G. (2008) Lipid mediators in innate immunity against tuberculosis: opposing roles of PGE2 and LXA4 in the induction of macrophage death. **J. Exp. Med.** 205:2791-2801.

250. Ji, R.R., Xu, Z.Z., Strichartz, G., Serhan, C.N. (2011) Emerging roles of resolvins in the resolution of inflammation and pain. **Trends Neurosci.** 34:599-609.

251. Serhan, C.N., Dalli, J., Karamnov, S., Choi, A., Park, C.K., Xu, Z.Z., Ji, R.R., Zhu, M., Petasis, N.A. (2012) Macrophage proresolving mediator maresin 1 stimulates tissue regeneration and controls pain. **FASEB J.** 26:1755-1765.

252. Bannenberg, G. Serhan, C.N. (2010) Specialized pro-resolving lipid mediators in the inflammatory response: An update. **Biochim. Biophys. Acta** 1801:1260-1273.

253. Serhan, C.N., Yacoubian, S., Yang, R. (2008) Anti-inflammatory and proresolving lipid mediators. **Annu. Rev. Pathol.** 3:279-312.

254. Prieto, P., Cuenca, J., Traves, P.G., Fernandez-Velasco, M., Martin-Sanz, P., Bosca, L. (2010) Lipoxin A4 impairment of apoptotic signaling in macrophages: implication of the PI3K/Akt and the ERK/Nrf-2 defense pathways. **Cell Death. Differ.** 17:1179-1188.

255. Chiang, N., Arita, M., Serhan, C.N. (2005) Anti-inflammatory circuitry: lipoxin, aspirin-triggered lipoxins and their receptor ALX. **Prostaglandins Leukot. Essent. Fatty Acids** 73:163-177.

256. Devchand, P.R., Arita, M., Hong, S., Bannenberg, G., Moussignac, R.L., Gronert, K., Serhan, C.N. (2003) Human ALX receptor regulates neutrophil recruitment in transgenic mice: roles in inflammation and host defense. **FASEB J.** 17:652-659.

257. Tamargo, J., Caballero, R., Gomez, R., Valenzuela, C., Delpon, E. (2004) Pharmacology of cardiac potassium channels. **Cardiovasc. Res.** 62:9-33.

258. Kang, D., La, J.H., Kim, E.J., Park, J.Y., Hong, S.G., Han, J. (2006) An endogenous acid-sensitive K+ channel expressed in COS-7 cells. **Biochem. Biophys. Res. Commun.** 341:1231-1236.

259. Po, S., Snyders, D.J., Baker, R., Tamkun, M.M., Bennett, P.B. (1992) Functional expression of an inactivating potassium channel cloned from human heart. **Circ. Res.** 71:732-736.

260. Maderna, P., Cottell, D.C., Toivonen, T., Dufton, N., Dalli, J., Perretti, M., Godson, C. (2010) FPR2/ALX receptor expression and internalization are critical for lipoxin A4 and annexin-derived peptide-stimulated phagocytosis. **FASEB J.** 24:4240-4249.

261. Maderna, P. Godson, C. (2005) Taking insult from injury: lipoxins and lipoxin receptor agonists and phagocytosis of apoptotic cells. **Prostaglandins Leukot. Essent. Fatty Acids** 73:179-187.

262. Souza, D.G., Fagundes, C.T., Amaral, F.A., Cisalpino, D., Sousa, L.P., Vieira, A.T., Pinho, V., Nicoli, J.R., Vieira, L.Q., Fierro, I.M., Teixeira, M.M. (2007) The required role of endogenously produced lipoxin A4 and annexin-1 for the production of IL-10 and inflammatory hyporesponsiveness in mice. **J. Immunol.** 179:8533-8543.

263. Sodin-Semrl, S., Spagnolo, A., Barbaro, B., Varga, J., Fiore, S. (2004) Lipoxin A4 counteracts synergistic activation of human fibroblast-like synoviocytes. **Int. J. Immunopathol. Pharmacol.** 17:15-25.

264. Brouwer, I.A., Zock, P.L., Camm, A.J., Bocker, D., Hauer, R.N., Wever, E.F., Dullemeijer, C., Ronden, J.E., Katan, M.B., Lubinski, A., Buschler, H., Schouten, E.G. (2006) Effect of fish oil on ventricular tachyarrhythmia and death in patients with implantable cardioverter defibrillators: the Study on Omega-3 Fatty Acids and Ventricular Arrhythmia (SOFA) randomized trial. **JAMA** 295:2613-2619.

265. Puttmann, M., Krug, H., von, O.E., Kattermann, R. (1993) Fast HPLC determination of serum free fatty acids in the picomole range. **Clin. Chem.** 39:825-832.

266. Albert, C.M., Campos, H., Stampfer, M.J., Ridker, P.M., Manson, J.E., Willett, W.C., Ma, J. (2002) Blood levels of long-chain n-3 fatty acids and the risk of sudden death. **N. Engl. J. Med.** 346:1113-1118.

267. Kitajka, K., Sinclair, A.J., Weisinger, R.S., Weisinger, H.S., Mathai, M., Jayasooriya, A.P., Halver, J.E., Puskas, L.G. (2004) Effects of dietary omega-3 polyunsaturated fatty acids on brain gene expression. **Proc. Natl. Acad. Sci. U. S. A** 101:10931-10936.

268. Jespersen, T., Membrez, M., Nicolas, C.S., Pitard, B., Staub, O., Olesen, S.P., Baro, I., Abriel, H. (2007) The KCNQ1 potassium channel is down-regulated by ubiquitylating enzymes of the Nedd4/Nedd4-like family. **Cardiovasc. Res** 74:64-74.

269. Roura-Ferrer, M., Sole, L., Oliveras, A., Dahan, R., Bielanska, J., Villarroel, A., Comes, N., Felipe, A. (2010) Impact of KCNE subunits on KCNQ1 (Kv7.1) channel membrane surface targeting. **J. Cell Physiol** 225:692-700.

270. Morenilla-Palao, C., Pertusa, M., Meseguer, V., Cabedo, H., Viana, F. (2009) Lipid raft segregation modulates TRPM8 channel activity. **J. Biol. Chem.** 284:9215-9224.

271. Abitbol, I., Peretz, A., Lerche, C., Busch, A.E., Attali, B. (1999) Stilbenes and fenamates rescue the loss of I(KS) channel function induced by an LQT5 mutation and other IsK mutants. **EMBO J** 18:4137-4148.

272. Smith, P.L., Baukrowitz, T., Yellen, G. (1996) The inward rectification mechanism of the HERG cardiac potassium channel. **Nature** 379:833-836.

273. Spector, P.S., Curran, M.E., Zou, A., Keating, M.T., Sanguinetti, M.C. (1996) Fast inactivation causes rectification of the I_{Kr} channel. **J. Gen. Physiol.** 107:611-619.

274. Schonherr, R. Heinemann, S.H. (1996) Molecular determinants for activation and inactivation of HERG, a human inward rectifier potassium channel. **J. Physiol. (Lond)** 493:635-642.

275. Silva, J. Rudy, Y. (2005) Subunit interaction determines IKs participation in cardiac repolarization and repolarization reserve. **Circulation** 112:1384-1391.

276. Rocchetti, M., Besana, A., Gurrola, G.B., Possani, L.D., Zaza, A. (2001) Rate dependency of delayed rectifier currents during the guinea-pig ventricular action potential. **J. Physiol** 534:721-732.

277. Jurkiewicz, N.K. Sanguinetti, M.C. (1993) Rate-dependent prolongation of cardiac action potentials by a methanesulfonanilide class III antiarrhythmic agent. Specific block of rapidly activating delayed rectifier K^+ current by dofetilide. **Circ. Res.** 72:75-83.

278. Viswanathan, P.C., Shaw, R.M., Rudy, Y. (1999) Effects of I_{Kr} and I_{Ks} heterogeneity on action potential duration and its rate dependence : a simulation study. **Circulation** 99:2466-2474.

279. Hund, T.J. Rudy, Y. (2004) Rate dependence and regulation of action potential and calcium transient in a canine cardiac ventricular cell model. **Circulation** 110:3168-3174.

280. Boyett, M.R. Jewell, B.R. (1978) A study of the factors responsible for rate-dependent shortening of the action potential in mammalian ventricular muscle. **J. Physiol** 285:359-380.

281. Carmeliet, E. (1977) Repolarisation and frequency in cardiac cells. **J. Physiol (Paris)** 73:903-923.

282. Chen, J., Zheng, R., Melman, Y.F., McDonald, T.V. (2009) Functional interactions between KCNE1 C-terminus and the KCNQ1 channel. **PLoS. One.** 4:e5143.

283. Beeton, C., Pennington, M.W., Wulff, H., Singh, S., Nugent, D., Crossley, G., Khaytin, I., Calabresi, P.A., Chen, C.Y., Gutman, G.A., Chandy, K.G. (2005) Targeting effector memory T cells with a selective peptide inhibitor of Kv1.3 channels for therapy of autoimmune diseases. **Mol. Pharmacol.** 67:1369-1381.

284. Beeton, C., Wulff, H., Barbaria, J., Clot-Faybesse, O., Pennington, M., Bernard, D., Cahalan, M.D., Chandy, K.G., Beraud, E. (2001) Selective blockade of T lymphocyte K(+) channels ameliorates experimental autoimmune encephalomyelitis, a model for multiple sclerosis. **Proc. Natl. Acad. Sci. U. S. A** 98:13942-13947.

285. Beeton, C., Barbaria, J., Giraud, P., Devaux, J., Benoliel, A.M., Gola, M., Sabatier, J.M., Bernard, D., Crest, M., Beraud, E. (2001) Selective blocking of voltage-gated K+ channels improves experimental autoimmune encephalomyelitis and inhibits T cell activation. **J. Immunol.** 166:936-944.

286. Rus, H., Pardo, C.A., Hu, L., Darrah, E., Cudrici, C., Niculescu, T., Niculescu, F., Mullen, K.M., Allie, R., Guo, L., Wulff, H., Beeton, C., Judge, S.I., Kerr, D.A., Knaus, H.G., Chandy, K.G., Calabresi, P.A. (2005) The voltage-gated potassium channel Kv1.3 is highly expressed on inflammatory infiltrates in multiple sclerosis brain. **Proc. Natl. Acad. Sci. U. S. A** 102:11094-11099.

287. DeCoursey, T.E., Kim, S.Y., Silver, M.R., Quandt, F.N. (1996) Ion channel expression in PMA-differentiated human THP-1 macrophages. **J. Membr. Biol.** 152:141-157.

288. Gallin, E.K. (1984) Calcium- and voltage-activated potassium channels in human macrophages. **Biophys. J.** 46:821-825.

289. Kotecha, S.A. Schlichter, L.C. (1999) A Kv1.5 to Kv1.3 switch in endogenous hippocampal microglia and a role in proliferation. **J. Neurosci.** 19:10680-10693.

290. Schilling, T., Quandt, F.N., Cherny, V.V., Zhou, W., Heinemann, U., DeCoursey, T.E., Eder, C. (2000) Upregulation of Kv1.3 K(+) channels in microglia deactivated by TGF-beta. **Am. J. Physiol Cell Physiol** 279:C1123-C1134.

291. Ypey, D.L. Clapham, D.E. (1984) Development of a delayed outward-rectifying K+ conductance in cultured mouse peritoneal macrophages. **Proc. Natl. Acad. Sci. U. S. A** 81:3083-3087.

292. Mackenzie, A.B., Chirakkal, H., North, R.A. (2003) Kv1.3 potassium channels in human alveolar macrophages. **Am. J. Physiol Lung Cell Mol. Physiol** 285:L862-L868.

293. Blunck, R., Scheel, O., Muller, M., Brandenburg, K., Seitzer, U., Seydel, U. (2001) New insights into endotoxin-induced activation of macrophages: involvement of a K+ channel in transmembrane signaling. **J. Immunol.** 166:1009-1015.

294. Ahluwalia, J., Tinker, A., Clapp, L.H., Duchen, M.R., Abramov, A.Y., Pope, S., Nobles, M., Segal, A.W. (2004) The large-conductance Ca2+-activated K+ channel is essential for innate immunity. **Nature** 427:853-858.

295. Khanna, R., Roy, L., Zhu, X., Schlichter, L.C. (2001) K+ channels and the microglial respiratory burst. **Am. J. Physiol Cell Physiol** 280:C796-C806.

296. Berridge, M.J., Lipp, P., Bootman, M.D. (2000) The versatility and universality of calcium signalling. **Nat. Rev. Mol. Cell Biol.** 1:11-21.

297. Prakriya, M., Feske, S., Gwack, Y., Srikanth, S., Rao, A., Hogan, P.G. (2006) Orai1 is an essential pore subunit of the CRAC channel. **Nature** 443:230-233.

298. Yeromin, A.V., Zhang, S.L., Jiang, W., Yu, Y., Safrina, O., Cahalan, M.D. (2006) Molecular identification of the CRAC channel by altered ion selectivity in a mutant of Orai. **Nature** 443:226-229.

299. Lin, C.S., Boltz, R.C., Blake, J.T., Nguyen, M., Talento, A., Fischer, P.A., Springer, M.S., Sigal, N.H., Slaughter, R.S., Garcia, M.L. (1993) Voltage-gated potassium channels regulate calcium-dependent pathways involved in human T lymphocyte activation. **J. Exp. Med.** 177:637-645.

300. Lampert, A., Muller, M.M., Berchtold, S., Lang, K.S., Palmada, M., Dobrovinskaya, O., Lang, F. (2003) Effect of dexamethasone on voltage-gated K+ channels in Jurkat T-lymphocytes. **Pflugers Arch.** 447:168-174.

301. Leifert, W.R., Dorian, C.L., Jahangiri, A., McMurchie, E.J. (2001) Dietary fish oil prevents asynchronous contractility and alters Ca(2+) handling in adult rat cardiomyocytes. **J. Nutr. Biochem.** 12:365-376.

302. Den Ruijter, H.M., Berecki, G., Opthof, T., Verkerk, A.O., Zock, P.L., Coronel, R. (2007) Pro- and antiarrhythmic properties of a diet rich in fish oil. **Cardiovasc. Res** 73:316-325.

303. Xiao, Y.F., Wright, S.N., Wang, G.K., Morgan, J.P., Leaf, A. (1998) Fatty acids suppress voltage-gated Na+ currents in HEK293t cells transfected with the alpha-subunit of the human cardiac Na+ channel. **Proc. Natl. Acad. Sci. U. S. A** 95:2680-2685.

304. Xiao, Y.F., Ke, Q., Wang, S.Y., Auktor, K., Yang, Y., Wang, G.K., Morgan, J.P., Leaf, A. (2001) Single point mutations affect fatty acid block of human myocardial sodium channel alpha subunit Na+ channels. **Proc. Natl. Acad. Sci. U. S. A** 98:3606-3611.

305. Li, G.R., Sun, H.Y., Zhang, X.H., Cheng, L.C., Chiu, S.W., Tse, H.F., Lau, C.P. (2009) Omega-3 polyunsaturated fatty acids inhibit transient outward and ultra-rapid delayed rectifier K+currents and Na+current in human atrial myocytes. **Cardiovasc. Res.** 81:286-293.

306. Bogdanov, K.Y., Spurgeon, H.A., Vinogradova, T.M., Lakatta, E.G. (1998) Modulation of the transient outward current in adult rat ventricular myocytes by polyunsaturated fatty acids. **Am J Physiol** 274:H571-H579.

307. Macleod, J.C., Macknight, A.D., Rodrigo, G.C. (1998) The electrical and mechanical response of adult guinea pig and rat ventricular myocytes to ω3 polyunsaturated fatty acids. **Eur. J Pharmacol.** 356:261-270.

308. Leifert, W.R., McMurchie, E.J., Saint, D.A. (1999) Inhibition of cardiac sodium currents in adult rat myocytes by n-3 polyunsaturated fatty acids. **J. Physiol** 520 Pt 3:671-679.

309. Jude, S., Roger, S., Martel, E., Besson, P., Richard, S., Bougnoux, P., Champeroux, P., Le Guennec, J.Y. (2006) Dietary long-chain omega-3 fatty acids of marine origin: a comparison of their protective effects on coronary heart disease and breast cancers. **Prog. Biophys. Mol. Biol.** 90:299-325.

310. Martens, J.R., O'Connell, K., Tamkun, M.M. (2004) Targeting of ion channels to membrane microdomains: localization of KV channels to lipid rafts. **Trends Pharmacol. Sci.** 25:16-21.

311. Pani, B. Singh, B.B. (2009) Lipid rafts/caveolae as microdomains of calcium signaling. **Cell Calcium** 45:625-633.

312. Jardin, I., Salido, G.M., Rosado, J.A. (2008) Role of lipid rafts in the interaction between hTRPC1, Orai1 and STIM1. **Channels (Austin.)** 2:401-403.

313. Romanenko, V.G., Fang, Y., Byfield, F., Travis, A.J., Vandenberg, C.A., Rothblat, G.H., Levitan, I. (2004) Cholesterol sensitivity and lipid raft targeting of Kir2.1 channels. **Biophys. J.** 87:3850-3861.

314. Abi-Char, J., Maguy, A., Coulombe, A., Balse, E., Ratajczak, P., Samuel, J.L., Nattel, S., Hatem, S.N. (2007) Membrane cholesterol modulates Kv1.5 potassium channel distribution and function in rat cardiomyocytes. **J. Physiol** 582:1205-1217.

315. Chun, Y.S., Shin, S., Kim, Y., Cho, H., Park, M.K., Kim, T.W., Voronov, S.V., Di, P.G., Suh, B.C., Chung, S. (2010) Cholesterol modulates ion channels via down-regulation of phosphatidylinositol 4,5-bisphosphate. **J. Neurochem.** 112:1286-1294.

316. Barbuti, A., Gravante, B., Riolfo, M., Milanesi, R., Terragni, B., DiFrancesco, D. (2004) Localization of pacemaker channels in lipid rafts regulates channel kinetics. **Circ. Res.** 94:1325-1331.

317. Epshtein, Y., Chopra, A.P., Rosenhouse-Dantsker, A., Kowalsky, G.B., Logothetis, D.E., Levitan, I. (2009) Identification of a C-terminus domain critical for the sensitivity of Kir2.1 to cholesterol. **Proc. Natl. Acad. Sci. U. S. A** 106:8055-8060.

318. Smithers, N., Bolivar, J.H., Lee, A.G., East, J.M. (2012) Characterizing the Fatty Acid Binding Site in the Cavity of Potassium Channel KcsA. **Biochem.** 51:7996-8002.

319. Gibor, G., Yakubovich, D., Rosenhouse-Dantsker, A., Peretz, A., Schottelndreier, H., Seebohm, G., Dascal, N., Logothetis, D.E., Paas, Y., Attali, B. (2007) An inactivation gate in the selectivity filter of KCNQ1 potassium channels. **Biophys. J.** 93:4159-4172.

320. Chung, D.Y., Chan, P.J., Bankston, J.R., Yang, L., Liu, G., Marx, S.O., Karlin, A., Kass, R.S. (2009) Location of KCNE1 relative to KCNQ1 in the I(KS) potassium channel by disulfide cross-linking of substituted cysteines. **Proc. Natl. Acad. Sci. U. S. A** 106:743-748.

321. Xu, X., Jiang, M., Hsu, K.L., Zhang, M., Tseng, G.N. (2008) KCNQ1 and KCNE1 in the IKs channel complex make state-dependent contacts in their extracellular domains. **J. Gen. Physiol** 131:589-603.

322. Tai, K.K. Goldstein, S.A. (1998) The conduction pore of a cardiac potassium channel. **Nature** 391:605-608.

323. Tapper, A.R. George, A.L., Jr. (2001) Location and orientation of minK within the I(Ks) potassium channel complex. **J. Biol. Chem.** 276:38249-38254.

324. Melman, Y.F., Krumerman, A., McDonald, T.V. (2002) A single transmembrane site in the KCNE-encoded proteins controls the specificity of KvLQT1 channel gating. **J. Biol. Chem.** 277:25187-25194.

325. Panaghie, G., Tai, K.K., Abbott, G.W. (2006) Interaction of KCNE subunits with the KCNQ1 K+ channel pore. **J. Physiol** 570:455-467.

326. Kang, C., Tian, C., Sonnichsen, F.D., Smith, J.A., Meiler, J., George, A.L., Jr., Vanoye, C.G., Kim, H.J., Sanders, C.R. (2008) Structure of KCNE1 and implications for how it modulates the KCNQ1 potassium channel. **Biochem.** 47:7999-8006.

327. Schimpf, R., Veltmann, C., Wolpert, C., Borggrefe, M. (2009) Channelopathies: Brugada syndrome, long QT syndrome, short QT syndrome, and CPVT. **Herz** 34:281-288.

8 APPENDIX 1: SUPPLEMENTAL MATERIAL

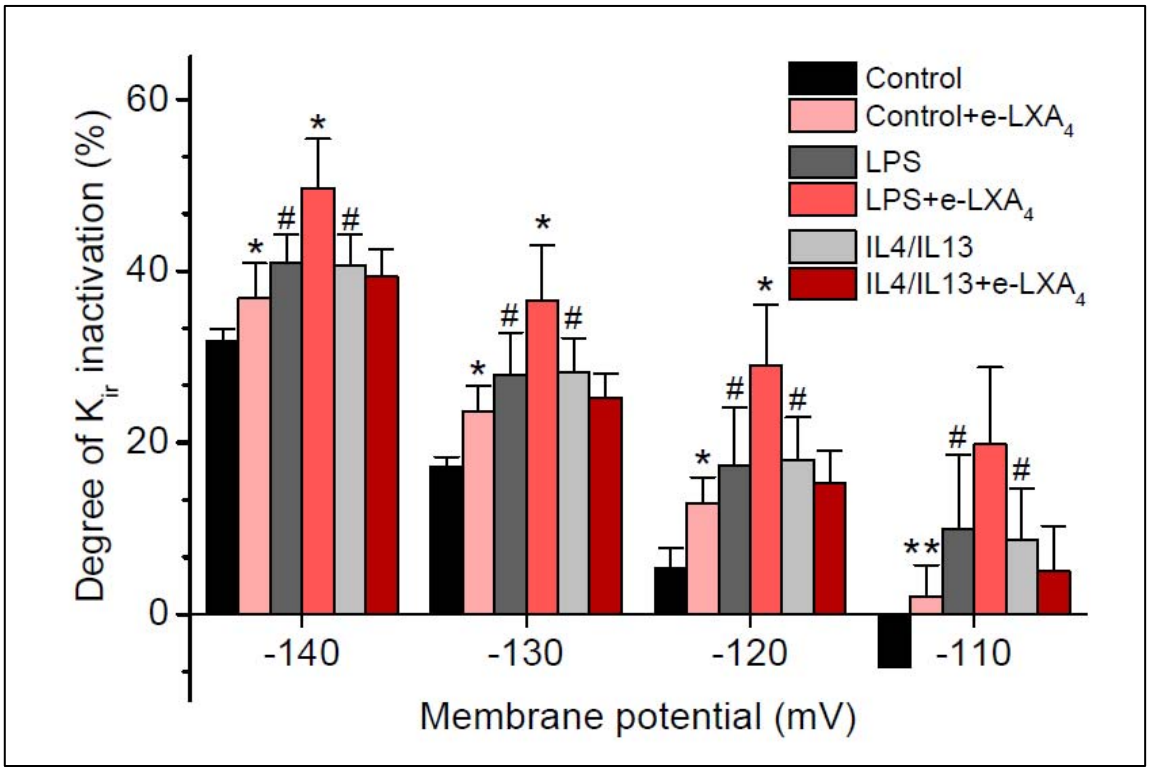

Figure S1. Acute effects of e-LXA$_4$ on K$_{ir}$ currents and degree of K$_{ir}$ inactivation. Representative traces of K$_{ir}$ currents recorded in control, LPS and IL4/IL13 activated BMDM. BMDM were not stimulated (A) treated with LPS (100 ng/ml) (B) or IL4/IL13 (20 ng/ml) for 18h (C). Current recordings were obtained in the absence and after perfusion with e-LXA$_4$ (500 nM) (A-C). Currents were elicited by applying hyper- and depolarizing pulses from a holding potential of -80 mV to different voltages from -140 to -40 mV in 10 mV steps (500ms duration). IV relationships in the absence and in the presence of e-LXA$_4$ (500 nM) in resting BMDM (D), or LPS (E) and IL4/IL13 (F) activated BMDM are shown. The degree of K$_{ir}$ inactivation was determined under these conditions (G). Data are expressed as the mean ± SEM. *P<0.05 *vs.* control; n>10 cells per group (Student's *t* test).

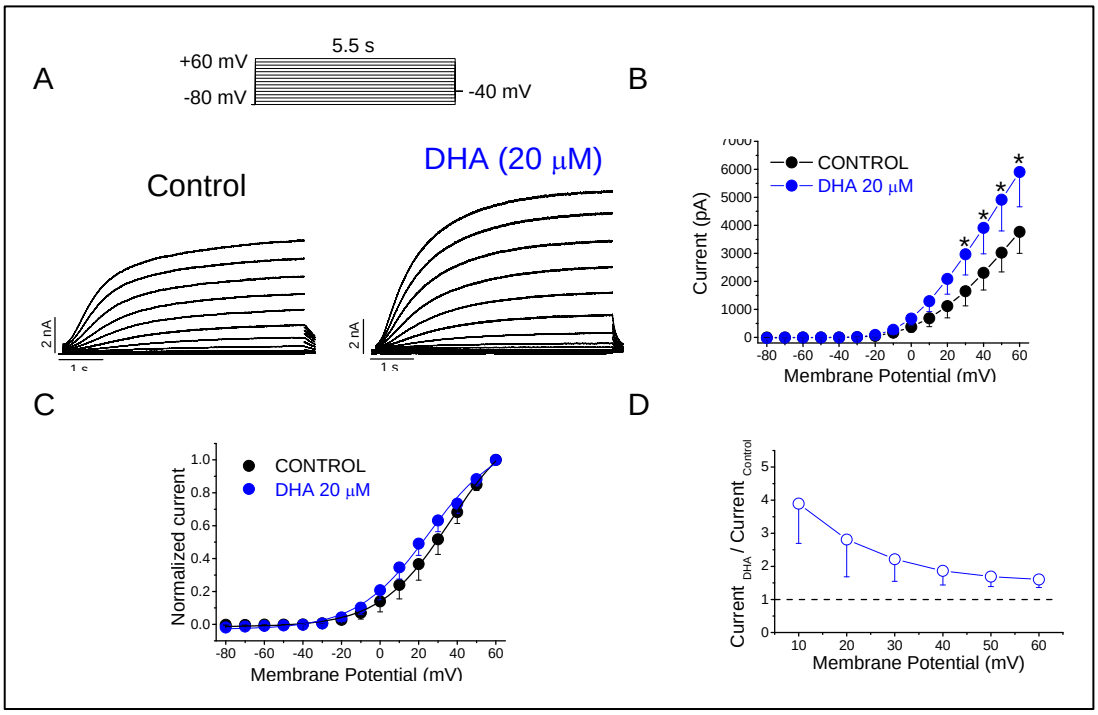

Figure S2. Voltage-dependent effects of acute DHA on K_V7.1/KCNE1 channels. **(A)** Currents were elicited in 10-mV increments to test potentials ranging from -80 to +60 mV from a holding potential of −80 mV in the absence and in the presence of DHA. **(B)** IV relationship obtained under control conditions and after perfusion with DHA. **(C)** Activation curves obtained under control conditions and after perfusion with DHA. Peak tail currents were measured, and the normalized data were fit to a Boltzmann function. The midpoint for the activation curve was V_{mid}=29.9±6.4 and 26.4±6.9 and the slope factor s=14.2±1.1 and 16.6±0.7 in the absence and the presence of DHA respectively (P>0.05, n=5) **(D)** Graph showing the ratio between the current obtained in the presence of DHA and that under control conditions.

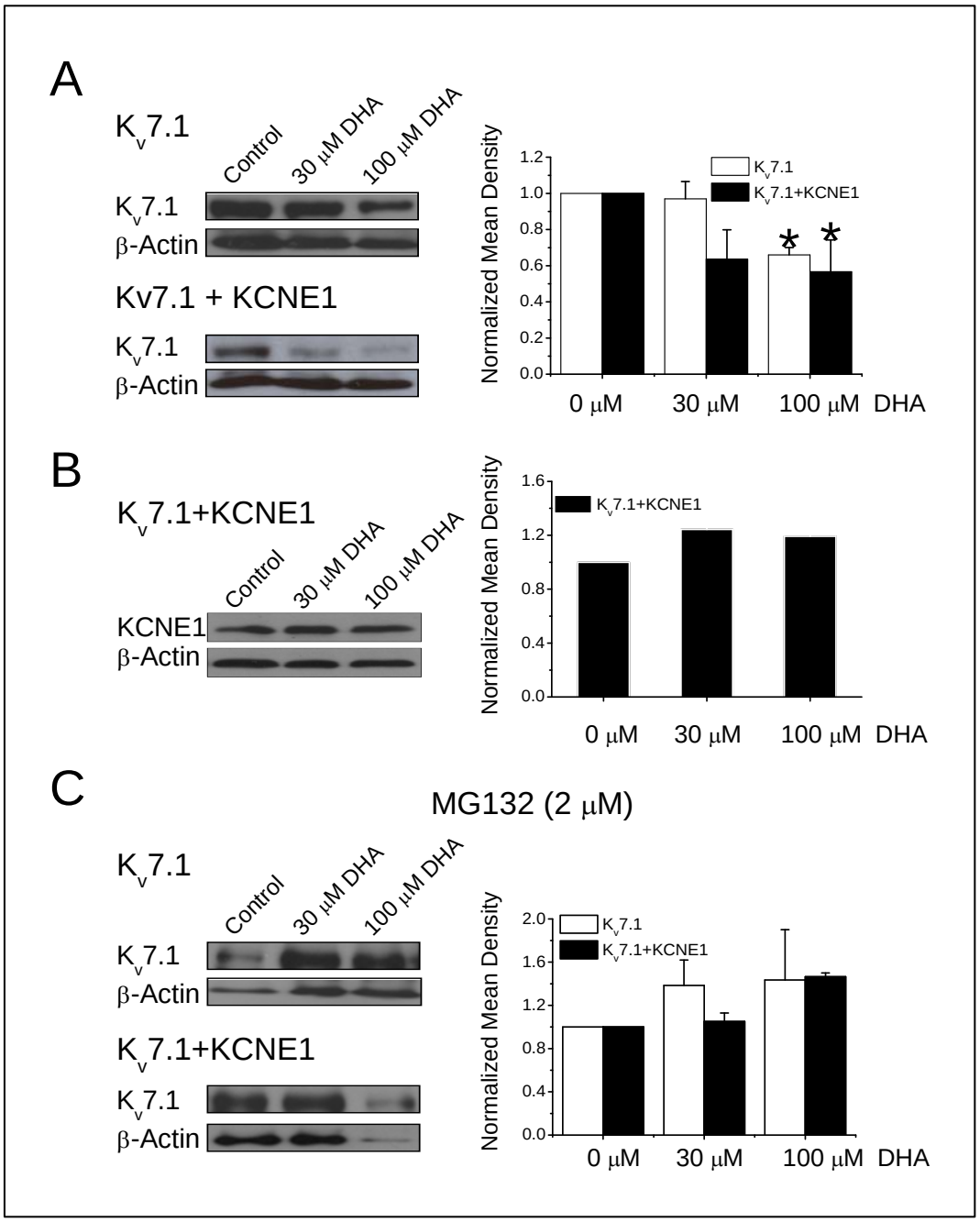

Figure S3. DHA decreases steady-state levels of K_v7.1 protein. **(A)**: Left: Shown are representative western blots that illustrate treatments with DHA. Note that DHA induces dose-dependent reductions of K_v7.1 protein. Cellular lysates were prepared from COS7 cells transiently expressing K_v7.1 and incubated for 48h with DHA at two concentrations (30 and 100 μM). Cellular lysates were prepared from COS-7 cells transiently expressing K_v7.1 incubated with DHA. Samples were subjected to SDS-PAGE, transferred to PVDF and probed with an antibody raised against K_v7.1. Right: Bar graph summarizing densitometry measurements used to compare protein levels for the treatments of DHA for 48 h. β-actin levels were used as a loading control (n=3 or 4; *:P<0.05). **(B)**: Representative western blots and graph showing the effects of DHA (0, 30 and 100 μM) on KCNE1 in cells transfected with K_v7.1+KCNE1). **(C)**: Representative western blots and graph showing the effects of DHA (0, 30 and 100 μM) on K_v7.1 in cells transfected with K_v7.1 or K_v7.1+KCNE1 in the presence of MG132 (proteosome inhibitor.*P<0.05, n=3-4)

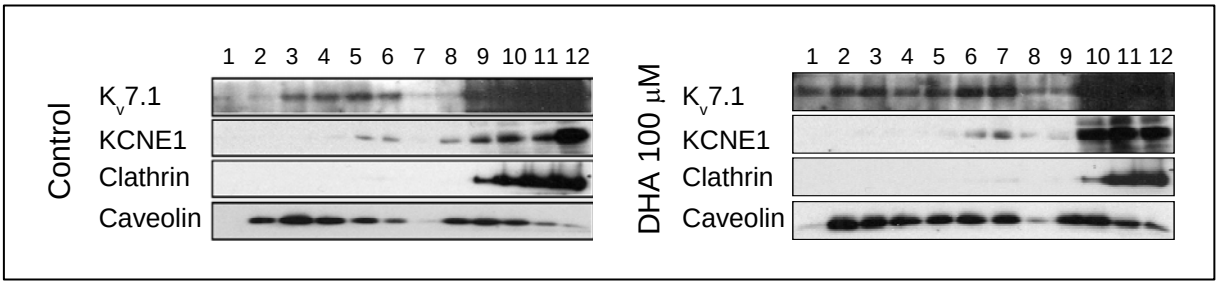

Figure S4. Effects of long term administration of DHA on K_v7.1 and KCNE1 location. Sucrose density gradient fractions of cells expressing K_v7.1 and KCNE1 in the absence or the presence of DHA. While caveolin indicated floating lipid rafts with low density, clathrin labeled non-raft fractions. K_v7.1 and KCNE1 colocalized with caveolin in low-buoyant density fractions (fractions 2-6) in control experiments, whereas DHA triggered a wider distribution of proteins (fractions 1-12) and rafts. Pictures are representative images of at least 3 independent lipid rafts extractions analysed by western blot.

Table S1A. Time-dependent effects of acute EPA in cholesterol depleted cells on the activation process of $K_V7.1$/KCNE1 channels. Currents were recorded for each experimental condition after applying a 12s depolarizing pulse at +60 mV and were fitted to a biexponential function or to a monoexponential function in the case of EPA. (P>0.05, n=4, *vs*. the control condition, P>0.05, n=4, MβCD *vs.* MβCD).

Activation kinetics						
CONTROL		**MβCD 10 mM**		**EPA 20 µM**	**MβCD 10 mM**	
τ_f (ms)	τ_s (ms)	τ_f (ms)	τ_s (ms)	τ_f (ms)	τ_f (ms)	τ_s (ms)
863±66	7296±1370	1065±186	5951±1324	7329±1696	928±76	5715±170

Table S1B. Time-dependent effects of acute EPA in cholesterol depleted cells on the deactivation process of $K_V7.1$/KCNE1 channels. Tail currents were recorded for each experimental condition at -40mV pulses after a depolarizing pulse to +60mV of 5.5s in duration and were fitted to a monoexponential function or a biexponential function in the case of EPA. (*P<0.05, n=4, *vs*. the control condition, P>0.05, n=4, MβCD *vs.* MβCD).

Deactivation kinetics				
CONTROL	**MβCD 10 mM**	**EPA 20 µM**		**MβCD 10 mM**
τ (ms)	τ (ms)	τ_f (ms)	τ_s (ms)	τ (ms)
584±89	272±45*	144±14	439±89	232±34*

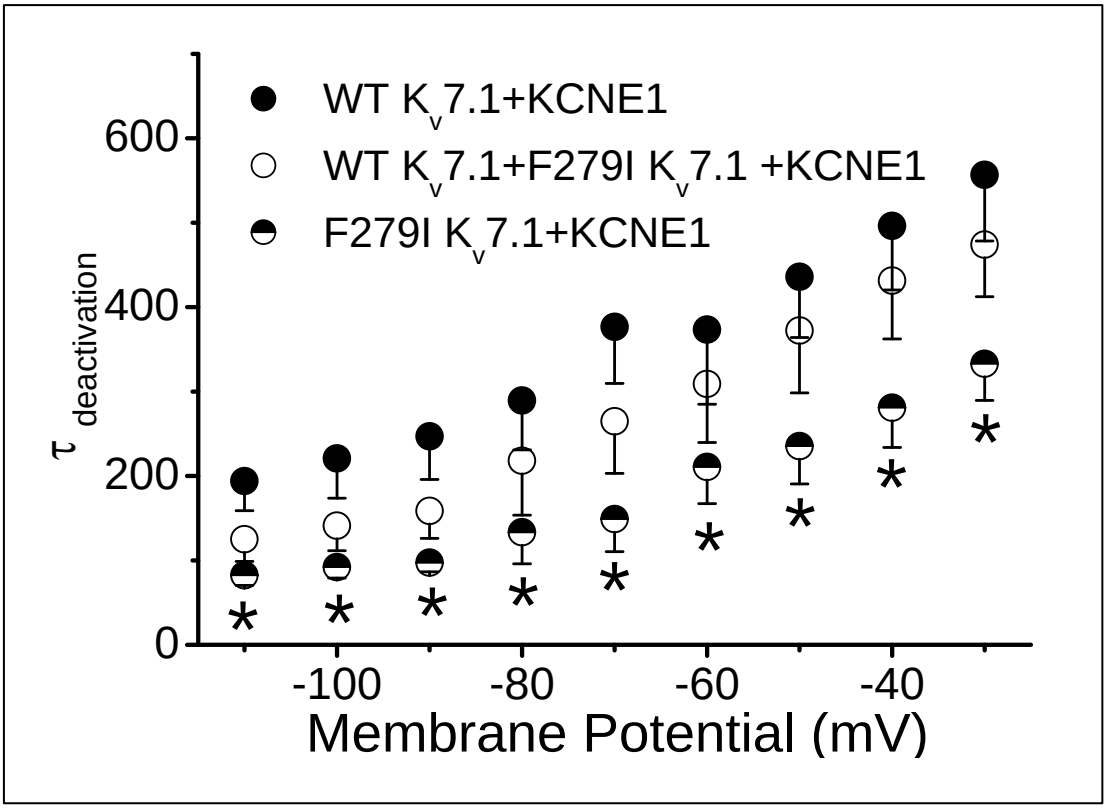

Figure S5. Comparison of deactivation time constants for the WT K_v7.1 channels expressed with the accessory subunit KCNE1 and for F279I K_v7.1/KCNE1 and WT/F279IK_v7.1/KCNE1 channel complexes. Deactivation time constants were obtained by fitting the tail currents to monoexponential decay functions and were plotted as a function of the repolarization potential. (*P<0.05, n=4-11, for WT/F279IK_v7.1/KCNE1 *vs*. the control condition).

9 APPENDIX 2: PUBLICATIONS

9.1 Original papers

Celecoxib blocks cardiac $K_v1.5$, $K_v4.3$ and $K_v7.1$ (KCNQ1) channels: effects on cardiac action potentials

Macías A*, **Moreno C***, Moral-Sanz J, Cogolludo A, David M, Alemanni M, Pérez-Vizcaíno F, Zaza A, Valenzuela C, González T. (* Both authors contributed equally to this work)

Abstract: Celecoxib is a COX-2 inhibitor that has been related to an increased cardiovascular risk and that exerts several actions on different targets. The aim of this study was to analyze the effects of this drug on human cardiac voltage-gated potassium channels K_v involved on cardiac repolarization $K_v1.5$ (I_{Kur}), $K_v4.3$+KChIP2 ($I_{to}1$)) and $K_v7.1$+KCNE1 (I_{Ks}) and to compare with another COX-2 inhibitor, rofecoxib. Currents were recorded in transfected mammalian cells by whole-cell patch-clamp. Celecoxib blocked all the Kv channels analyzed and rofecoxib was always less potent, except on $K_v4.3$+KChIP2 channels. $K_v1.5$ block increased in the voltage range of channel activation, decreasing at potentials positive to 0 mV. The drug modified the activation curve of the channels that became biphasic. Block was frequency-dependent, increasing at fastest frequencies. Celecoxib effects were not altered by TEA_{out} in R487Y mutant $K_v1.5$ channels but the kinetics of block were slower and the degree of block was smaller with TEA_{in}, indicating that celecoxib acts from the cytosolic side. We confirmed the blocking properties of celecoxib on native K_v currents from rat vascular cells, where $K_v1.5$ are the main contributors ($IC_{50}\approx$ 7 μM). Finally, we demonstrate that celecoxib prolongs the action potential duration in mouse cardiac myocytes and shortens it in guinea pig cardiac myocytes, suggesting that K_v block induced by celecoxib may be of clinical relevance. **J Mol Cell Cardiol.** 2010 Dec;49(6):984-92.

Protein kinase C (PKC) activity regulates functional effects of $K_v\beta1.3$ subunit on $K_v1.5$ channels: identification of a cardiac $K_v1.5$ channelosome

David M, Macías Á, **Moreno C**, Prieto Á, Martínez-Mármol R, Vicente R, González T, Felipe A, Tamkun MM, Valenzuela C.

Abstract: $K_v1.5$ channels are the primary channels contributing to the ultrarapid outward potassium current (I_{Kur}). The regulatory $K_v\beta1.3$ subunit converts $K_v1.5$ channels from delayed rectifiers with a modest degree of slow inactivation to channels with both fast and slow inactivation components. Previous studies have shown that inhibition of PKC with calphostin C abolishes the fast inactivation induced by $K_v\beta1.3$. In this study, we investigated the mechanisms underlying this phenomenon using electrophysiological, biochemical, and confocal microscopy approaches. To achieve this, we used HEK293 cells (which lack $K_v\beta$ subunits) transiently cotransfected with $K_v1.5$+$K_v\beta1.3$ and also rat ventricular and atrial tissue to study native α-β subunit interactions. Immunocytochemistry assays demonstrated that these channel subunits colocalize in control conditions and after calphostin C treatment. Moreover, coimmunoprecipitation studies showed that $K_v1.5$ and $K_v\beta1.3$ remain associated after PKC inhibition. After knocking down all PKC isoforms by siRNA or inhibiting PKC with calphostin C, $K_v\beta1.3$-induced fast inactivation at +60 mV was abolished. However, depolarization to +100 mV revealed $K_v\beta1.3$-induced inactivation, indicating that PKC inhibition causes a dramatic positive shift of the inactivation

curve. Our results demonstrate that calphostin C-mediated abolishment of fast inactivation is not due to the dissociation of K_v1.5 and K_vβ1.3. Finally, immunoprecipitation and immunocytochemistry experiments revealed an association between K_v1.5, K_vβ1.3, the receptor for activated C kinase (RACK1), PKCβI, PKCβII, and PKCθ in HEK293 cells. A very similar K_v1.5 channelosome was found in rat ventricular tissue but not in atrial tissue. **J Biol Chem**. 2012 Jun 15;287(25):21416-28.

9.2 Reviews

Kv1.5-Kv beta interactions: molecular determinants and pharmacological consequences.

González T, David M, **Moreno C**, Macías A, Valenzuela C.

Abstract: K_v1.5 channels are homotetramers of alpha-pore subunits mainly present in human atrium and pulmonary vasculature. Thus, K_v1.5 is a pharmacological target for cardiovascular diseases. K_v beta 1.3 assemblies with K_v alpha 1.5 and modifies its gating and pharmacology. A further knowledge of alpha-beta interactions and pharmacology will lead a better design of new drugs. **Mini Rev Med Chem.** 2010 Jun;10(7):635-42.

Stereoselective interactions between local anesthetics and ion channels.

Valenzuela C, **Moreno C**, de la Cruz A, Macías Á, Prieto Á, González T.Abstract: Local anesthetics are useful probes of ion channel function and structure. Stereoselective interactions are especially interesting because they can reveal three-dimensional relationships between drugs and channels with otherwise identical biophysical and physicochemical properties. Furthermore, stereoselectivity suggests direct and specific receptor-mediated action, and identification of such stereospecific interactions may have important clinical consequences. The fact that drug targets are able to discriminate between the enantiomers present in a racemic drug is the consequence of the ordered asymmetric macromolecular units that form living cells. However, almost 25% of the drugs used in the clinical practice are racemic mixtures, and their individual enantiomers frequently differ in both their pharmacodynamic and pharmacokinetic profiles. Moreover, their effects can be similar to or different from the pharmacological effect of the drug and may contribute to the undesired effects of the drug. In other cases, the pharmacological effects induced by the two enantiomers on the molecular target are opposite. In the present manuscript, we will review the stereoselective effects of bupivacaine-like local anesthetics on cardiac sodium and potassium channels. **Chirality**. 2012 Nov;24(11):944-50.

Effects of n-3 Polyunsaturated Fatty Acids on Cardiac Ion Channels

Moreno C, Macías A, Prieto A, de la Cruz A, González T, Valenzuela C.

Abstract: Dietary n-3 polyunsaturated fatty acids (PUFAs) have been reported to exhibit antiarrhythmic properties, and these effects have been attributed to their capability to modulate ion channels. In the present review, we will focus on the effects of PUFAs on a cardiac sodium channel (Na_v1.5) and two potassium channels involved in

cardiac atrial and ventricular repolarization (K_v) (K_v1.5 and K_v11.1). n-3 PUFAs of marine (docosahexaenoic, DHA and eicosapentaenoic acid, EPA) and plant origin (alpha-linolenic acid, ALA) block K_v1.5 and K_v11.1 channels at physiological concentrations. Moreover, DHA and EPA decrease the expression levels of K_v1.5, whereas ALA does not. DHA and EPA also decrease the magnitude of the currents elicited by the activation of K_v1.5 and calcium channels. These effects on sodium and calcium channels should theoretically shorten the cardiac action potential duration (APD), whereas the blocking actions of n-3 PUFAs on K_v channels would be expected to produce a lengthening of cardiac action potential. Indeed, the effects of n-3 PUFAs on the cardiac APD and, therefore, on cardiac arrhythmias vary depending on the method of application, the animal model, and the underlying cardiac pathology. **Front Physiol.** 2012;3:245.

Polyunsaturated Fatty acids modify the gating of kv channels.

Moreno C, Macias A, Prieto A, De La Cruz A, Valenzuela C.

Abstract: Polyunsaturated fatty acids (PUFAs) have been reported to exhibit antiarrhythmic properties, which are attributed to their capability to modulate ion channels. This PUFAs ability has been reported to be due to their effects on the gating properties of ion channels. In the present review, we will focus on the role of PUFAs on the gating of two K_v channels, K_v1.5 and K_v11.1. K_v1.5 channels are blocked by n-3 PUFAs of marine (docosahexaenoic acid (DHA) and eicosapentaenoic acid] and plant origin (alpha-linolenic acid, ALA) at physiological concentrations. The blockade of K_v1.5 channels by PUFAs steeply increased in the range of membrane potentials coinciding with those of K_v1.5 channel activation, suggesting that PUFAs-channel binding may derive a significant fraction of its voltage sensitivity through the coupling to channel gating. A similar shift in the activation voltage was noted for the effects of n-6 arachidonic acid (AA) and DHA on K_v1.1, K_v1.2, and K_v11.1 channels. PUFAs- K_v1.5 channel interaction is time-dependent, producing a fast decay of the current upon depolarization. Thus, K_v1.5 channel opening is a prerequisite for the PUFA-channel interaction. Similar to the K_v1.5 channels, the blockade of K_v11.1 channels by AA and DHA steeply increased in the range of membrane potentials that coincided with the range of K_v11.1 channel activation, suggesting that the PUFAs- K_v channel interactions are also coupled to channel gating. Furthermore, AA regulates the inactivation process in other K_v channels, introducing a fast voltage-dependent inactivation in non-inactivating K_v channels. These results have been explained within the framework that AA closes voltage-dependent potassium channels by inducing conformational changes in the selectivity filter, suggesting that K_v channel gating is lipid dependent. **Front Pharmacol.** 2012;3:163.

9.3 Publications in progress

Modulation of K_v and K_{ir} currents by 15-epi-lipoxin-A_4 in activated murine macrophages. Implications in innate immunity

Moreno C,‖ Prieto P,‖ Macías A,‖ Santillana MP,‖ Través PG, Boscá L,¶ and Valenzuela C.¶ ‖ CM, PP, AM and

MP-S contributed equally to this work. ¶ Corresponding authors

Abstract: Potassium channels play a pivotal role in the modulation of macrophage physiology. Blockade of voltage dependent potassium channels (K_v) channels by specific antagonists decreases macrophage cytokine production and inhibits proliferation. In the presence of aspirin, acetylated COX-2 loses activity required to form prostaglandin but maintains oxygenase activity to produce 15*R*-HETE from arachidonate. This intermediate product is transformed via 5-LOX into epimeric lipoxins, termed 15-epi-lipoxins (e-LXA_4). K_v channels have been proposed as anti-inflammatory targets. Therefore, we studied the effects of e-LXA_4 on early signaling and on K_v and inward rectifier potassium channels (K_{ir}) in mice bone marrow-derived macrophages (BMDM). Experiments were performed in BMDM and electrophysiological recordings were performed by the whole-cell patch-clamp technique. Treatment of BMDM with e-LXA_4 inhibited LPS-dependent activation of NF-κB and IKKβ activity, at the same time that protected against LPS activation-dependent apoptosis. In addition, acute treatment of LPS-stimulated BMDM with e-LXA_4 resulted in a decrease of K_v currents, compatible with attenuation of the inflammatory response. More importantly, long-term treatment of LPS-stimulated BMDM with e-LXA_4 significantly reverted LPS effects on K_v and K_{ir} currents. Under these conditions, e-LXA_4 decreased calcium influx *vs.* that observed in LPS-stimulated BMDM. These effects were mediated, at least in part, via the lipoxin receptor (ALX), since were partially reverted in the presence of a selective ALX receptor antagonist. We provide evidence for a new mechanism by which e-LXA_4 contributes to inflammation resolution consisting in the reversion of LPS effects on K_v and K_{ir} currents in macrophages.

Effects of n-3 polyunsaturated fatty acids on the function, expression and localization of K_v7.1 channels

Moreno C, Oliveras A, Kharche S, Guizy M, Comes N, Starý T, Loussouarn G, Severi S, Felipe A, Valenzuela C.

Abstract: Dietary polyunsaturated fatty acids (PUFAs) have been reported to exhibit antiarrhythmic properties, which have been attributed to their ability to modulate ion channels. In this work we analyzed the effects of EPA and DHA on the current and the expression of K_v7.1+KCNE1 channels transiently expressed in COS7 cells by using patch-clamp, Western blot, and lipid rafts extraction techniques. Perfusion of cells with EPA and DHA (20 μM) increased K_v7.1+KCNE1 current. This effect was accompanied by an acceleration of the deactivation kinetics and slower activation kinetics. Both PUFAs shifted the activation curve towards negative potentials. After incubation the cells during 48 h with EPA, K_v7.1 current magnitude decreased and the activation curve was shifted to more positive potentials. Under these conditions, EPA decreased the expression of K_v7.1 but not of KCNE1. This decrease in the K_v7.1 protein expression was prevented in the presence of a proteasome inhibitor MG132, suggesting that PUFAs can favor a degradation of K_v7.1 via proteasome. Also, DHA and EPA impaired the localization of K_v7.1 in lipid rafts. Electrophysiological experiments with methyl-β-cyclodextrin (MβCD) demonstrated that removal of cholesterol with MβCD increased the K_v7.1 magnitude current. After cholesterol depletion with MβCD, EPA produces similar effects than those produced acutely and they could be reverted after wash-out with external drug-free solution, suggesting a direct effect on the channel. These results demonstrate

that EPA and DHA: 1) increase the K_v7.1+KCNE1 magnitude, 2) induce K_v7.1 degradation via proteasome and 3) modify the membrane localization of this channel.

A New KCNQ1 mutation responsible of short QT syndrome located at the S5 segment

Moreno C, Muñoz C, de la Cruz A, Salar M, Gimeno JR, Lambiasse P, Felipe A, Valenzuela C.

Abstract: Mutations involving cardiac ion channels result in abnormal action potential (AP) formation or propagation, leading to cardiac arrhythmias. They constitute approximately 10–20% of all sudden cardiac death (SCD). The short QT syndrome is a new congenital entity characterized by a shortened QTc interval in the ECG and a lack of adaptation during increasing heart rates. In the present Doctoral Thesis, we used the *patch-clamp* technique to characterize the novel F279I K_v7.1 mutation found on a 23 years old man with a QTc of 356 ms and a familial history of SCD. In the absence of KCNE1, WT and F279I K_v7.1 currents had similar biophysical properties. However, functional analysis of F279I K_v7.1 (alone or co-expressed with the WT channel, in the presence of KCNE1) revealed a pronounced shift of the half-activation potential and an acceleration of the activation kinetics leading to a gain of function in I_{Ks}. We conclude that the F279I mutation would predict to augment substantially repolarizing current during the AP due to an impaired coupling of the K_v7.1 gating modulation induced by KCNE1.